

MATHEMATICAL MODELLING OF AIR
ENTRAINMENT IN WEB HANDLING
APPLICATIONS

By

TAJUDDIN

"

Bachelor of Engineering

N.E.D University of Engineering & Technology

Karachi, Pakistan

1985

Submitted to the Faculty of the
Graduate College of the
Oklahoma State University
in partial fulfillment of
the requirements for
the Degree of
MASTER OF SCIENCE
December, 1987



MATHEMATICAL MODELLING OF AIR
ENTRAINMENT IN WEB HANDLING
APPLICATIONS

Thesis Approved:

Elvitt O. Thomas

Thesis Adviser

John J. Shelton

James F. Good

Dean of the Graduate College

PREFACE

I wish to express my sincere gratitude to my advisor, Dr. F. O. Thomas for his esteemed guidance, concern, and invaluable help during this work and during my stay at Oklahoma State University. Without his valuable suggestions and constructive guidance, the completion of this project would have been impossible. I also thank him for helping me in writing this thesis despite his demanding schedule.

I would also take this opportunity to thank my committee members, Dr. J. Shelton and Dr. K. Good, for their initial advisement in the course of this work. Special thanks are also due to Web Handling Research Center for the financial support I received during the course of this work.

I am especially indebted to my father and mother, Mr. and Mrs. Nazar Ali and other family members for their constant support and moral encouragement.

TABLE OF CONTENTS

Chapter	Page
I. INTRODUCTION.	1
1.1. Background.	1
1.2. Problem Statement	7
II. MATHEMATICAL FORMULATION.	8
2.1. Problem Formulation	8
2.2. Basic Equations	8
2.2.1. General Lubrication Equation- Hydrodynamic Aspects of the Problem	10
2.2.2. Web Equilibrium Equation.	17
2.3. Governing Differential Equation	40
2.4. Pressure Distribution	43
2.5. Summary of the Simplified Governing Equations	46
2.6. Qualitative Analysis Based on Governing Equations	47
III. SOLUTION OF THE GOVERNING DIFFERENTIAL EQUATION.	51
3.1. Mathematical Description of the Problem	51
3.2. Boundary conditions	53
3.3. Numerical Solution.	55
3.3.1. Inlet Region Solution	57
3.3.2. Exit Region Solution.	58
3.3.3. Numerical Integration Method.	61
3.4. Discussion of the Numerical Results	63
3.5. Constant Gap Film Thickness for Various Web Handling Applications	82
IV. STRATEGY FOR CONTROLLING AIR ENTRAINMENT.	83
4.1. Modification of the Model	84
4.2. Controlling Air Entrainment Via Rider Roller.	92

Chapter	Page
4.3. Modification of the Computer Code to Account for Rider Roller Effects	108
4.4. Significance of the Normalized Quantities and Discussion of Results	111
4.5. An Example of Air Film Thickness control	130
V. CONCLUSIONS AND RECOMMENDATIONS	138
5.1. Conclusions	138
5.5. Recommendations for Future Work	140
A SELECTED BIBLIOGRAPHY.	145
APPENDICES	146
APPENDIX A - NORMALIZATION FOR THE DERIVATION OF THE REYNOLDS LUBRICATION EQUATION	147
APPENDIX B - COMPARISON OF THE ORDER OF MAGNITUDE IN THE DERIVATION OF REYNOLDS EQUATION	150
APPENDIX C - SIMPLIFYING STEPS IN THE DERIVATION OF THE REYNOLDS EQUATION	152
APPENDIX D - FORCE AND MOMENT EQUATIONS FOR THE WEB ELEMENT.	155
APPENDIX E - SIMPLIFIED FORCE AND MOMENT EQUATIONS FOR THE WEB ELEMENT.	158
APPENDIX F - DERIVATION OF THE FORCE EQUILIBRIUM EQUATION	161
APPENDIX G - COUPLED NUMERICAL PROCEDURE OF RUNGE-KUTTA AND MILNE PREDICTOR-CORRECTOR METHODS.	163
APPENDIX H - EQUATION FOR WEB-RIDER ROLLER CLEARANCE.	167
APPENDIX I - COMPUTER PROGRAM LISTINGS.	172

LIST OF TABLES

Table	Page
I. Numerical Results of Inlet Region Solution	64
II. Numerical Results of Exit Region Solution	65
III. Numerical Values of Constant Gap Film Thickness Length of the Inlet Region for Different Parameters.	82

LIST OF FIGURES

Figure	Page
1. Schematic Presentation of Web-Roller Interaction	2
2. Typical Problem in Winding Process Due to Air Entrainment	4
3. The Foil Bearing.	6
4. Geometric Configuration of the Problem with Coordinate System	9
5. Air Film Flow Channel	15
6. Cartesian Coordinate System on Web.	19
7. Element of Web with Various Stresses.	20
8. Element of Web with Various Forces and Moments	21
9. Deflections and Rotations of Web.	28
10. The Three Regions in Web-Roller Interacton.	49
11. Schematic Presentation of Inlet and Exit Transition Regions.	52
12. Air Film Thickness in the Inlet Region.	68
13. Plot of η vs H' - Inlet Region.	69
14. Plot of η vs H'' - Inlet Region	70
15. Plot of η vs H''' - Inlet Region.	71
16. Air Film Pressure in the Inlet Region	72
17. Air Film Thickness in the Exit Region	73
18. "Undulation" Near the Exit Transition Region.	74

Figure	Page
19. Plot of η vs H' - Exit Region	75
20. Plot of η vs H'' - Exit Region.	76
21. Plot of η vs H''' - Exit Region	77
22. Air Film Pressure in the Exit Region.	78
23. Effect of Relative Speed U on Constant Gap Film Thickness.	80
24. Effect of Tension T on Constant Gap Film Thickness.	81
25. The Modified Geometry	85
26. Web Element Under Various Forces and Moments	87
27. Pressure Due to Rider Roller in Both the Inlet and Uniformity Region	93
28. Rider Roller Pressure Fully in the Inlet Region.	94
29. Definition of the Transformed Angle	100
30. Sketch Illustrating Method of Increasing Rider Roller Pressure	114
31. Sketch Illustrating Method of Varying Rider Roller Size	116
32. Effect of Rider Roller Size on Constant Gap Film Thickness - Normalized	117
33. Rider Roller Pressure for Three Different K_1 Values ($BN=5.0$, $ETC=1.0$)	119
34. Pressure in the Air Film for Three Different K_1 Values ($BN=5.0$, $ETC=1.0$)	120
35. Sketch Illustrating Method of Varying Rider Roller Location	122
36. Effect of Rider Roller Location on Constant Gap Film Thickness - Normalized.	124
37. Rider Roller Pressure for Three Different η_c Values ($BN=5.0$, $K_1=0.5$).	125

Figure	Page
38. Pressure in the Air Film for Three Different η_c Values (BN=5.0, $K_1=0.5$).	126
39. Effect of Imposed Pressure on Constant Gap Film Thickness - Normalized	128
40. Rider Roller Pressure for Three Different Δ Values (ETC=1.0, $K_1=0.5$).	131
41. Pressure in the Air Film for Three Different Δ Values (ETC=1.0, $K_1=0.5$).	132
42. Effect of Rider Roller Size on Constant Gap Film Thickness - Dimensional.	134
43. Effect of Rider Roller Location on Constant Gap Film Thickness - Dimensional.	135
44. Effect of Imposed Pressure on Constant Gap Film Thickness - Dimensional.	137

NOMENCLATURE

b	- Half width of the web
c	- Clearance between the web and rider roller
c_m	- Minimum clearance between the web and rider roller
c_I, c_{II}	- Dimensional clearances in the two regions defined in Figure 27
C_1, C_2, C_3, C_4, C_5	- Constants of integration
C_I, C_{II}	- Normalized clearance for c_I, c_{II}
$D=(Et^3)/(12(1-\nu^2))$	- Flexure rigidity
E	- Modulus of elasticity
F_x, F_y, F_z	- Body forces along x-, y- and z-directions, respectively
G	- Shear Modulus
h	- air film thickness
h_0	- Constant gap film thickness
$H=h/h_0$	- Normalized air film thickness
K_1, K_2	- Defined by equations (4.2.5) and (4.2.6)
l	- Characteristic length
M_x, M_y	- Bending moments per unit length of sections of web perpendicular to x- and y- directions, respectively

M_{xy}	- Twisting moment per unit length of sections of web perpendicular to x-axis
N_x, N_y	- Normal forces per unit length of sections perpendicular to x- and y-directions, respectively
N_{xy}	- Shearing force in direction of y-axis per unit length of section perpendicular to x-axis
p	- Air film pressure
p_a	- Ambient pressure
p_r	- Rider roller pressure
$\bar{p} = p/p_a$	- Normalized pressure
$\bar{p} = h_0/T \{ T/(6\mu U) \}^{2/3} p$	- Normalized pressure
$\bar{p}_R = pR/T$	- Normalized pressure
$\bar{p}_R = h_0/T \{ T/(6\mu U) \}^{2/3} p_r$	- Normalized rider roller pressure
Q_x, Q_y	- Transverse shearing force parallel to z-axis per unit length of section perpendicular to x- and y-directions
r_x, r_y	- Radii of curvature of the middle surface of the web in xz- and yz-planes, respectively
R	- Radius of supporting roller
$R_0 = R + h_0$	- Sum of roller radius and constant gap film thickness
t	- Time (section 2.2.1)
t	- Thickness of the web
T	- Reduced tension in the web
T_0	- Tension of the web
$\bar{u}, \bar{v}, \bar{w}$	- Components of velocity of air

	under the web
u, v, w	- Components of displacement
u_0, v_0	- Middle surface displacement (at $z=0$)
U	- Sum of the web and the supporting roller speed
U_i	- Characterstic velocity
U_n	- Sum of the web and the rider roller speed
U_R	- Velocity of Roller (x-direction)
U_w	- Velocity of web (x-direction)
$U = u/U_i$	- Normalized u velocity
V_R	- Velocity of Roller (y-direction)
V_w	- Velocity of web (y-direction)
$V = (\bar{v}l)/(U_i b)$	- Normalized v velocity
w	- load due to rider roller
$W = (\bar{w}l)/(U_i h)$	- Normalized w velocity
x, y, z	- Rectangular coordinates
x_c	- dimensional distance of point of minimum clearance
x_n	- x-coordinate defined at point of minimum clearance
$X = x/l$	- Normalized x-coordinate
$Y = y/b$	- Normalized y-coordinate
$Z = z/h$	- Normalized z-coordinate
ρ	- Air density
ν	- Kinematic viscosity (section 2.2.1)
ν	- Poisson's ratio

μ	- Coefficient of viscosity
$\sigma_x, \sigma_y, \sigma_z$	- Normal components of stress parallel to x-, y- and z-directions
τ	- Total shear force
$\tau_{xy}, \tau_{yz}, \tau_{zx}$	- Shearing stress components
τ_a	- Shearing force per unit area on the web due to air under it
σ	- Mass per unit area of the web
α, β	- Rotations in x- and y-directions
ϵ_x, ϵ_y	- Normal strains
$\epsilon_{xz}, \epsilon_{yz}$	- Shearing strains
$\gamma_{xy}, \gamma_{yz}, \gamma_{zx}$	- Shearing strains
$\eta = (x/h_0) \left\{ (6\mu U)/T \right\}^{1/3}$	- Normalized x-coordinate
η_c	- Normalized distance of point of minimum clearance
ψ_I, ψ_{II}	- Transformed angles
ψ_{Io}	- Transformed angle defined by equation (4.2.33)
Λ	- Defined by equation (4.2.13)

CHAPTER I

INTRODUCTION

1.1 Background

A web may be defined as any material manufactured in continuous strips. Many materials are processed in web form which requires techniques for their transportation and manipulation. These techniques may be collectively termed web handling. Web handling is therefore quite important in industries involved with paper products, plastic films, magnetic tapes, packaging processes, printing applications and textiles, to name but a few.

An integral component of any web handling application is the passage of the web material over a supporting roller as shown in Figure 1 which also depicts the phenomenon of air entrainment. Due to the small but finite viscosity of air, the air in contact with the web and roller is drawn toward the region where the web meets the roller (which is known as the nip). Due to this air entrainment, the web rides on an air film which acts as a lubricant and prevents perfect surface to surface contact between the web and the roller. The thickness of the air

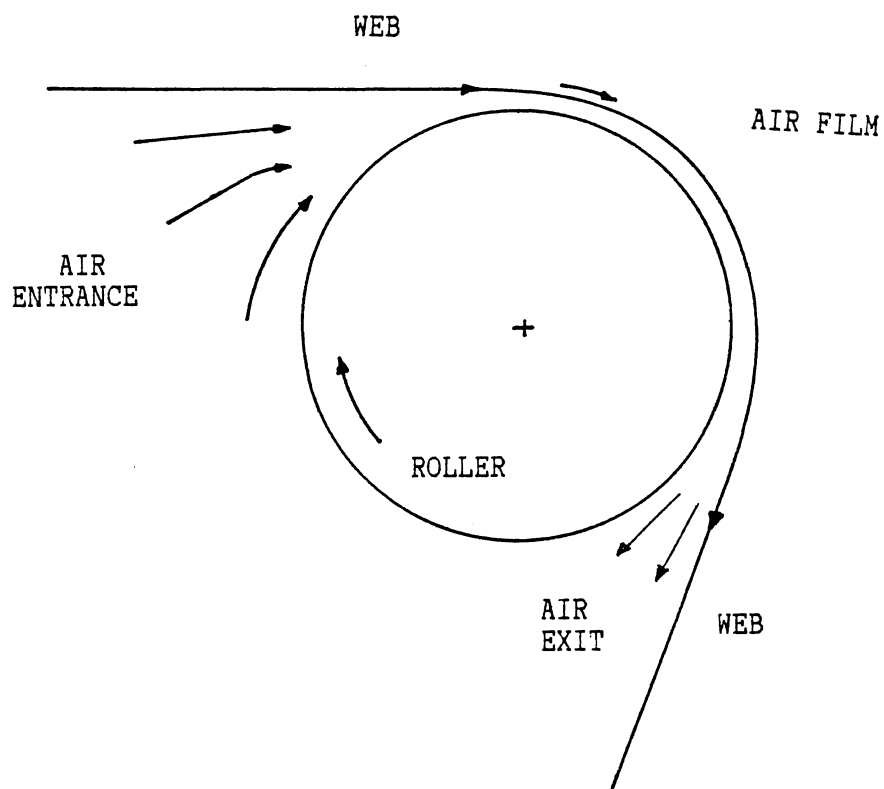


Figure 1. Schematic Presentation of Web-Roller Interaction

film between the web and the roller is expected to depend on parameters such as the sum of the web and the roller speed, viscosity of air, tension in the web and the size of the roller. The air entrainment phenomenon is an important consideration in determining the coefficient of friction between the web and roller. It is apparent that if too much air is entrained, the result will be instability to lateral disturbances and related difficulties in guiding the web.

The phenomenon of air entrainment is also an important concern in winding, the process by which a web material is wrapped into wound rolls. If too much air is entrained, surface to surface contact between adjacent layers of the material is severely reduced which results in a reduction of resistance to transverse directed disturbances. This can lead to roll formation failure due to "telescoping". Further, entrapped air in the roll causes formation of tires, balloons and bubbles (see Figure 2) which cause deformation of the web and consequently become one reason for wrinkle formation. On the other hand, if too little air is entrained, the coefficient of friction between adjacent layers of the material is very high leading to poor longitudinal transmission of tension. The absence of ample air film between the adjacent layers of material prevents minor irregularities from being smoothed out and results in their growth. These propagate outward as the roll is formed and can lead to gauge bands and may even

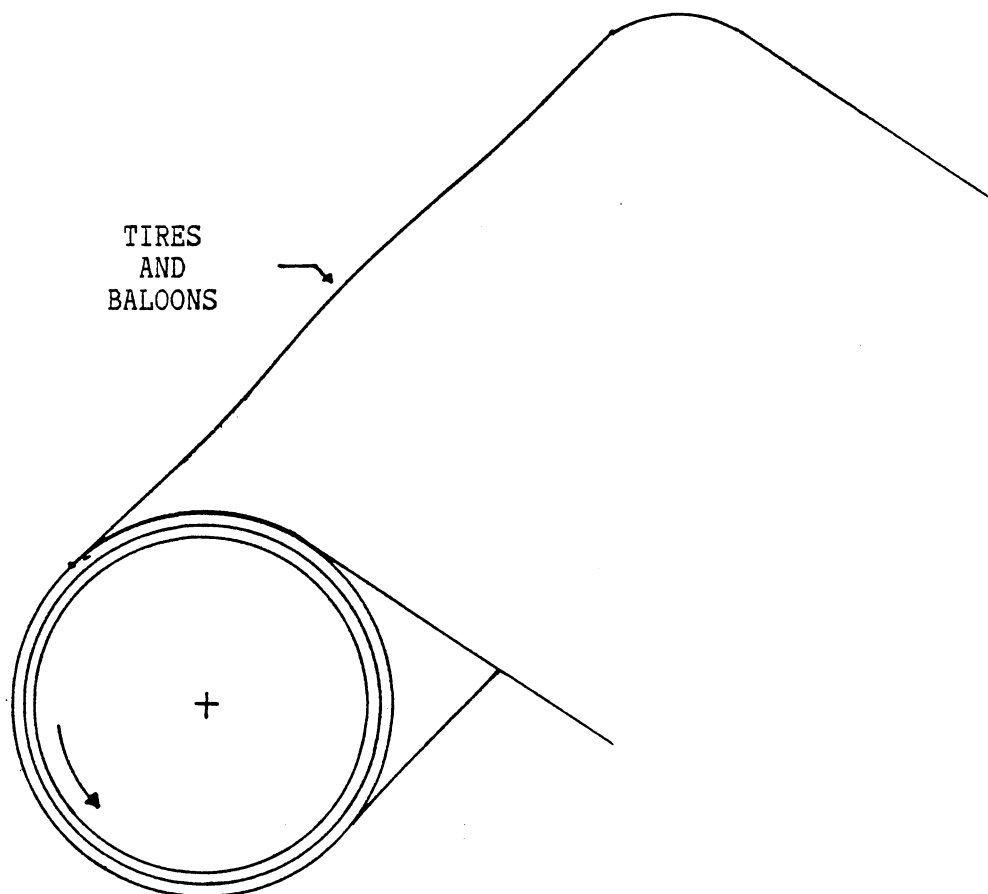


Figure 2. Typical Problem in Winding Process Due to Air Entrainment

locally yield the material.

From the above discussion it is clear that air entrainment effects play an important role in a variety of web handling applications. This is particularly true as line speeds continue to increase. It is widely recognized by industrial practitioners that a paucity of fundamental knowledge regarding air entrainment is a major hurdle in understanding the dynamics of winding and the instabilities encountered in a variety of web handling applications. Despite the recognized importance of air entrainment, there is at present, very little published work available. One effort in this regard is a work concerning air entrainment in winding by Knox & Sweeney (1). These authors suggested the application of foil bearing theory to model fluid film effects in winding since the winding process is geometrically similar to the foil bearing problem. Based upon their analysis an expression for nominal air film thickness was obtained.

It is appropriate to next review briefly foil bearing literature. A foil bearing consists of a rotating shaft which is supported by a stationary foil. Alternately, the shaft may be stationary and the foil moving with a certain speed over the shaft. The angle of wrap may vary from zero to 180 degrees. A typical foil bearing geometry is shown in Figure 3. The first major publication regarding foil bearings was that of Block and van Rossum (2). This work gives an approximate expression for the film thickness in

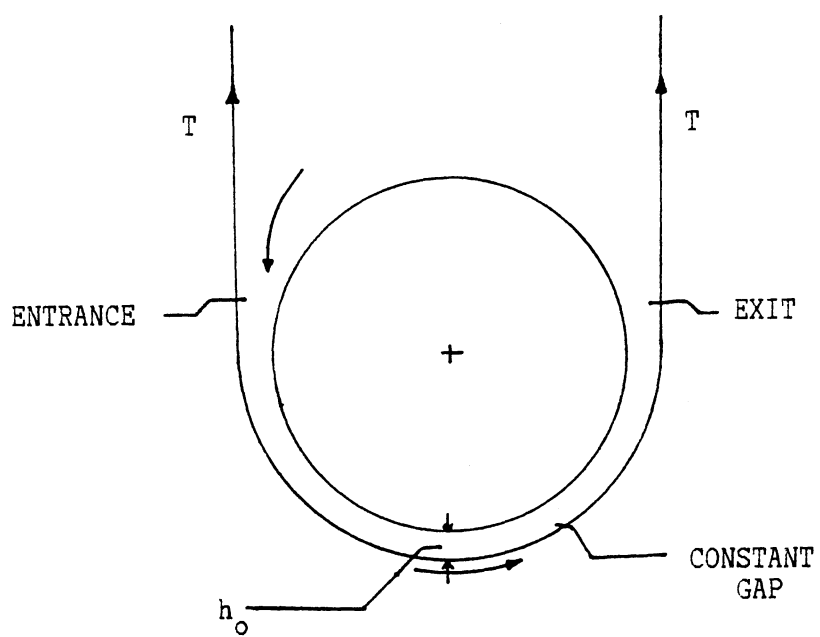


Figure 3. The Foil Bearing

the uniform gap region. Gross (3) introduced the fundamental differential equations for foil bearings and presented methods for their linearization. Langlois (4) analyzed lightly loaded foil bearing at zero angle of wrap. Baumeister (5) derived a set of six different foil bearing governing differential equations, each based on different physical assumptions. These were solved for gap clearance in order to determine the effect of the assumptions. Eshel and Elrod (6) discussed the theory of the infinitely wide, perfectly flexible self acting foil bearing while E. J. Barlow (7) discussed the numerical technique for the solution of the governing differential equation for an infinitely wide, self-acting foil bearing.

1.2 Problem Statement

The purpose of the present work is to develop a mathematical model that allows one to predict analytically the air film thickness between a web and a supporting roller. In addition, strategy for controlling the air film thickness will be developed and modelled. Geometrically the problem for which the model will be developed is defined in Figure 1. Due to local geometrical similarity between the nip of a wound roll and web over a supporting roller, it is expected that dynamic mechanisms will be similar in both cases. Hence the results of the work to be presented should also be applicable to the winding problem.

CHAPTER II

MATHEMATICAL FORMULATION

2.1 Problem Formulation

Figure 4 shows schematically the basic geometric configuration of the problem and the coordinate system that will be used for the mathematical formulation. It may be seen that a thin web of spanwise width $2b$ and thickness t passes over an infinitely long roller of radius R , which may be stationary or may be rotating. The web is assumed to be under uniform tension and is travelling with a velocity U_w over the roller in the direction of arc length of the web. The roller is assumed to have an inflexible surface and is completely impermeable.

The mathematical formulation of the problem is obtained from a "first principles" approach. The prediction of air film thickness and pressure requires a coupling of the relevant hydrodynamics of the air film with the web equilibrium dynamics. These two analyses are thus necessary for developing the required mathematical model.

2.2 Basic Equations

In this section the partial differential equations

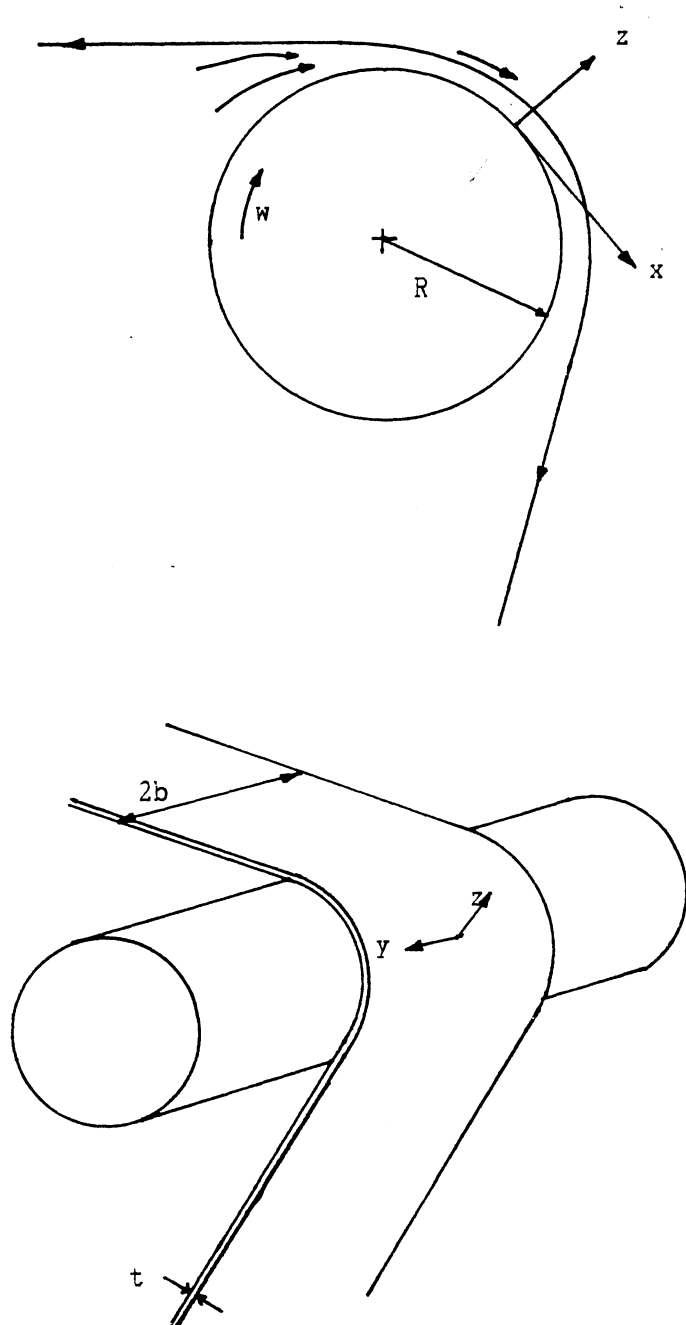


Figure 4. Geometric Configuration of the Problem with Coordinate System

governing both the hydrodynamic lubrication and the web equilibrium are developed. Since nearly every web handling application involves an air film thickness which is much smaller than the radius of curvature of the lubricating film, it is satisfactory to work with a Cartesian coordinate system. A similar argument holds for the analysis of equilibrium of the web, since most web materials are very thin.

2.2.1 General Lubrication Equation - Hydrodynamic Aspects of the Problem

The basic equations of viscous fluid flow are the Navier-Stokes equations which are derived by applying the principle of conservation of momentum to a fluid. The component form of these equations are

$$\begin{aligned} \frac{\partial \bar{u}}{\partial t} + \bar{u} \frac{\partial \bar{u}}{\partial x} + \bar{v} \frac{\partial \bar{u}}{\partial y} + \bar{w} \frac{\partial \bar{u}}{\partial z} = F_x / \rho - \frac{\partial p}{\partial x} / \rho + \nu \left[\frac{\partial^2 \bar{u}}{\partial x^2} + \frac{\partial^2 \bar{u}}{\partial y^2} + \frac{\partial^2 \bar{u}}{\partial z^2} \right] \\ - 2/3 \frac{\partial \mu}{\partial x} (\nabla \cdot \mathbf{V}) / \rho + 1/\rho \left[2 \frac{\partial \mu}{\partial x} \left\{ \frac{\partial \bar{u}}{\partial x} \right\} + \frac{\partial \mu}{\partial y} \left\{ \frac{\partial \bar{v}}{\partial x} + \frac{\partial \bar{u}}{\partial y} \right\} + \frac{\partial \mu}{\partial z} \left\{ \frac{\partial \bar{w}}{\partial x} + \frac{\partial \bar{u}}{\partial z} \right\} \right] \end{aligned} \quad (2.2.1)$$

$$\begin{aligned} \frac{\partial \bar{v}}{\partial t} + \bar{u} \frac{\partial \bar{v}}{\partial x} + \bar{v} \frac{\partial \bar{v}}{\partial y} + \bar{w} \frac{\partial \bar{v}}{\partial z} = F_y / \rho - \frac{\partial p}{\partial y} / \rho + \nu \left[\frac{\partial^2 \bar{v}}{\partial x^2} + \frac{\partial^2 \bar{v}}{\partial y^2} + \frac{\partial^2 \bar{v}}{\partial z^2} \right] \\ - 2/3 \frac{\partial \mu}{\partial y} (\nabla \cdot \mathbf{V}) / \rho + 1/\rho \left[\frac{\partial \mu}{\partial x} \left\{ \frac{\partial \bar{v}}{\partial x} + \frac{\partial \bar{u}}{\partial y} \right\} + 2 \frac{\partial \mu}{\partial y} \frac{\partial \bar{v}}{\partial y} + \frac{\partial \mu}{\partial z} \left\{ \frac{\partial \bar{w}}{\partial y} + \frac{\partial \bar{v}}{\partial z} \right\} \right] \end{aligned} \quad (2.2.2)$$

$$\begin{aligned}
\frac{\partial \bar{w}}{\partial t} + \bar{u} \frac{\partial \bar{w}}{\partial x} + \bar{v} \frac{\partial \bar{w}}{\partial y} + \bar{w} \frac{\partial \bar{w}}{\partial z} &= F_z / \rho - \frac{\partial p}{\partial z} / \rho + \nu \left[\frac{\partial^2 \bar{w}}{\partial x^2} + \frac{\partial^2 \bar{w}}{\partial y^2} + \frac{\partial^2 \bar{w}}{\partial z^2} \right] \\
-2/3 \frac{\partial \mu}{\partial z} (\nabla \cdot \mathbf{V}) / \rho + 1/\rho \left[\frac{\partial \mu}{\partial x} \left\{ \frac{\partial \bar{w}}{\partial x} + \frac{\partial \bar{u}}{\partial z} \right\} + \frac{\partial \mu}{\partial y} \left\{ \frac{\partial \bar{w}}{\partial y} + \frac{\partial \bar{v}}{\partial z} \right\} + 2 \frac{\partial \mu}{\partial z} \frac{\partial \bar{w}}{\partial z} \right]
\end{aligned}
\tag{2.2.3}$$

In addition, the equation of mass conservation is given by

$$\frac{\partial \rho}{\partial t} + \nabla \cdot (\rho \mathbf{V}) = 0$$

or,

$$\frac{\partial \rho}{\partial t} + \frac{\partial}{\partial x} (\rho \bar{u}) + \frac{\partial}{\partial y} (\rho \bar{v}) + \frac{\partial}{\partial z} (\rho \bar{w}) = 0 \tag{2.2.4}$$

where $\bar{u}, \bar{v}, \bar{w}$ are the velocity components and F_x, F_y, F_z are the body forces along the x, y, z coordinate directions respectively, ρ is the density of air, ν is the kinematic viscosity, $\mathbf{V} = i\bar{u} + j\bar{v} + k\bar{w}$ is the velocity vector and $\nabla = i \frac{\partial}{\partial x} + j \frac{\partial}{\partial y} + k \frac{\partial}{\partial z}$ is the gradient operator.

Assuming viscosity to be constant and neglecting the effects of body forces, equations (2.2.1) through (2.2.3) reduce to

$$\begin{aligned}
\frac{\partial \bar{u}}{\partial t} + \bar{u} \frac{\partial \bar{u}}{\partial x} + \bar{v} \frac{\partial \bar{u}}{\partial y} + \bar{w} \frac{\partial \bar{u}}{\partial z} &= -1/\rho \frac{\partial p}{\partial x} + \nu \left[\frac{\partial^2 \bar{u}}{\partial x^2} + \frac{\partial^2 \bar{u}}{\partial y^2} + \frac{\partial^2 \bar{u}}{\partial z^2} \right]
\end{aligned}
\tag{2.2.5}$$

$$\frac{\partial \bar{v}}{\partial t} + \bar{u} \frac{\partial \bar{v}}{\partial \bar{x}} + \bar{v} \frac{\partial \bar{v}}{\partial \bar{y}} + \bar{w} \frac{\partial \bar{v}}{\partial \bar{z}} = -1/\rho \frac{\partial \bar{p}}{\partial \bar{y}} + \nu \left[\frac{\partial^2 \bar{v}}{\partial \bar{x}^2} + \frac{\partial^2 \bar{v}}{\partial \bar{y}^2} + \frac{\partial^2 \bar{v}}{\partial \bar{z}^2} \right] \quad (2.2.6)$$

$$\frac{\partial \bar{w}}{\partial t} + \bar{u} \frac{\partial \bar{w}}{\partial \bar{x}} + \bar{v} \frac{\partial \bar{w}}{\partial \bar{y}} + \bar{w} \frac{\partial \bar{w}}{\partial \bar{z}} = -1/\rho \frac{\partial \bar{p}}{\partial \bar{z}} + \nu \left[\frac{\partial^2 \bar{w}}{\partial \bar{x}^2} + \frac{\partial^2 \bar{w}}{\partial \bar{y}^2} + \frac{\partial^2 \bar{w}}{\partial \bar{z}^2} \right] \quad (2.2.7)$$

Non-dimensionalizing equations (2.2.4) through (2.2.7) with following normalization

$$\begin{aligned} \bar{x} &= x/l & \bar{u} &= \hat{u}/U_i \\ \bar{y} &= y/b & \bar{v} &= (\bar{v}l)/(U_i b) \\ \bar{z} &= z/h & \bar{w} &= (\bar{w}l)/(U_i h) \\ \bar{p} &= p/p_a \end{aligned} \quad (2.2.8)$$

In above normalization l and U_i are the characteristic length and velocity in the web arc direction, h is the air film thickness and p_a is the ambient pressure. A mathematical justification for choosing normalized expressions for \bar{v} & \bar{w} as cited above is given in Appendix A. Substituting these normalized quantities into equations (2.2.5) through (2.2.7) and then neglecting higher order terms of ratio of the film thickness h to the characteristic length l (see Appendix B), we obtain

$$(h^2 p_a) / (\mu U_i l) \frac{\partial P}{\partial X} = -\frac{\partial}{\partial Z} - \frac{U}{Z^2} \quad (2.2.9)$$

$$(h^2 p_a l) / (\mu b^2 U_i) \frac{\partial P}{\partial Y} = \frac{\partial}{\partial Z} - \frac{U}{Z^2} \quad (2.2.10)$$

$$\frac{\partial P}{\partial Z} = 0 \quad (2.2.11)$$

Transforming these normalized equations back into dimensional form yields

$$\frac{\partial p}{\partial x} = \mu \frac{\partial}{\partial z} - \frac{\bar{u}}{z^2} \quad (2.2.12)$$

$$\frac{\partial p}{\partial y} = \mu \frac{\partial}{\partial z} - \frac{\bar{v}}{z^2} \quad (2.2.13)$$

$$\frac{\partial p}{\partial z} = 0 \quad (2.2.14)$$

Equation (2.2.14) tells us that pressure along z-direction is constant, i.e. there is no significant hydrostatic variation in pressure across the film thickness. While equations (2.2.12) & (2.2.13) after double integration give us following expressions for velocity components \bar{u} & \bar{v}

$$\bar{u} = 1/(2\mu) \frac{\partial p}{\partial x} z^2 + C_1 z + C_2 \quad (2.2.15a)$$

$$\bar{v} = 1/(2\mu) \frac{\partial p}{\partial y} z^2 + C_3 z + C_4 \quad (2.2.15b)$$

Let us first assume that the roller is stationary and the web is moving with a speed U_w in x-direction. Applying appropriate boundary conditions at the web and roller surfaces we get following expressions for velocity

$$\bar{u} = z/(2\mu) \frac{\partial p}{\partial x} (z-h) + (U_w z)/h \quad (2.2.16a)$$

$$\bar{v} = z/(2\mu) \frac{\partial p}{\partial y} (z-h) + (V_w z)/h \quad (2.2.16b)$$

where V_w is the speed of web in the spanwise direction.

The surface velocities are shown in Figure 5 which also shows the lubricant flow channel of the problem. Now replacing velocity component \bar{w} in the continuity equation (2.2.4) by

$$\bar{w} = \frac{\partial h}{\partial t} \quad (2.2.17)$$

we get

$$\frac{\partial p}{\partial t} + \frac{\partial}{\partial x}(\rho \bar{u}) + \frac{\partial}{\partial y}(\rho \bar{v}) + \frac{\partial}{\partial z}(\rho \frac{\partial h}{\partial t}) = 0 \quad (2.2.18)$$

Integrating the above equation with respect to z from 0 to h , we get

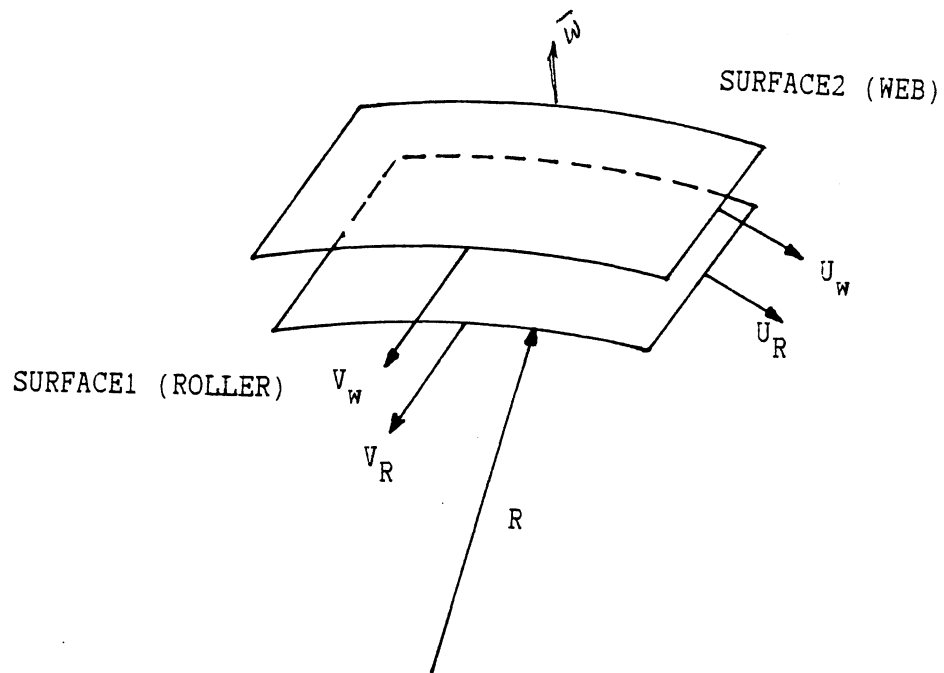


Figure 5. Air Film Flow Channel

$$\int_0^h \frac{\partial}{\partial x} (\rho \bar{u}) dz + \int_0^h \frac{\partial}{\partial y} (\rho \bar{v}) dz + \frac{\partial}{\partial t} (\rho h) = 0 \quad (2.2.19)$$

Substituting velocity components from equations (2.2.16a) & (2.2.16b) into the above equation and then applying Leibnitz's rule we obtain following equation (see Appendix C).

$$\begin{aligned} \frac{\partial}{\partial x} [(\rho h^3)/\mu \frac{\partial p}{\partial x}] + \frac{\partial}{\partial y} [(\rho h^3)/\mu \frac{\partial p}{\partial y}] &= 6 \frac{\partial}{\partial x} [\rho U_w h] + 6 \frac{\partial}{\partial y} [\rho V_w h] \\ &+ 12 \frac{\partial}{\partial t} [\rho h] \end{aligned} \quad (2.2.20)$$

The above equation may be written in a general form as

$$\nabla \cdot \left\{ (\rho h^3)/\mu \nabla p \right\} = 6 \left\{ \nabla \cdot (\rho h U) \right\} + 12 \frac{\partial}{\partial t} \{ \rho h \} \quad (2.2.21)$$

where

$$\nabla = i \frac{\partial}{\partial x} + j \frac{\partial}{\partial y}$$

and,

$$U = i U_w + j V_w$$

This is the hydrodynamic lubrication equation applicable for the motion of a web over an isolated roller. This is a general unsteady lubrication equation that includes the web motion along both the arc of the web and axis of the roller.

Now if we assume that the roller is rotating with certain speed along with the motion of the web then we



2-D Reynolds = η_0

obtain an equation similar to equation (2.2.17) with U_w & V_w being replaced by sum of web and roller speeds in x & y directions, respectively. Mathematically, for this case, velocity vector will be

$$U = i(U_w + U_r) + j(V_w + V_r)$$

2.2.2 Web Equilibrium Equation

In order to determine the position of the web relative to the roller, an equation relating the displacement of the web to the applied tension is required. Such an equation is termed the equilibrium equation.

We assume that the web is bent into a cylindrical shell with an added deformation due to anticlastic bending. Deviations caused by the anticlastic effects and the tension variation in the web arc direction will be assumed to be small, i.e. of the same order of magnitude as the web thickness. Under these assumptions we can apply the theory of thin cylindrical shells under small deformations with an additional study of bending stresses caused by bending of the web while wrapping around the roller. It is further assumed that the web resists lateral loads by the action of bending and transverse shear stresses.

Let us assume that a cartesian coordinate system x, y, z has been defined on the middle surface of the web and cut an element from the web by cutting along two pairs of

adjacent coordinate lines as shown in Figure 6. The cuts are made so that the four sides of the web element of dimensions dx , dy are normal to the middle surface of the web. Such an element of thickness dz has been shaded in Figure 7 which also shows various stresses acting on the web. Because of the curvature of the web in the x -coordinate direction, the length of the web element is not simply dx but

$$dx\left\{\frac{(r_x + z)}{r_x}\right\} \equiv dx\left\{1 + \frac{z}{r_x}\right\}$$

where r_x is the principal radius of curvature in the web motion direction, z is the distance from the middle surface. The normal force transmitted through this element will be

$$\sigma_y dx \left\{ \frac{(r_x + z)}{r_x} \right\} dz$$

The total normal force acting on area $(dx t)$ may be found by integrating the above expression between the limits $-t/2$ to $t/2$. Now Figure 8 shows a web element with various forces and moments acting on it. N_x & N_y are the normal forces, N_{xy} & N_{yx} are the shearing forces, Q_x & Q_y are the transverse forces, M_x & M_y are the moments, M_{yx} & M_{xy} are the twisting moments (These forces and moments

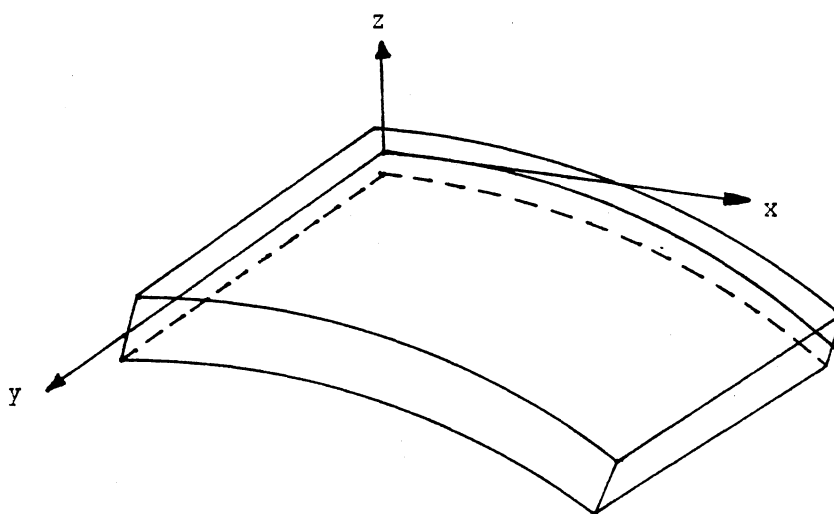


Figure 6. Cartesian Coordinate System on Web

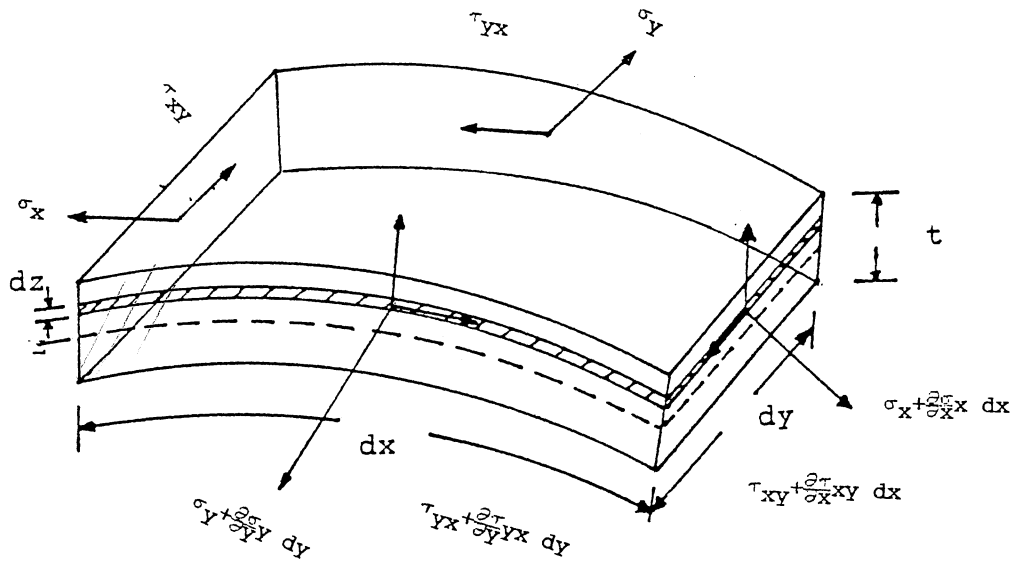


Figure 7. Element of Web with Various Stresses

$dx \rightarrow$

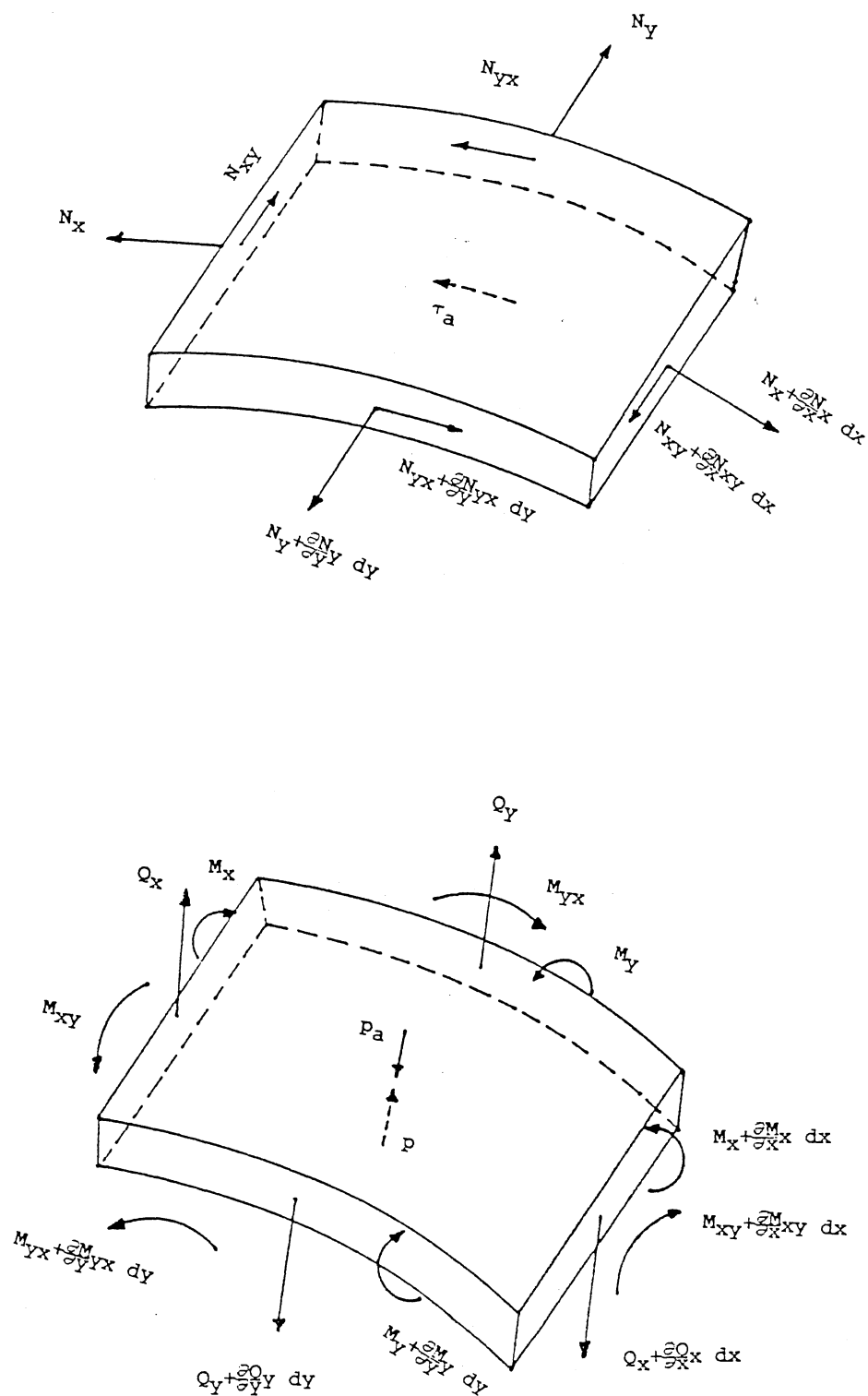


Figure 8. Element of Web with Various Forces and Moments

are all on a per unit length basis). Referring to this figure the total normal force acting on the element in y-coordinate direction is $N_y dx$. This force must be equal to the force obtained by integrating the above expression across the thickness. Equating these two and dropping out dx from both sides we get

$$N_y = \int_{-t/2}^{t/2} \sigma_y(r_x + z)/r_x dz \quad (2.2.22)$$

In the same way the shearing stresses τ_{yx} & τ_{yz} must be integrated to obtain the shearing force N_{yx} and the transverse force Q_y respectively.

$$N_{yx} = \int_{-t/2}^{t/2} (\tau_{yx}(r_x + z)/r_x) dz \quad (2.2.23)$$

$$Q_y = - \int_{-t/2}^{t/2} \tau_{yz}(r_x + z)/r_x dz \quad (2.2.24)$$

The negative sign with the equation for the shear stress resultant Q_y stipulates that a positive transverse

force shall have a direction opposite to its corresponding shear stress. An analysis similar to above leads us to evaluate three more force equations, N_x , N_{xy} , Q_x , for the remaining three stress resultants. These equations are cited in Appendix D.

When the stresses within the element are not distributed uniformly across the thickness of the web, some of them have moments with respect to the center of the section. Since these moments influence the equilibrium of the web element, we must consider them. The non-uniformity of shear stress τ_{ij} , across the thickness results in their resultant lying anywhere in the plane of the cross-section and has a moment with respect to an axis which is normal to the section and passes through the center of the line element d_j . The moments, due to stresses shown in Figure 7, are defined in Appendix D. The negative signs with these equations are arbitrarily chosen.

From the equations defined in Appendix D it can be seen that $\tau_{xy} = \tau_{yx}$ does not imply that shear forces N_{xy} & N_{yx} are same. The only condition that makes them equal is when $r_x = r_y$. Since in our case the thickness of the web is very small as compared to the principal radii of curvature along both x & y -coordinate directions, the difference between N_{xy} & N_{yx} will be small and can be safely neglected. Also note from the moment equations

that the moments are not zero when stresses are independent of z , i.e. stresses uniformly distributed across the thickness. This is so because we are considering curvatures in both x & y -coordinate directions. Also note that transverse shearing stresses τ_{xz} & τ_{yz} do not lead to moments.

In our problem, for a certain finite angle of wrap of the web, there always exists curvature in the x -coordinate direction, whose radius value depends upon the angle of wrap of the web. But for the y -coordinate direction, even if the side leakages are not negligible, the radius of curvature is very large, therefore, the term $(r_y + z)/r_y$ approaches unity. With this condition general equations of Appendix D reduce to equations of Appendix E which will be used in developing the web equilibrium equation.

Equilibrium Equation The force and moments defined above have to satisfy six conditions of equilibrium, three of them concerning the force components and the other three concerning the moments. Referring to Figure 7 and applying the condition of force equilibrium in the y -coordinate direction we have

$$\left\{ \sigma_y + \frac{\partial \sigma}{\partial y} y \, dy \right\} dx \left\{ (r_x + z)/r_x \right\} dz - \sigma_y dx \left\{ (r_x + z)/r_x \right\} dz +$$

$$\left\{ \tau_{xy} + \frac{\partial \tau}{\partial x} xy \, dx \right\} dy \, dz - \tau_{xy} dy \, dz = 0$$

or,

$$\frac{\partial T}{\partial X}xy + \frac{\partial \sigma}{\partial Y}Y\{(r_x + z)/r_x\} = 0 \quad (2.2.25)$$

Integrating the above equation and then applying Leibnitz's rule we get the following force equilibrium equation for the y-coordinate direction (Refer to Appendix F)

$$\frac{\partial N}{\partial X}xy + \frac{\partial N}{\partial Y}Y = 0 \quad (2.2.26)$$

A similar force balancing in both the x & z-coordinate directions gives us the remaining two force equilibrium equations. These are

$$\frac{\partial N}{\partial X}x + \frac{\partial N}{\partial Y}Yx + Q_x \frac{\partial^2 w}{\partial X^2} = 0 \quad (2.2.27)$$

$$\frac{\partial O}{\partial X}x + \frac{\partial O}{\partial Y}Y = 0 \quad (2.2.28)$$

In equation (2.2.27) the last term on the left hand side represents the contribution of the transverse shear force Q_x due to the curvature of the web along its arc length; w is the radial displacement of the web. The above three equations are developed by balancing the forces obtained by integrating stresses across the thickness of the web. Besides such forces, there are some external

forces acting on the web which should be considered for the true equilibrium of the web. These forces, some of which are shown in Figure 8, are as follows:

1. Shearing force on the web due to presence of air film beneath it; τ_a . (Due to No-slip condition),

2. A net force due to the pressure in the air film and the ambient pressure; $(p - p_a)$.



3. Hoop force due to the curvature of the web. This force affects the equilibrium equation of the normal shear force (Flugge (8)).

4. Centrifugal force due to the motion of the web over a supporting roller.

The addition of these forces to the equilibrium equations result in the following modified set of equilibrium equations

$$\frac{\partial N}{\partial X}x + \frac{\partial N}{\partial Y}yx + Q_x \frac{\partial^2}{\partial X^2} - W^2 - \tau_a = 0 \quad (2.2.29)$$

$$\frac{\partial N}{\partial X}xy + \frac{\partial N}{\partial Y}y = 0 \quad (2.2.30)$$

$$\frac{\partial Q}{\partial X}x + \frac{\partial Q}{\partial Y}y - (p - p_a) + \frac{\partial^2}{\partial X^2} - W^2 \sigma U_w - \frac{\partial^2}{\partial X^2} N_x = 0 \quad (2.2.31)$$

The fourth term on the left hand side of the last equation is the term due to centrifugal force which causes the tension in the web to be reduced. If T_0 is

the tension in the web then the reduced tension will be $(T_0 - \sigma U_w^2)$, where σ is the mass per unit area of the web. The term $\frac{\partial^2 w}{\partial x^2}$ in the equilibrium equations represents the effects of the curvature in the web motion direction, w , as mentioned earlier, is the radial displacement of the web (see Figure 9).

The equations of equilibrium concerning the moments may be derived in a fashion similar to the derivation of force equilibrium equations. These moment equilibrium equations are

$$\frac{\partial M}{\partial x} + \frac{\partial M}{\partial y} - Q_x = 0 \quad (2.2.32)$$

$$\frac{\partial M}{\partial x} + \frac{\partial M}{\partial y} - Q_y = 0 \quad (2.2.33)$$

Since the transverse shearing stresses τ_{xz} & τ_{yz} do not lead to moments, only two equations concerning the moments could be derived. Now since the force and moment equilibrium equations contain more unknowns than the number of equations, the problem is indeterminate, and it is necessary to study the deformation of the web.

Web Deformation Since most webs are thin we establish simple kinematic relations of deformation based on thin shell or thin plate theory. This may be done in two different ways. We may start with the fundamental equations

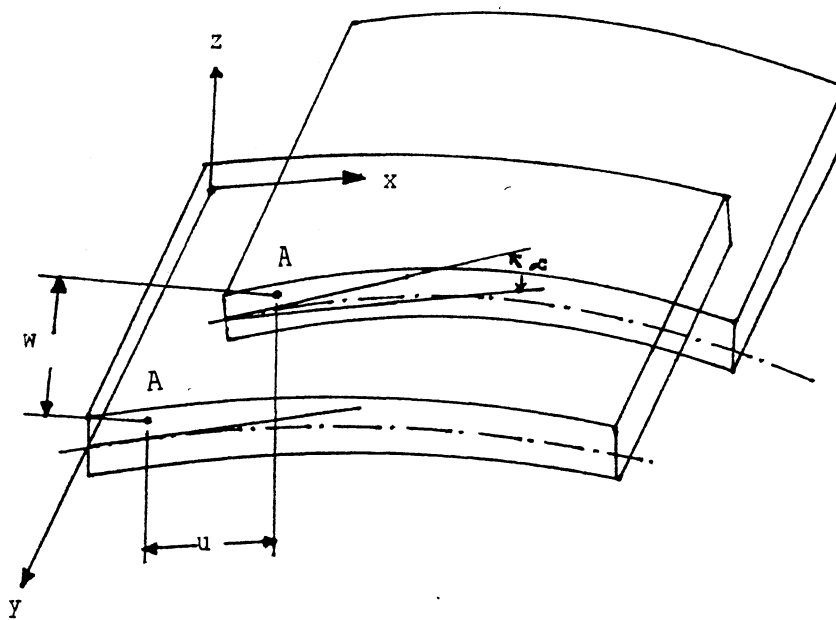


Figure 9. Deflections and Rotations of Web

of three-dimensional elasticity and investigate which terms become unimportant when the thickness is made small compared with other dimensions; or we may try to use the basic assumptions and then develop the necessary kinematic relations. We choose the second approach which is more physically intuitive. The basic assumptions which are necessary for our problem of web motion over a supporting roller and which are based on the theory of thin shells or thin plates, are as follows:

1. A lineal element of the web extending through the web thickness, normal to the mid-surface x - y plane, in the unstressed state, on the application of load, undergoes at most a translation and a rotation with respect to the original coordinate system and remains normal to the deformed middle surface.

This assumption may be stated in the following two simple statements:

- 1a. A lineal element through the thickness does not elongate or contract.

- 1b. The lineal element remains straight upon load application.

2. For all kinematic relations the distance z of a point (point A in Figure 9) from the middle surface may be considered as unaffected by the deformation of the web.

3. The web resists lateral and in-plane loads by bending and transverse shear stresses, not through blocklike compression or tension in the thickness

direction. This results in a stress system in which σ_z may be considered negligible compared with σ_x and σ_y .

Applied to the web, the first assumption means that we neglect the deformations due to the transverse shear forces Q_x & Q_y . The second assumption means that whatever happens in the z-direction regarding stress or strain is without significance.

4. In order to keep our equations linear we make an additional assumption. All displacements are small, i.e. they are negligible compared with the principal radii of curvature. Also their first derivatives, i.e. the slopes, are negligible compared with unity.

From these assumptions we establish the kinematic relations of the web. Defining the two in-plane displacements in the most general forms as

$$u = u_0(x,y) + z\alpha(x,y) \quad (2.2.34a)$$

$$v = v_0(x,y) + z\beta(x,y) \quad (2.2.34b)$$

where u_0 & v_0 are middle surface displacements (at $z=0$) and α & β are the rotations and are defined in Figure 9. Assumption (1a) requires that $\epsilon_z = 0$; which means that the lateral deflection w is a function of x & y only. Assumption (1b) requires that for any z , ϵ_{xz} & ϵ_{yz} are

constant at any specific location(x,y) on the web middle surface, for all z. The second part of assumption (1) requires that the constant should be zero; hence

$$\epsilon_{xz} = \epsilon_{yz} = 0 \quad (2.2.35)$$

The stress-strain relationships in terms of displacements are

$$\epsilon_x = \frac{\partial u}{\partial x} = (\sigma_x - \nu\sigma_y)/E \quad (2.2.36)$$

$$\epsilon_y = \frac{\partial v}{\partial y} = (\sigma_y - \nu\sigma_x)/E \quad (2.2.37)$$

$$\gamma_{xy} = \frac{\partial u}{\partial y} + \frac{\partial v}{\partial x} = \tau_{xy}/G \quad (2.2.38)$$

$$\gamma_{xz} = \frac{\partial w}{\partial x} + \frac{\partial u}{\partial z} = \tau_{xz}/G \quad (2.2.39)$$

$$\gamma_{yz} = \frac{\partial v}{\partial z} + \frac{\partial w}{\partial y} = \tau_{yz}/G \quad (2.2.40)$$

where ϵ 's are the normal strain, γ 's are the shear strains, E is the modulus of elasticity, ν is the Poisson's ratio and $G = E/(2(1+\nu))$ is the shear modulus. Now the condition of $\epsilon_{xz} = \epsilon_{yz} = 0$ implies that

$$\frac{\partial u}{\partial z} = - \frac{\partial w}{\partial x} \quad (2.2.41a)$$

and,

$$\frac{\partial v}{\partial z} = - \frac{\partial w}{\partial y} \quad (2.2.41b)$$

Using equation (2.2.34), we may write

$$\alpha = - \frac{\partial w}{\partial x} \quad (2.2.42a)$$

$$\beta = - \frac{\partial w}{\partial y} \quad (2.2.42b)$$

$$\frac{\partial u}{\partial x} = \frac{\partial u}{\partial x} + z \frac{\partial \alpha}{\partial x} \quad (2.2.42c)$$

and,

$$\frac{\partial v}{\partial y} = \frac{\partial v}{\partial y} + z \frac{\partial \beta}{\partial y} \quad (2.2.42d)$$

Using above expressions, equation (2.2.36) simplifies to

$$\frac{\partial u}{\partial x} + z \frac{\partial \alpha}{\partial x} = (\sigma_x - \nu \sigma_y) / E \quad (2.2.43)$$

Multiplying the above equation by z and then integrating across the thickness yields

$$\int_{-t/2}^{t/2} z \frac{\partial u}{\partial x} dz + \int_{-t/2}^{t/2} z^2 \frac{\partial \alpha}{\partial x} dz = \int_{-t/2}^{t/2} \{ (\sigma_x - \nu \sigma_y) / E \} z dz \quad (2.2.44)$$

It was mentioned earlier that the principal radius of curvature r_x is very large compared to thickness of the web, thus we may disregard the terms z/r_x from the

equations of Appendix E. Applying Leibnitz's rule and substituting appropriate expression for the resulting integral, the above equation may be written as

$$-\frac{\partial^2}{\partial Y^2} \frac{W}{X^2} \left[t^3/12 \right] = - (M_X - \nu M_Y)/E \quad (2.2.45)$$

A similar analysis with equations (2.2.37) & (2.2.38) result in the following equations

$$-\frac{\partial^2}{\partial X^2} \frac{W}{Y^2} \left[t^3/12 \right] = - (M_Y - \nu M_X)/E \quad (2.2.46)$$

$$-\frac{\partial^2}{\partial X \partial Y} \frac{W}{Y} \left[t^3/6 \right] = - M_{XY}/G \quad (2.2.47)$$

Solving equations (2.2.45) & (2.2.46) we get the following equations for moments as a function of web deviation from the roller, w.

$$M_X = D \left[\frac{\partial^2}{\partial Y^2} \frac{W}{X^2} + \nu \frac{\partial^2}{\partial X^2} \frac{W}{Y^2} \right] \quad (2.2.48)$$

$$M_Y = D \left[\frac{\partial^2}{\partial X^2} \frac{W}{Y^2} + \nu \frac{\partial^2}{\partial Y^2} \frac{W}{X^2} \right] \quad (2.2.49)$$

where $D = (Et^3)/(12(1-\nu^2))$ is the flexure rigidity of the web material. Equation (2.2.47) may be written as

$$M_{xy} = \left[(Et^3)/(12(1+\nu)) \right] \frac{\partial^2 w}{\partial x \partial y} \quad (2.2.50)$$

A similar approach may be adopted to obtain the equations for normal and shear forces.

$$N_x = \left\{ (Et)/(1-\nu^2) \right\} \left[\frac{\partial u_0}{\partial x} + \nu \frac{\partial v_0}{\partial y} \right] \quad (2.2.51)$$

$$N_y = \left\{ (Et)/(1-\nu^2) \right\} \left[\frac{\partial v_0}{\partial y} + \nu \frac{\partial u_0}{\partial x} \right] \quad (2.2.52)$$

$$N_{xy} = \left\{ (Et)/2(1+\nu) \right\} \left[\frac{\partial u_0}{\partial y} + \nu \frac{\partial v_0}{\partial x} \right] \quad (2.2.53)$$

The above equations (in which u_0 & v_0 are the middle surface displacements not attributed to tension T_0) describe only the in-plane force and deformation behavior. The inclusion of tension along the web arc direction results in the following modified set of force equations:

$$N_x = \left\{ (Et)/(1-\nu^2) \right\} \left[\frac{\partial u_0}{\partial x} + \nu \frac{\partial v_0}{\partial y} \right] + T_0 \quad (2.2.54)$$

$$N_y = \left\{ (Et)/(1-\nu^2) \right\} \left[\frac{\partial v_0}{\partial y} + \nu \frac{\partial u_0}{\partial x} \right] + \nu T_0 \quad (2.2.55)$$

$$N_{xy} = \left\{ (Et)/(2(1+\nu)) \right\} \left[\frac{\partial u_0}{\partial y} + \frac{\partial v_0}{\partial x} \right] \quad (2.2.56)$$

Equations (2.2.31) through (2.2.33) and equations (2.2.48) through (2.2.50) are the governing equations for the lateral deflections, bending and shearing action of the web element, while equations (2.2.29), (2.2.30) & equations (2.2.54) through (2.2.56) are the governing equations for the in-plane stress resultants and in-plane mid-surface displacements. In order to relate these eleven equations to a differential equation that governs the equilibrium of the web, it is necessary to define the shape of the air film between the web and the roller. From the basic geometry of the problem we have a condition that far from the roller the air film thickness is comparable with the radius of the roller R and the pressure there approaches the ambient pressure. In this region the air film shape is assumed to be parabolic. The parabolic film assumption is expected to provide satisfactory results for our web handling applications as it does for various pertinent applications (like gear teeth meshing and slider bearings which support the magnetic elements used for memory devices, etc). Mathematically, the air film in this region is approximated by

$$h = x^2/(2R) + w(x,y) \quad (2.2.57)$$

where $w(x,y)$ is the radial displacement of the web (see Figure 9). A mathematical proof of approximating

parabolic film assumption for a foil bearing is given by W.A.Gross (3). From equation (2.2.57) we may write

$$\frac{\partial^2 w}{\partial x^2} = \frac{\partial^2 h}{\partial x^2} - 1/R \quad (2.2.58)$$

$$\frac{\partial^2 w}{\partial y^2} = \frac{\partial^2 h}{\partial y^2} \quad (2.2.59)$$

This parabolic film approximation will be used in reducing the governing equations to a differential equation for the web equilibrium. Differentiating equation (2.2.32) with respect to x and equation (2.2.33) with respect to y and substituting the resulting equations in equation (2.2.31) we obtain

$$\frac{\partial}{\partial x} \left[\frac{\partial M}{\partial x^2} \right] + 2 \frac{\partial}{\partial x} \frac{\partial M}{\partial x \partial y} + \frac{\partial}{\partial y} \left[\frac{\partial M}{\partial y^2} \right] - (p - p_a) + \sigma U_w \frac{\partial^2 w}{\partial x^2} - N_x \frac{\partial^2 w}{\partial x^2} = 0 \quad (2.2.60)$$

Double differentiation of equations (2.2.48), (2.2.49), & (2.2.50) with respect to x , y , and x and y , respectively and substituting the expression for $\frac{\partial^2 w}{\partial y^2}$ from equation (2.2.59) we obtain the following equations

$$\frac{\partial^2}{\partial X^2} \left[\frac{\partial^2}{\partial X^2} \frac{M}{X^2} \right] = D \left[\frac{\partial^4}{\partial X^4} W + \nu \frac{\partial^4}{\partial X^2 \partial Y^2} h \right] \quad (2.2.61)$$

$$\frac{\partial^2}{\partial Y^2} \left[\frac{\partial^2}{\partial Y^2} M \right] = D \left[\frac{\partial^4}{\partial Y^4} h + \nu \frac{\partial^4}{\partial X^2 \partial Y^2} h \right] \quad (2.2.62)$$

$$\frac{\partial^2}{\partial X \partial Y} M_{XY} = \left\{ (Et^3)/(12(1+\nu)) \right\} \left[\frac{\partial^4}{\partial X^2 \partial Y^2} h \right] \quad (2.2.63)$$

Substituting the above equations and the equation for N_X in equation (2.2.60) we obtain

$$\begin{aligned} & D \left[\frac{\partial^4}{\partial X^4} W + \nu \frac{\partial^4}{\partial X^2 \partial Y^2} h + \frac{\partial^4}{\partial Y^4} h + \nu \frac{\partial^4}{\partial X^2 \partial Y^2} h \right] + \\ & 2 \left\{ (Et^3)/(12(1+\nu)) \right\} \frac{\partial^4}{\partial X^2 \partial Y^2} h - (p-p_a) + \sigma U_w \frac{\partial^2}{\partial X^2} W - \\ & \frac{\partial^2}{\partial X^2} W \left[(Et)/(1-\nu^2) \left\{ \frac{\partial u_0}{\partial X} + \nu \frac{\partial v_0}{\partial Y} \right\} + T_0 \right] = 0 \end{aligned}$$

or,

$$\begin{aligned} & \left\{ (Et^3)/(12(1-\nu^2)) \right\} \left[\frac{\partial^4}{\partial X^4} W + \frac{\partial^4}{\partial Y^4} h + 2 \frac{\partial^4}{\partial X^2 \partial Y^2} h \right] - (p-p_a) + \\ & \sigma U_w \frac{\partial^2}{\partial X^2} W - \frac{\partial^2}{\partial X^2} W \left[(Et)/(1-\nu^2) \left\{ \frac{\partial u_0}{\partial X} + \nu \frac{\partial v_0}{\partial Y} \right\} + T_0 \right] = 0 \end{aligned} \quad (2.2.64)$$

From assumption (4) it may be inferred that the normal force N_x due to displacement alone is negligible compared to that due to the tension in the web. This leads to a simplified form of the above equation.

$$\left\{ (Et^3)/(12(1-\nu^2)) \right\} \left[\frac{\partial^4 w}{\partial x^4} + \frac{\partial^4 h}{\partial y^4} + 2 \frac{\partial^2 w}{\partial x^2} \frac{\partial^2 h}{\partial y^2} \right] - (p-p_a) + \sigma U_w \frac{\partial^2 w}{\partial x^2} - T_O \frac{\partial^2 w}{\partial x^2} = 0 \quad (2.2.65)$$

Substituting the expression for $\frac{\partial^2 w}{\partial x^2}$ from equation (2.2.58) in the above equation we obtain

$$\left\{ (Et^3)/(12(1-\nu^2)) \right\} \left[\frac{\partial^4 h}{\partial x^4} + 2 \frac{\partial^2 h}{\partial x^2} \frac{\partial^2 h}{\partial y^2} + \frac{\partial^4 h}{\partial y^4} \right] - (p-p_a) + \left\{ \frac{\partial^2 h}{\partial x^2} - 1/R \right\} [\sigma U_w - T_O] = 0$$

or,

$$\left\{ (Et^3)/(12(1-\nu^2)) \right\} [\vartheta^2 \vartheta^2 h] - (p-p_a) + \left\{ \frac{\partial^2 h}{\partial x^2} - 1/R \right\} [\sigma U_w - T_O] = 0 \quad (2.2.66)$$

where ϑ^2 is given by

$$\nabla^2 = \frac{\partial^2}{\partial X^2} + \frac{\partial^2}{\partial Y^2}$$

The above equation is the general equilibrium equation for a thin web. This equation and equation (2.2.21), together with the appropriate boundary conditions, describe the system of web motion over a supporting roller. It is important to examine equation (2.2.66) when $R \rightarrow \infty$. For this condition it becomes the equation of an infinitely wide plate under tension. The first term in equation (2.2.66) expresses the flexibility of the web; the third term, which is the result of tension in the web, usually dominates in most web handling applications. The first term may become predominant when the web material is such that the elastic deformation has to be taken into account. It is also interesting to note that this equation is similar to the one derived by E.J Barlow (9) for a foil bearing problem. The only difference is the additional term in the equation of Barlow which expresses the curvature of the foil in the foil width direction and which is the cause for the non-linearity of the partial differential equation. Without this term equations for normal forces (N_x & N_y) are simply that of a thin plate under tension. One important conclusion from this comparison is that the resulting web equilibrium equation will be non-linear if the radius of curvature in the web width is not very large compared to the radius of curvature in the web length direction.

Physically, this is possible when side leakages are considerable.

Determination of the air film thickness between the web and the roller requires the simultaneous solution of the Reynolds lubrication equation and the web equilibrium equation.

2.3 Governing Differential Equation

We make certain assumptions based upon physical analysis of the problem. Since in most web handling applications, the width of the web is much greater than the air film thickness, we may neglect the end effects. This assumption reduces the Reynolds lubrication equation (equation (2.2.21)) to a one-dimensional ordinary differential equation. Since the pressure developed in the air film is expected not to be significant, we will initially assume the air to be incompressible. These two assumptions along with the previously made assumption of constant viscosity reduce equation (2.2.21) to

$$\frac{d}{dx} \left\{ h^3 \frac{dp}{dx} \right\} = 6\mu U \frac{dh}{dx} \quad (2.3.1)$$

where U is the algebraic sum of the velocity of the web and the roller. As discussed in the last section, since the web material in most web handling applications is very thin, the bending term in the equilibrium equation may

be neglected compared to the term due to the tension (Ref. Timoshenko(10)). The resulting equilibrium equation will be that for a perfectly flexible web and may be written as

$$p - p_a = \left\{ \frac{d}{d} - \frac{h}{x^2} \right\}^2 [\sigma U_w - T_0] \quad (2.3.2)$$

Let T be defined as the reduced tension;

$$T = T_0 - \sigma U_w \quad (2.3.3)$$

Since the mass per unit area of the web (i.e. σ) is very small, the difference between the tension T_0 and the reduced tension T will not be significant. However, the difference may be significant at high web speeds. Now equation (2.3.2) may be written as

$$p - p_a = T \left\{ 1/R - \frac{d}{d} - \frac{h}{x^2} \right\}^2$$

or,

$$p - p_a = (T/R) \left\{ 1 - R \frac{d}{d} - \frac{h}{x^2} \right\}^2 \quad (2.3.4)$$

Now integrating equation (2.3.1) we get

$$h^3 \frac{dp}{dx} = 6\mu U(h-h_0) \quad (2.3.5)$$

where h_0 is the constant of integration and defines the film thickness at the point where $\frac{dp}{dx} = 0$. Now differentiating equation (2.3.4) with respect to x we get

$$\frac{dp}{dx} = (T/R) \left\{ -R \frac{d^3 h}{dx^3} \right\}$$

or,

$$\frac{dp}{dx} = -T \frac{d^3 h}{dx^3} \quad \checkmark \quad (2.3.6)$$

Eliminating the pressure gradient term by combining equations (2.3.5) & (2.3.6) we get

$$\frac{d^3 h}{dx^3} = \frac{12\mu U}{T} \left\{ \frac{(h_0 - h)}{h^3} \right\} \quad \checkmark \quad (2.3.7)$$

Let us define a normalized film thickness as

$$H = h/h_0 \quad \checkmark \quad (2.3.8)$$

Substituting equation (2.3.8) in equation (2.3.7)

$$h_0 \frac{d^3 H}{dx^3} = \left\{ \frac{6\mu U h_0}{T h_0^3} \right\} \left[\frac{(1-H)}{H^3} \right] \quad \checkmark$$

or,

$$\left\{ \frac{T h_0^3}{6\mu U} \right\} \frac{d^3 H}{dx^3} = \left[\frac{(1-H)}{H^3} \right] \quad \checkmark \quad (2.3.9)$$

Let us now define the normalized x-coordinate as

$$\eta \equiv (x/h_0) \left\{ (6\mu U)/T \right\}^{1/3} \quad (2.3.10a)$$

From this we may write

$$x = (\eta h_0) \left\{ T/(6\mu U) \right\}^{1/3} \quad (2.3.10b)$$

With the above normalization we may write equation

(2.3.9) as

$$\frac{d^3 H}{d\eta^3} = \left[(1-H)/H^3 \right] \quad (2.3.11)$$

This is the governing, third-order non-linear, differential equation, the solution of which will allow us to determine the air-film thickness between the web and roller.

2.4 Pressure Distribution

The pressure profile in the air film may be obtained by considering the equation (2.3.6)

$$\frac{dp}{dx} = -T \frac{d^3 h}{dx^3} \quad (2.4.1)$$

Substituting dimensionless variables from equations (2.3.8) and (2.3.10) in the above equation we may write

$$(h_0/T) \left\{ T/(6\mu U) \right\}^{2/3} \frac{dp}{dr} = - \frac{d^3 H}{dr^3} \quad \checkmark \quad (2.4.2)$$

Let us define a non-dimensional pressure as

$$P = (h_0/T) \left\{ T/(6\mu U) \right\}^{2/3} p \quad (2.4.3)$$

Substituting the above non-dimensional pressure in equation (2.4.2) we obtain

$$\frac{dP}{dr} = - \frac{d^3 H}{dr^3} \quad (2.4.4)$$

This equation may be solved to obtain the pressure distribution. An alternate approach is to use equation (2.3.4)

$$p - p_a = T/R - T \frac{d^2 h}{dx^2}$$

or,

$$p - p_a = T/R - (T/h_0) \left\{ (6\mu U)/T \right\}^{2/3} \frac{d^2 H}{dr^2}$$

which may be written as (after multiplying it by $(h_0/T) \left\{ T/(6\mu U) \right\}^{2/3}$)

$$P - P_a = (h_0/R) \left\{ T/(6\mu U) \right\}^{2/3} - \frac{d^2 H}{dr^2}$$

using equation (3.2.1) the above equation may be written as

$$P - P_a = \left[\frac{d^2 H^2}{\eta^2} \right]_{\eta \rightarrow \infty} - \frac{d^2 H^2}{\eta^2} \quad (2.4.5)$$

where P is the non-dimensional pressure in the air film given by equation (2.4.3) and P_a is the non-dimensional ambient pressure, given by

$$P_a = (h_0/T) \{ T / (6\mu U) \}^{2/3} P_a \quad (2.4.6)$$

and the expression for $\left[\frac{d^2 H^2}{\eta^2} \right]_{\eta \rightarrow \infty}$ is derived in section (3.2) (see equation (3.2.1)).

The advantage of using equation (2.4.4) over equation (2.4.5) is that it enables the estimation of air film pressure without knowing the numerical value of $\left[\frac{d^2 H^2}{\eta^2} \right]_{\eta \rightarrow \infty}$.

Now equation (2.4.5) is the normalized form of equation (2.3.4). In this equation the normalized pressure P is defined by equation (2.4.3). The dimensional equation (equation (2.3.4)) can also be transformed into a normalized equation by using the following normalized pressure

$$P_N = p(R/T) \quad (2.4.7)$$

Now equation (2.3.4) may be written as

$$p(R/T) - p_a(R/T) = 1 - R \frac{d^2 h}{dx^2}$$

using normalized equations (2.3.8) & (2.3.10b), the above equation may be written as

$$p(R/T) - p_a(R/T) = 1 - \left[R / \left\{ h_0 (T/6\mu U)^{2/3} \right\} \right] \frac{d^2 H_2}{d\eta^2}$$

which may be simplified to (by using equations (2.4.7) & (3.2.1))

$$P_N - P_{a_N} = 1 - \left\{ \frac{d^2 H_2}{d\eta^2} / \frac{d^2 H_2}{d\eta^2} \right\}_{\eta \rightarrow \infty} \quad (2.4.8)$$

where $P_{a_N} = p_a(R/T)$ is a new non-dimensional ambient pressure.

2.5 Summary of The Simplified Governing Equations

The simplified one-dimensional Reynolds equation is

$$\frac{d}{dx} \left(h^3 \frac{dp}{dx} \right) = 6\mu U \frac{dh}{dx} \quad (2.5.1)$$

and the simplified equilibrium equation of the web is

$$p - p_a = T \left\{ 1/R - \frac{d}{d} \frac{h^2}{x^2} \right\} \quad (2.5.2)$$

The governing differential equation is obtained from combination of the above two equations and by introducing non-dimensional variables $H=h/h_0$ & $\eta=(x/h_0) \left\{ (6\mu U)/T \right\}^{1/3}$

$$\frac{d^3 H}{d\eta^3} = \left[(1-H)/H^3 \right] \quad (2.5.3)$$

The pressure distribution in the air film may be obtained from any of the following three equations

$$\frac{dP}{d\eta} = - \frac{d^3 H}{d\eta^3} \quad (2.5.4)$$

$$P - P_a = \left[\frac{d^2 H}{d\eta^2} \right]_{\eta \rightarrow \infty} - \frac{d^2 H}{d\eta^2} \quad (2.5.5)$$

$$P_N - P_{a_N} = 1 - \left\{ \frac{d^2 H}{d\eta^2} / \left[\frac{d^2 H}{d\eta^2} \right]_{\eta \rightarrow \infty} \right\} \quad (2.5.6)$$

2.6 Qualitative Analysis Based on Governing Equations

Since one of the surfaces (i.e web) of the lubricating channel is flexible, an increase in pressure in the air film will cause an increase in the air gap. But from the simplified form of the Reynolds equation (2.3.5) it can be

seen that an increase in the air gap will result in a decrease in pressure gradient. Thus the result of combining the Reynolds equation and equilibrium equation will always result in a smoothing of the pressure peaks. This, physically, means that for the problem of web motion over a supporting roller, most of the region has constant pressure. The absence of pressure gradient in such a region is possible only when the air film thickness is constant. Such a region is termed the constant gap region or uniformity region and according to equation (2.3.5) has a film thickness h_0 (Figure 10 shows how this region separates the entrance and the exit regions).

In the entrance region the pressure increases from ambient to the pressure in the uniformity region. This requires a positive pressure gradient. We note from the one-dimensional Reynolds equation (2.3.5) that $\frac{dp}{dx}$ is positive only when $h > h_0$ which clearly satisfies the physical situation. A positive pressure gradient is thus compatible with a decrease in the air film from "infinity" to the constant gap film thickness h_0 . (Note that the film thickness at "infinity" refers to film thickness at a point where pressure approaches ambient pressure).

In the exit region the pressure decreases from the constant gap region pressure to ambient while the air film thickness increases from h_0 to some infinity. This requires a negative pressure gradient. But from the Reynolds

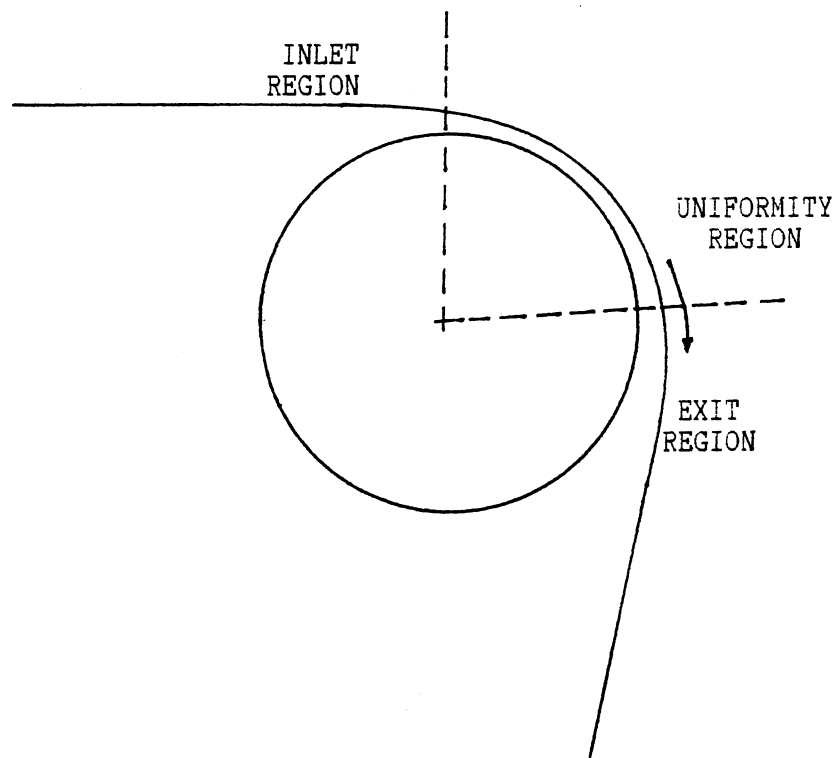


Figure 10. The Three Regions in Web-Roller Interaction

equation (2.3.5) we observe that a negative pressure gradient can exist only if $h < h_0$, which is incompatible with the increasing gap. The increase in film thickness is therefore preceded by a region where $h < h_0$ in which the pressure decreases to below ambient, followed by a region of increasing film thickness and increasing pressure. Thus theoretically it is observed that the air film profile in both inlet and exit regions is different. There is a gradual reduction in air film thickness in the inlet region as we approach uniformity region while there are some oscillations of the web in the exit region which diminish in amplitude as we move towards the exit transition region.

Another conclusion may be obtained by referring equation (2.3.4). Since the web is surrounded by atmospheric pressure in the region far away from the roller, equations (2.3.4) & (2.2.58) show that the radius of curvature must be infinite; that is, the web becomes straight in that region, as is physically correct.

CHAPTER III

SOLUTION OF THE GOVERNING DIFFERENTIAL EQUATION

3.1 Mathematical Description of the Problem

The qualitative analysis of the last chapter leads to the important conclusion that the entrance and the exit regions are separated by a constant gap region and that the air film thickness variation in both the inlet and the exit regions is different.

The derivation of the governing equation (equation (2.3.11)) is based on a coordinate system in which the independent variable η is taken positive in the direction of the web motion. From the coordinate system shown in Figure 11 it may be observed that for a differential equation that defines the air film profile in the inlet region, we have to define the independent variable in the direction opposite to the web motion. The governing differential equation is altered only by a change of sign. In general then, the governing differential equation may be written as

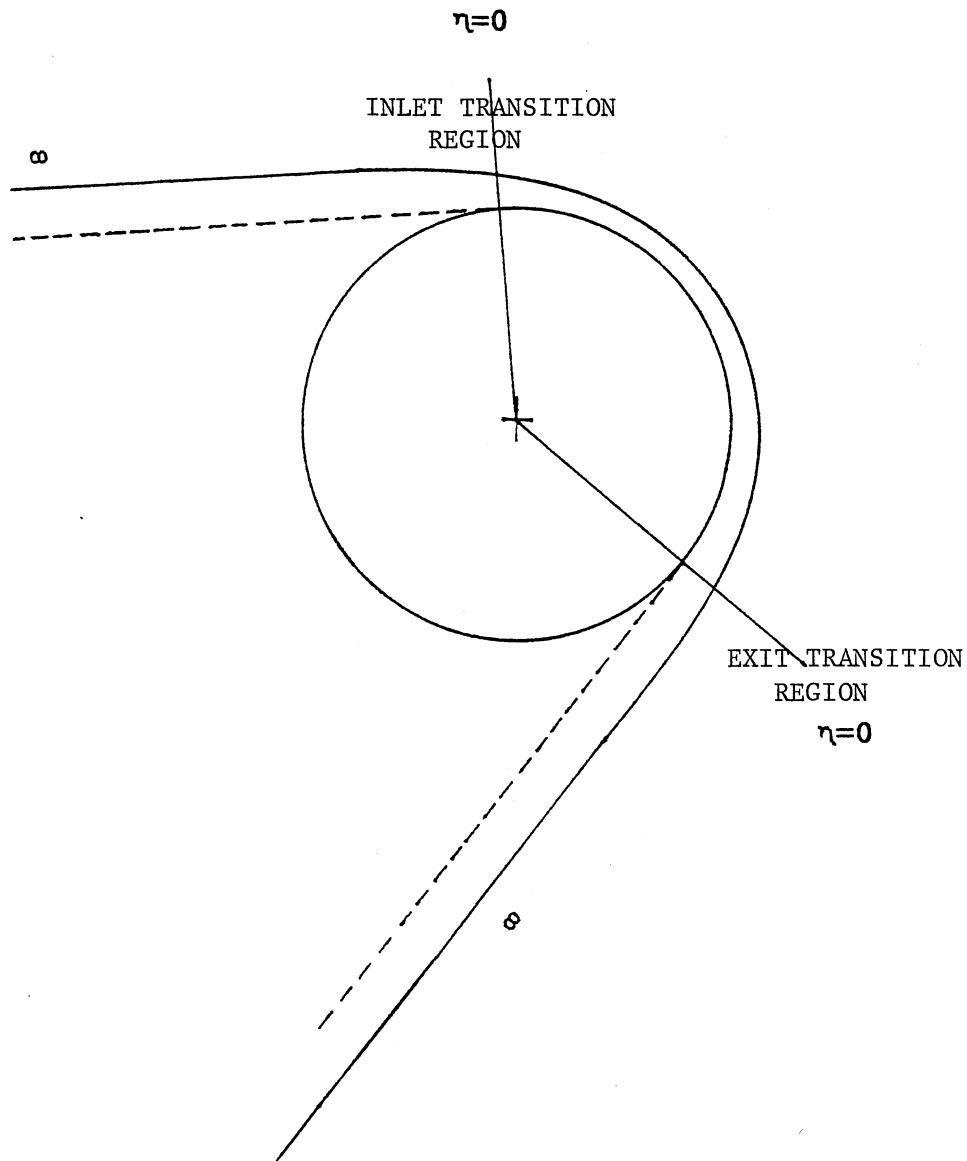


Figure 11. Schematic Representation of Inlet and Exit Transition Regions.

$$\frac{d^3 H}{d\eta^3} = \pm \left\{ (H - 1)/H^3 \right\}$$

or,

$$H''' = \pm \left\{ (H - 1)/H^3 \right\} \quad (3.1.1)$$

where the upper sign applies to the inlet condition while the lower sign applies to the exit condition. The problem is solved in two parts, and it is possible to construct the entire air film thickness variation by integrating equation (3.1.1) outward from the region of uniformity toward the inlet region in one case and the exit region in the other, with appropriate boundary conditions. Observe that the variable η is set equal to zero at the two transition regions for the two separate solutions. The two transition boundaries are located approximately at the points where the tangents to the roller match the given web directions far from the roller. Such tangents are shown in Figure 11. It can be observed from this figure that at the transition points the normalized film thickness H does not necessarily have a value of exactly unity, but is close to unity.

3.2 Boundary Conditions

The appropriate boundary conditions for the present problem will be now developed. Since the web is surrounded by the atmospheric pressure in a region "far" from the

roller, in both the inlet and the exit regions, we have from equation (2.3.4)

$$\left. \frac{d^2 b}{dx^2} \right]_{x \rightarrow \infty} = 1/R$$

where the infinity condition is valid for both the inlet and the exit regions. Using normalized parameters from equations (2.3.8) and (2.3.10b), above condition may be written as

$$\left. \frac{d^2 H}{d\eta^2} \right]_{\eta \rightarrow \infty} = (h_0/R) \left\{ T/(6\mu U) \right\}^{2/3} \quad (3.2.1)$$

The significance of the above equation is that if we know the numerical value of $H''(\infty)$ it enables us to determine the constant gap film thickness, as a function of various dimensional parameters. Equation (3.2.1) may be solved for the constant gap film thickness as

$$h_0 = R \left\{ (6\mu U)/T \right\}^{2/3} \left. \frac{d^2 H}{d\eta^2} \right]_{\eta \rightarrow \infty} \quad (3.2.2)$$

Since $\left. \frac{dw}{dx} \right]_{\eta \rightarrow \infty} = 0$ we may write from equation (2.2.57)

$$\left. \frac{dh}{dx} \right]_{x \rightarrow \infty} = x/R$$

or,

$$\left. \frac{dH}{d\eta} \right]_{\eta \rightarrow \infty} = \eta (h_0/R) \{T/(6\mu U)\}^{2/3}$$

or,

$$\left. \frac{dH}{d\eta} \right]_{\eta \rightarrow \infty} = \eta \left. \frac{d^2 H}{d\eta^2} \right]_{\eta \rightarrow \infty} \quad (3.2.3)$$

Another useful boundary condition is that at the entrance and exit transition regions the film thickness approaches unity; i.e.

$$\left. H \right]_{\eta \rightarrow 0} \simeq 1 \quad (3.2.4)$$

3.3 Numerical Solution

We know that the governing equation is a non-linear, third order differential equation. A practical solution results from a simple linearization. Since near the transition regions the normalized film thickness H is nearly unity, we may write

$$H \simeq 1 + \Delta H \quad (3.3.1)$$

where ΔH is some small quantity. Substituting the above

equation in equation (3.1.1) we get

$$\Delta H'''' = \pm \Delta H$$

or,

$$\Delta H'''' \mp \Delta H = 0 \quad (3.3.2)$$

The solution of this equation is given by

$$\Delta H = C_1 e^{\pm \eta} + e^{\mp \eta/2} \{ C_2 \cos(\sqrt{3} \eta/2) + C_3 \sin(\sqrt{3} \eta/2) \} \quad (3.3.3)$$

where $C_1, C_2,$ & C_3 are constants of integration. The above equation may also be written as

$$\Delta H = C_1 e^{\pm \eta} + C_4 e^{\mp \eta/2} \sin\{\sqrt{3} \eta/2 + C_5\} \quad (3.3.4)$$

where C_4 & C_5 are new constants of integration. This solution of the linearized form of the governing differential equation is essentially valid near the uniformity region where H is nearly unity. The numerical values obtained from the above equation may be further used to provide initial values in the integration of equation (3.1.1) in the region away from the constant gap region where the change in the film thickness is high. Let us now examine the significance of equation (3.3.3)(or equation

(3.3.4)) in obtaining complete solutions in the inlet and the exit region.

3.3.1 Inlet Region Solution

Equation (3.3.3) for the inlet region is

$$\Delta H = C_1 e^{\eta} + e^{-\eta/2} \{ C_2 \cos(\sqrt{3} \eta/2) + C_3 \sin(\sqrt{3} \eta/2) \} \quad (3.3.5)$$

In the uniformity region, η is large and negative. For such a large and negative value of η the first term in equation (3.3.5) becomes very small. Thus the second term will be of the order of ΔH . Since x is of the order of R , η will be of the order of R/h_0 (see equation (2.3.10)), thus e^{R/h_0} times the bracketed term will be of the order of ΔH . Since $R \gg h_0$ (and since ΔH is small quantity) C_2 and C_3 has to be very small so that ΔH will remain bounded at $\eta \rightarrow -\infty$. From these arguments we have anywhere near the inlet transition region

$$\Delta H = C_1 e^{\eta} \quad (3.3.6)$$

so that,

$$\Delta H' = C_1 e^{\eta} \quad (3.3.7)$$

$$\Delta H'' = C_1 e^{\eta} \quad (3.3.8)$$

From equation (3.3.1) we have then

$$H = 1 + C_1 e^\eta \quad (3.3.9)$$

$$H' = C_1 e^\eta \quad (3.3.10)$$

$$H'' = C_1 e^\eta \quad (3.3.11)$$

Equations (3.3.9) through (3.3.11) may be used along with equations (3.3.2) & (3.1.1) to obtain the air film thickness in the inlet region. It is convenient to start integration somewhere in the uniformity region, close to the transition region. Initial values for the inlet solution are chosen by assignment of an arbitrary small value of $C_1 e^\eta$ which determine H and its derivatives from the last three equations. With these initial values the inlet region is integrated until the boundary condition (3.2.3) is satisfied; or until $H'''(\infty)$ differs from zero by a prescribed small number.

3.3.2 Exit Region Solution

Equation (3.3.3) for the exit region is

$$\Delta H = C_1 e^{-\eta} + e^{\eta/2} \{ C_2 \cos(\sqrt{3} \eta/2) + C_3 \sin(\sqrt{3} \eta/2) \} \quad (3.3.12)$$

It is expected that for large and negative η , the

second term is small, so that $C_1 e^{-\eta}$ is of the order of ΔH . In other words, $C_1 e^{R/h_0}$ is of the order of ΔH . In order that ΔH remains bounded at $\eta = -\infty$, C_1 should be very small (since $R \gg h_0$). Thus for the region close to the exit transition region we have

$$\Delta H = e^{\eta/2} \{ C_2 \cos(\sqrt{3} \eta/2) + C_3 \sin(\sqrt{3} \eta/2) \} \quad (3.3.13)$$

From the above equation we may write

$$\begin{aligned} \Delta H' = & C_2 \left\{ (1/2) e^{\eta/2} \cos(\sqrt{3} \eta/2) - (\sqrt{3}/2) e^{\eta/2} \sin(\sqrt{3} \eta/2) \right\} + \\ & C_3 \left\{ (1/2) e^{\eta/2} \sin(\sqrt{3} \eta/2) + (\sqrt{3}/2) e^{\eta/2} \cos(\sqrt{3} \eta/2) \right\} \end{aligned} \quad (3.3.14)$$

and,

$$\begin{aligned} \Delta H'' = & -C_2 \left\{ (1/2) e^{\eta/2} \cos(\sqrt{3} \eta/2) + (\sqrt{3}/2) e^{\eta/2} \sin(\sqrt{3} \eta/2) \right\} \\ & - C_3 \left\{ (1/2) e^{\eta/2} \sin(\sqrt{3} \eta/2) - (\sqrt{3}/2) e^{\eta/2} \cos(\sqrt{3} \eta/2) \right\} \end{aligned} \quad (3.3.15)$$

From the last three equations we may write

$$\Delta H(0) = C_2 \quad (3.3.16)$$

$$\Delta H'(0) = (1/2)C_2 + (\sqrt{3}/2)C_3 \quad (3.3.17)$$

$$\Delta H''(0) = -(1/2)C_2 + (\sqrt{3}/2)C_3 \quad (3.3.18)$$

Unlike the inlet region, where $\Delta H = \Delta H' = \Delta H''$, in the exit region $\Delta H \neq \Delta H' \neq \Delta H''$ and two constants are involved in the equations of these three. For such a case we choose an arbitrary value of C_2 and then pick a value of C_3 and substitute them in the above three equations to obtain ΔH and its derivatives. We then use these values as initial values of ΔH , $\Delta H'$ & $\Delta H''$ and march the solution of the differential equation for the exit region. This determines $H''(\infty)$. Since the web at a distance far away from the roller, at both the inlet and the exit regions, is surrounded by the same atmospheric pressure, we must have

$$H_i'' \Big|_{\eta \rightarrow \infty} = H_e'' \Big|_{\eta \rightarrow \infty} \quad (3.3.19)$$

that is, the same value of $H''(\infty)$ is required for both inlet and exit region solutions. If the chosen values of C_2 & C_3 do not satisfy the above condition we choose a new set of values of C_2 & C_3 . This trial and error procedure

continues until the above condition is satisfied. This gives us air film thickness variation in the exit region.

The pressure distribution in the inlet and the exit regions may be obtained by incorporating equation (2.4.4) in the above numerical solution.

3.3.3 Numerical Integration Method

Since one of the boundary conditions for the present problem is set at infinity, which is numerically undefined, it is obvious that the range of integration of the problem involves a large number of steps. It is necessary for such a case to use a method having a small per-step truncation error so that the cumulative error is minimized. The Milne predictor-corrector method with variable step size, which has a per-step error of order $(\Delta\eta)^5$, is used for the inlet and the exit region solutions of the differential equation. Due to its very low per-step error this method is considerably more accurate than many other numerical methods. However, this method does have the disadvantage of not being self-starting, though, as we shall see later, the advantages of it will camouflage this disadvantage. Although the fourth-order Runge-Kutta method is self-starting and has the same order of the per-step error as the Milne method, the former is not preferred because of the fact that the change in film thickness away from the transition regions is high

(whereas it is low near the transition regions) causing the Runge-Kutta method to give unsatisfactory results for higher order derivatives. In addition to this, it has been found that the estimation of the per-step error in Milne method is far easier than in Runge-Kutta method (James (11) pp- 356-403).

A computer code for the purpose of solving the governing differential equation was written in FORTRAN. This code uses a coupled numerical technique of Runge-Kutta method and Milne predictor-corrector method, the details of which is given in Appendix G. The six starting values required for the Milne method are computed through the Runge-Kutta method with small interval of constant size. Since the integration process is started somewhere in the uniformity region, the linearized form of the differential equation (equation (3.3.2)) is used in the Runge-Kutta method for computing six starting values of each H and its derivatives. These values are then further used in the integration process by the Milne method. The step size in this method is automatically controlled so that the relative error in H for each step is less than some small number assigned in advance.

One problem that remains in the above numerical scheme is determining the point in the uniformity region where we should start the numerical integration. This problem is solved by first arbitrarily choosing a small negative value of η (negative value is chosen since the integration must

be started in the uniformity region). Using this value the numerical solution of the governing differential equation (equation (3.1.1)) is obtained. From this solution the intercept of the asymptote of the H' -curve with the η -axis is determined. If this intercept does not meet at $\eta=0$ then the arbitrarily chosen value of η is changed. This trial-and-error procedure is continued until we arrive at a solution which gives the intercept of the asymptote of H' -curve at $\eta=0$. This point is further elaborated in the next section.

Two listings of the computer program which give complete solutions of the air film thickness and the pressure distribution in the inlet and the exit region are provided in Appendix I.

3.4 Discussion of the Numerical Results

Numerical values of the air film thickness and the pressure in the air film are given in Table I & II. The solutions are also depicted graphically in Figures 12 through 22. Observe from the plots of η VS H (Figures 12 and 18), which also show the film thickness variation, the different web behaviour in the inlet and the exit region. This air film thickness variation obtained from the numerical solution in both regions is compatible with the conclusions obtained from the qualitative analysis of the governing differential equations in the last chapter.

TABLE I

NUMERICAL RESULTS OF INLET REGION SOLUTION

ETA	H	H'	H''	H'''	P
-7.5000	0.1000E+01	0.5000E-03	0.5000E-03	0.5000E-03	0.1000E+01
-7.2500	0.1001E+01	0.6420E-03	0.6420E-03	0.6420E-03	0.9990E+00
-7.0000	0.1001E+01	0.8243E-03	0.8243E-03	0.8243E-03	0.9987E+00
-6.7500	0.1001E+01	0.1058E-02	0.1058E-02	0.1058E-02	0.9984E+00
-6.5000	0.1001E+01	0.1359E-02	0.1359E-02	0.1359E-02	0.9979E+00
-6.2500	0.1002E+01	0.1745E-02	0.1745E-02	0.1745E-02	0.9973E+00
-5.7500	0.1003E+01	0.2876E-02	0.2870E-02	0.2852E-02	0.9955E+00
-5.2500	0.1005E+01	0.4735E-02	0.4715E-02	0.4675E-02	0.9927E+00
-4.7500	0.1008E+01	0.7786E-02	0.7732E-02	0.7629E-02	0.9880E+00
-4.2500	0.1013E+01	0.1278E-01	0.1264E-01	0.1237E-01	0.9803E+00
-3.7500	0.1021E+01	0.2092E-01	0.2055E-01	0.1983E-01	0.9680E+00
-3.2500	0.1035E+01	0.3411E-01	0.3313E-01	0.3125E-01	0.9485E+00
-2.7500	0.1057E+01	0.5521E-01	0.5268E-01	0.4793E-01	0.9181E+00
-2.2500	0.1092E+01	0.8842E-01	0.8206E-01	0.7055E-01	0.8724E+00
-1.7500	0.1148E+01	0.1394E+00	0.1240E+00	0.9778E-01	0.8071E+00
-1.2500	0.1235E+01	0.2148E+00	0.1798E+00	0.1248E+00	0.7203E+00
-0.7500	0.1368E+01	0.3212E+00	0.2475E+00	0.1437E+00	0.6151E+00
-0.2500	0.1562E+01	0.4632E+00	0.3210E+00	0.1475E+00	0.5008E+00
0.2500	0.1837E+01	0.6418E+00	0.3922E+00	0.1350E+00	0.3900E+00
0.7500	0.2210E+01	0.8539E+00	0.4543E+00	0.1121E+00	0.2935E+00
1.2500	0.2696E+01	0.1094E+01	0.5039E+00	0.8656E-01	0.2163E+00
1.7500	0.3307E+01	0.1356E+01	0.5413E+00	0.6378E-01	0.1582E+00
2.2500	0.4054E+01	0.1634E+01	0.5685E+00	0.4583E-01	0.1159E+00
2.7500	0.4943E+01	0.1923E+01	0.5879E+00	0.3265E-01	0.8566E-01
3.2500	0.5978E+01	0.2221E+01	0.6018E+00	0.2330E-01	0.6412E-01
3.7500	0.7164E+01	0.2524E+01	0.6117E+00	0.1676E-01	0.4870E-01
4.2500	0.8503E+01	0.2832E+01	0.6189E+00	0.1220E-01	0.3754E-01
4.7500	0.9997E+01	0.3143E+01	0.6241E+00	0.9006E-02	0.2937E-01
5.2500	0.1165E+02	0.3456E+01	0.6280E+00	0.6740E-02	0.2329E-01
5.7500	0.1345E+02	0.3770E+01	0.6310E+00	0.5115E-02	0.1872E-01
6.2500	0.1542E+02	0.4087E+01	0.6332E+00	0.3934E-02	0.1522E-01
7.0000	0.1866E+02	0.4562E+01	0.6357E+00	0.2718E-02	0.1139E-01
7.5000	0.2102E+02	0.4881E+01	0.6369E+00	0.2155E-02	0.9510E-02
8.0000	0.2354E+02	0.5199E+01	0.6379E+00	0.1728E-02	0.8008E-02
8.5000	0.2622E+02	0.5518E+01	0.6386E+00	0.1399E-02	0.6798E-02
9.0000	0.2906E+02	0.5838E+01	0.6393E+00	0.1143E-02	0.5813E-02
9.5000	0.3206E+02	0.6158E+01	0.6398E+00	0.9427E-03	0.5005E-02
10.0000	0.3522E+02	0.6478E+01	0.6402E+00	0.7834E-03	0.4336E-02
10.5000	0.3854E+02	0.6798E+01	0.6406E+00	0.6559E-03	0.3778E-02
11.5000	0.4565E+02	0.7439E+01	0.6411E+00	0.4693E-03	0.2913E-02
12.5000	0.5341E+02	0.8080E+01	0.6415E+00	0.3439E-03	0.2287E-02
13.5000	0.6181E+02	0.8722E+01	0.6418E+00	0.2575E-03	0.1823E-02
14.5000	0.7086E+02	0.9364E+01	0.6421E+00	0.1964E-03	0.1473E-02
15.5000	0.8054E+02	0.1001E+02	0.6422E+00	0.1522E-03	0.1203E-02
16.5000	0.9087E+02	0.1065E+02	0.6424E+00	0.1198E-03	0.9934E-03
17.5000	0.1018E+03	0.1129E+02	0.6425E+00	0.9548E-04	0.8265E-03
18.5000	0.1134E+03	0.1193E+02	0.6426E+00	0.7701E-04	0.6934E-03
20.5000	0.1386E+03	0.1322E+02	0.6427E+00	0.5168E-04	0.4962E-03
22.5000	0.1663E+03	0.1450E+02	0.6428E+00	0.3593E-04	0.3619E-03
24.5000	0.1966E+03	0.1579E+02	0.6428E+00	0.2574E-04	0.2669E-03
26.5000	0.2295E+03	0.1708E+02	0.6429E+00	0.1891E-04	0.1983E-03
28.5000	0.2649E+03	0.1836E+02	0.6429E+00	0.1420E-04	0.1471E-03
30.5000	0.3029E+03	0.1965E+02	0.6429E+00	0.1086E-04	0.1086E-03
38.5000	0.4807E+03	0.2479E+02	0.6430E+00	0.4319E-05	0.2178E-04
42.5000	0.5850E+03	0.2736E+02	0.6430E+00	0.2917E-05	-0.5061E-06
46.5000	0.6996E+03	0.2993E+02	0.6430E+00	0.2040E-05	-0.1560E-04
50.5000	0.8245E+03	0.3251E+02	0.6430E+00	0.1469E-05	-0.2653E-04
54.5000	0.9596E+03	0.3508E+02	0.6430E+00	0.1085E-05	-0.3427E-04

TABLE II
 NUMERICAL RESULTS OF EXIT REGION SOLUTION

ETA	H	H'	H''	H'''	P
-13.0000	0.9997E+00	0.4600E-05	0.2600E-03	0.2600E-03	0.1000E+01
-12.7500	0.9997E+00	0.7805E-04	0.3271E-03	0.2620E-03	0.9995E+00
-12.5000	0.9998E+00	0.1678E-03	0.3893E-03	0.2316E-03	0.9994E+00
-12.2500	0.9998E+00	0.2718E-03	0.4409E-03	0.1769E-03	0.9993E+00
-12.0000	0.9999E+00	0.3868E-03	0.4755E-03	0.9478E-04	0.9993E+00
-11.7500	0.1000E+01	0.5075E-03	0.4858E-03	-0.1696E-04	0.9992E+00
-11.0000	0.1001E+01	0.8253E-03	0.2977E-03	-0.5246E-03	0.9995E+00
-10.0000	0.1001E+01	0.7173E-03	-0.6582E-03	-0.1371E-02	0.1001E+01
-9.0000	0.1002E+01	-0.7044E-03	-0.2213E-02	-0.1508E-02	0.1003E+01
-8.0000	0.9995E+00	-0.3451E-02	-0.2948E-02	0.4976E-03	0.1005E+01
-7.0000	0.9948E+00	-0.5454E-02	-0.2584E-03	0.5251E-02	0.1000E+01
-6.2500	0.9911E+00	-0.3784E-02	0.5212E-02	0.9140E-02	0.9919E+00
-5.5000	0.9904E+00	0.2887E-02	0.1267E-01	0.9866E-02	0.9803E+00
-4.7500	0.9968E+00	0.1476E-01	0.1816E-01	0.3265E-02	0.9718E+00
-4.0000	0.1013E+01	0.2802E-01	0.1524E-01	-0.1245E-01	0.9763E+00
-3.2500	0.1037E+01	0.3403E-01	-0.1819E-02	-0.3318E-01	0.1003E+01
-2.5000	0.1059E+01	0.2156E-01	-0.3355E-01	-0.4992E-01	0.1052E+01
-1.7500	0.1062E+01	-0.1831E-01	-0.7308E-01	-0.5206E-01	0.1114E+01
-1.0000	0.1025E+01	-0.8607E-01	-0.1041E+00	-0.2302E-01	0.1162E+01
-0.3750	0.9503E+00	-0.1516E+00	-0.9735E-01	0.5791E-01	0.1151E+01
0.2500	0.8405E+00	-0.1904E+00	-0.5048E-02	0.2687E+00	0.1008E+01
0.8750	0.7351E+00	-0.1171E+00	0.2822E+00	0.6669E+00	0.5611E+00
1.4375	0.7355E+00	0.1580E+00	0.6969E+00	0.6650E+00	-0.8376E-01
2.0000	0.9500E+00	0.6237E+00	0.8994E+00	0.5832E-01	-0.3988E+00
2.5625	0.1442E+01	0.1122E+01	0.8526E+00	-0.1474E+00	-0.3260E+00
3.1250	0.2204E+01	0.1579E+01	0.7765E+00	-0.1125E+00	-0.2076E+00
3.7500	0.3338E+01	0.2046E+01	0.7229E+00	-0.6285E-01	-0.1242E+00
4.3750	0.4756E+01	0.2487E+01	0.6933E+00	-0.3492E-01	-0.7818E-01
5.0000	0.6445E+01	0.2915E+01	0.6765E+00	-0.2034E-01	-0.5208E-01
5.7500	0.8820E+01	0.3418E+01	0.6650E+00	-0.1140E-01	-0.3418E-01
6.5000	0.1157E+02	0.3914E+01	0.6583E+00	-0.6825E-02	-0.2383E-01
7.2500	0.1469E+02	0.4406E+01	0.6542E+00	-0.4319E-02	-0.1747E-01
8.0000	0.1942E+02	0.5058E+01	0.6509E+00	-0.2515E-02	-0.1231E-01
9.2500	0.2481E+02	0.5708E+01	0.6489E+00	-0.1560E-02	-0.9212E-02
10.2500	0.3084E+02	0.6356E+01	0.6477E+00	-0.1017E-02	-0.7246E-02
11.2500	0.3752E+02	0.7004E+01	0.6468E+00	-0.6915E-03	-0.5937E-02
12.7500	0.4875E+02	0.7973E+01	0.6460E+00	-0.4121E-03	-0.4684E-02
13.7500	0.5705E+02	0.8619E+01	0.6457E+00	-0.3019E-03	-0.4134E-02
14.7500	0.6599E+02	0.9264E+01	0.6454E+00	-0.2262E-03	-0.3727E-02
15.7500	0.7557E+02	0.9910E+01	0.6452E+00	-0.1728E-03	-0.3419E-02
16.7500	0.8581E+02	0.1055E+02	0.6450E+00	-0.1342E-03	-0.3182E-02
17.7500	0.9668E+02	0.1120E+02	0.6449E+00	-0.1059E-03	-0.2996E-02
18.7500	0.1082E+03	0.1184E+02	0.6448E+00	-0.8462E-04	-0.2849E-02
22.7500	0.1607E+03	0.1442E+02	0.6446E+00	-0.3846E-04	-0.2489E-02
24.7500	0.1909E+03	0.1571E+02	0.6445E+00	-0.2730E-04	-0.2388E-02
26.7500	0.2236E+03	0.1700E+02	0.6445E+00	-0.1991E-04	-0.2315E-02
28.7500	0.2589E+03	0.1829E+02	0.6445E+00	-0.1486E-04	-0.2261E-02
30.7500	0.2968E+03	0.1958E+02	0.6444E+00	-0.1132E-04	-0.2221E-02
32.7500	0.3372E+03	0.2087E+02	0.6444E+00	-0.8768E-05	-0.2190E-02
40.7500	0.5248E+03	0.2602E+02	0.6444E+00	-0.3624E-05	-0.2119E-02
44.7500	0.6340E+03	0.2860E+02	0.6444E+00	-0.2484E-05	-0.2100E-02
48.7500	0.7536E+03	0.3118E+02	0.6443E+00	-0.1759E-05	-0.2087E-02
52.7500	0.8834E+03	0.3376E+02	0.6443E+00	-0.1280E-05	-0.2077E-02
56.7500	0.1024E+04	0.3633E+02	0.6443E+00	-0.9534E-06	-0.2071E-02

It is obvious from these plots that there is a gradual increase in the air film thickness near the inlet transition region (Figure 12) whereas, there is a sinusoidal behaviour (undulation) of the web near the exit transition region. This sinusoidal behavior of the web is shown in Figure 18 which is an enlarged plot of Figure 17 near the exit transition region. An important point to observe from these plots (ETA VS H) is that the normalized air film thickness H does not have a value of exactly unity at the two transition points, i.e. the points where we defined $\eta=0$ for the two separate solutions in the inlet and the exit region. This fact has already been observed geometrically from Figure 11. Another important fact to observe from these two plots is that the constant gap film thickness is not the minimum film thickness; infact, minimum film thickness occurs somewhere in the exit region and is approximately 71.6% of the nominal clearance (see Figure 18).

The significance of ETA VS H' plot (Figures 13 and 19) is that it enables us to locate graphically the point of tangency, i.e. the transition point. The point of tangency is located by finding the intercept of the asymptote of H'-curve with the η -axis (see Figures 13 and 19). This curve helps us in the trial-and-error procedure of locating the point in the uniformity region where we should start the integration process (The numerical results given in Tables I and II are for the final solution when the

tangency point is located at approximately $\eta=0$ for the two regions):

As discussed in section 3.2, the constant gap film thickness may be determined if the numerical value of $H''(\infty)$ is known. From the numerical results and from equation (3.2.2) we may write the constant gap film thickness as

$$h_0 = 0.643 R \left\{ (6\mu U)/T \right\}^{2/3} \quad (3.4.1)$$

or,

$$h_0 = 0.643 R \left\{ (6\mu(U_W + U_R)) / (T_0 - \sigma U_W)^2 \right\}^{2/3} \quad (3.4.2)$$

The numerical value of $H''(\infty)=0.643$ may also be obtained from the asymptote value of H'' (see Figure 14). Since the inlet and exit region solutions must give the same constant gap film thickness, the asymptotic value of H'' from Figure 20 (exit region) is the same as obtained from Figure 14 (inlet region).

Figure 16 and Figure 22 show the pressure distribution in the inlet and exit region, respectively. These pressure curves are obtained for the normalized pressure equation given by equation (2.4.8) (in this and the subsequent pressure curves P_n represents the normalized pressure \bar{P}_n define by equation (2.4.7)). This distribution of the pressure in both regions corroborate the results of the

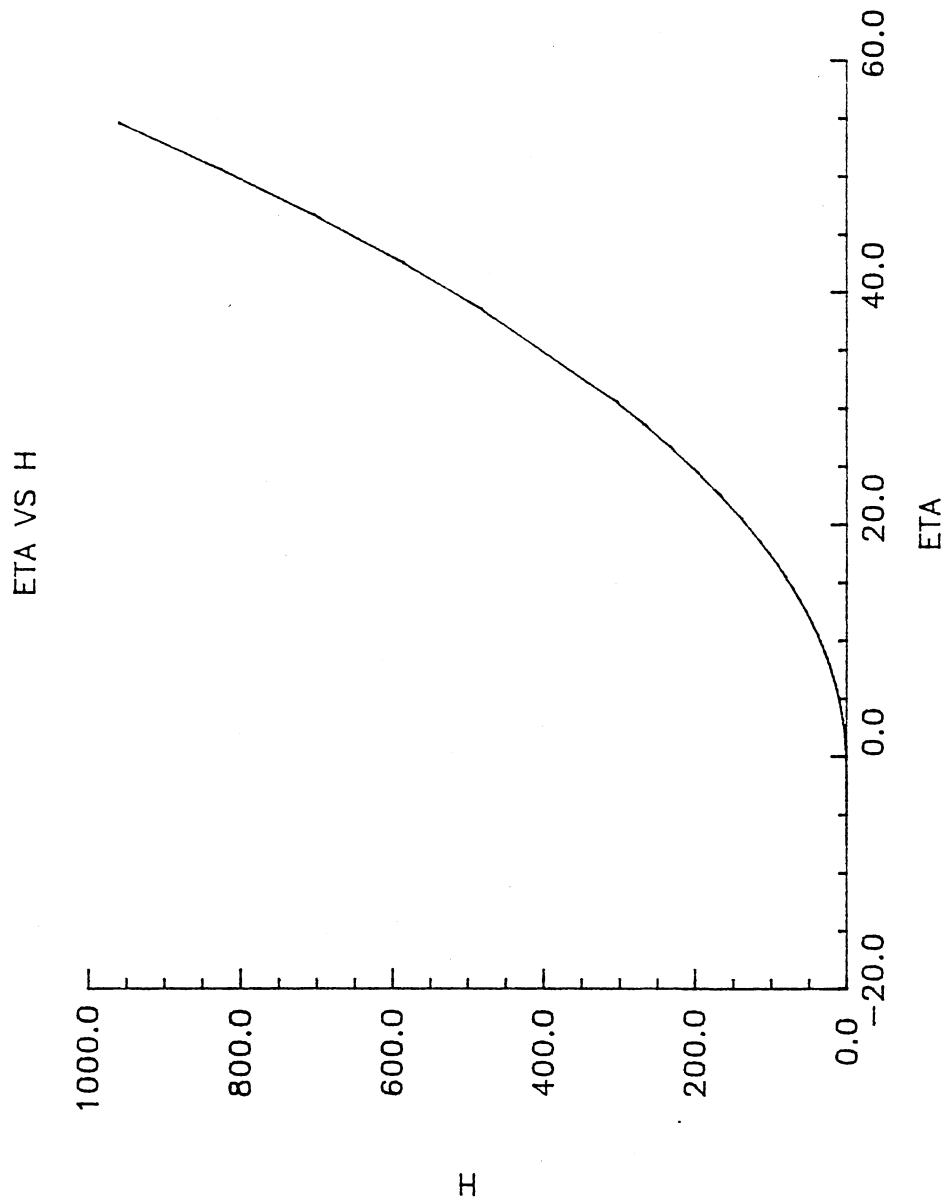


Figure 12. Air Film Thickness In the Inlet Region

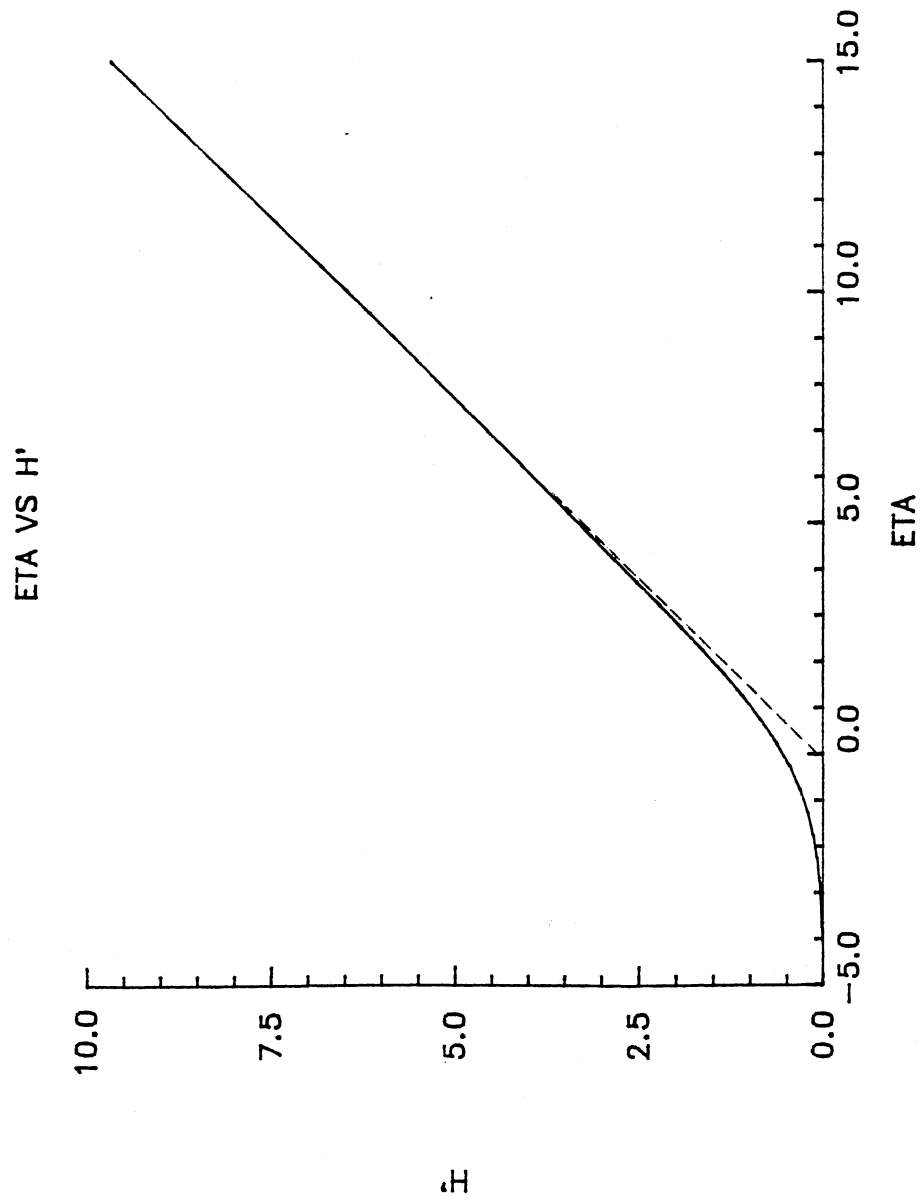


Figure 13. Plot of η VS H' - Inlet Region

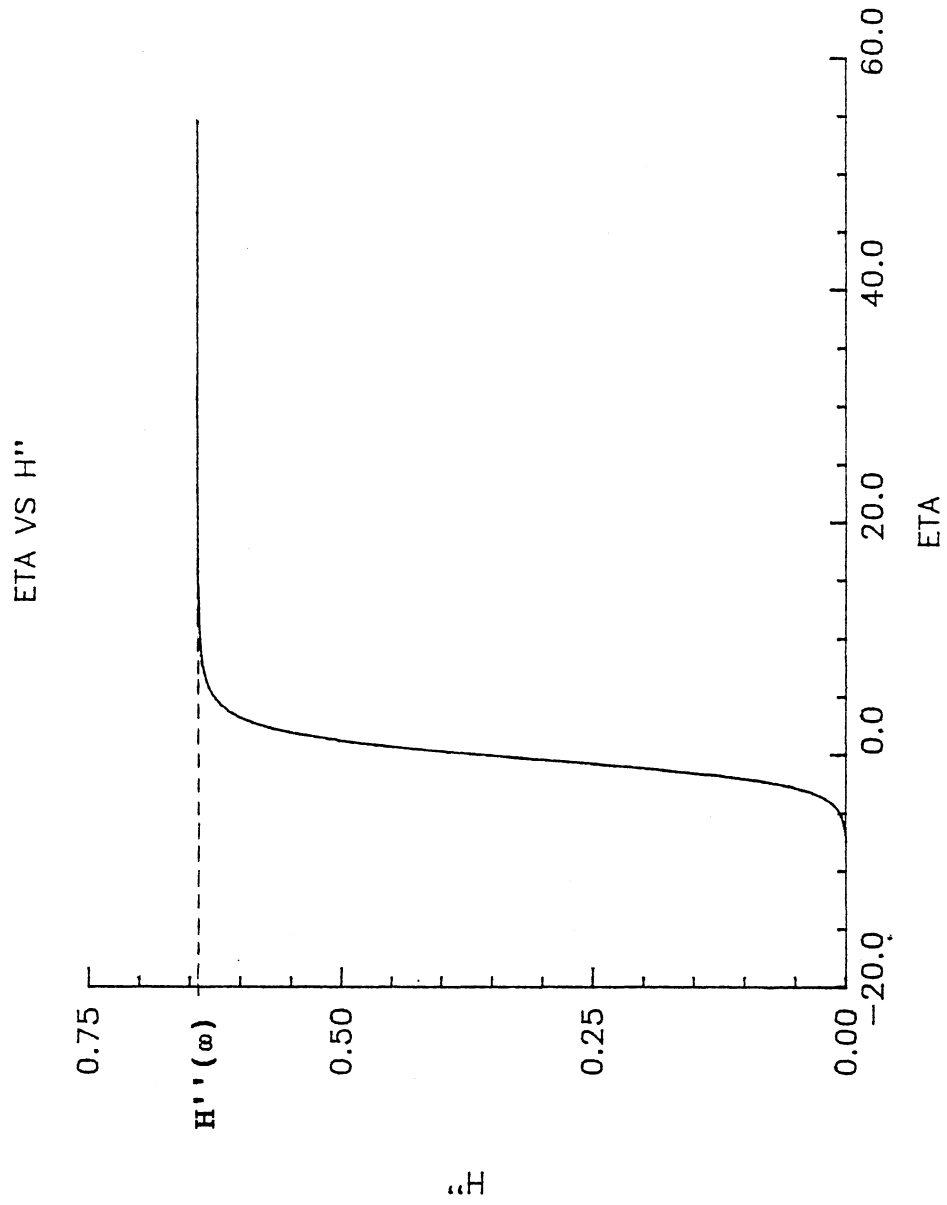


Figure 14. Plot of η VS H''' - Inlet Region

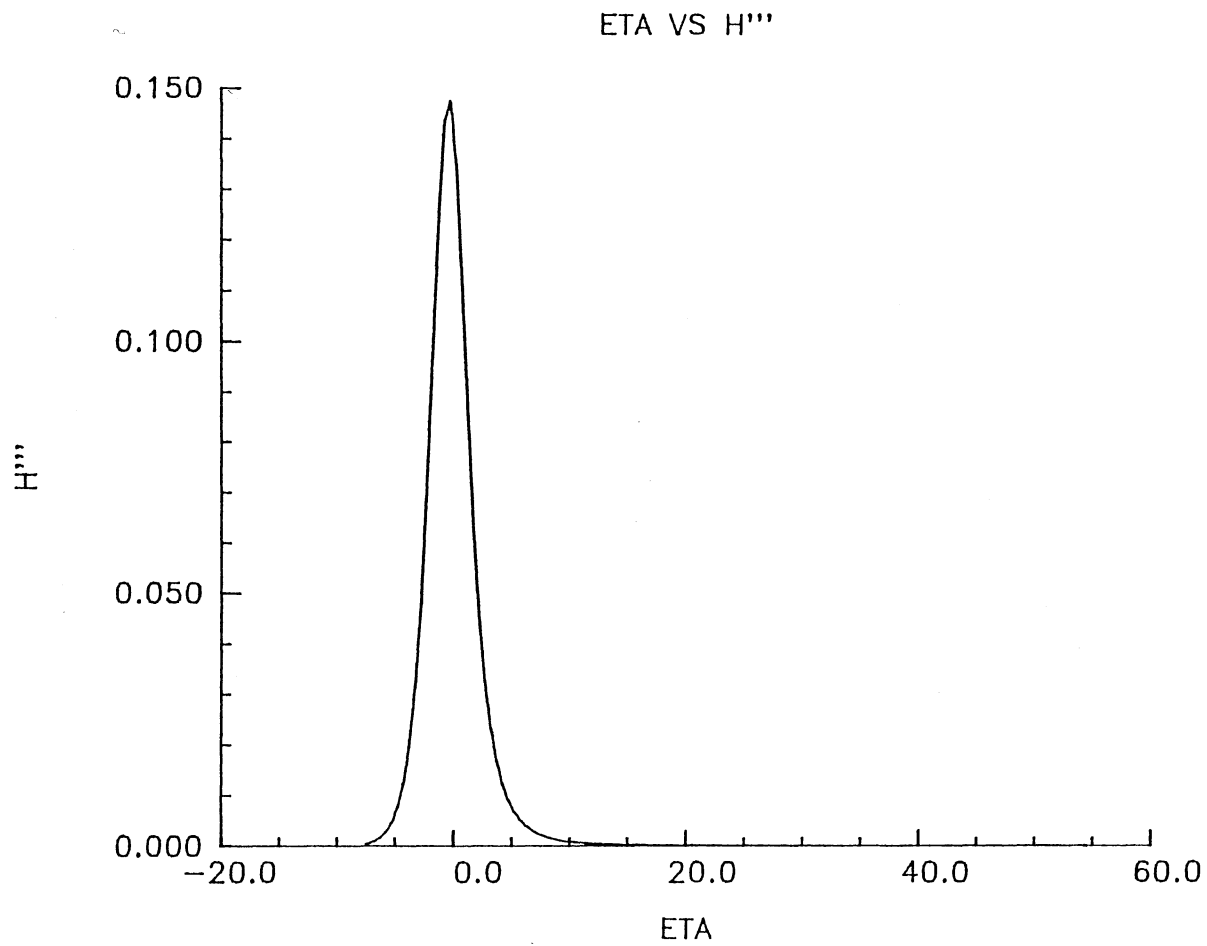


Figure 15. Plot of ETA vs H''' - Inlet Region.

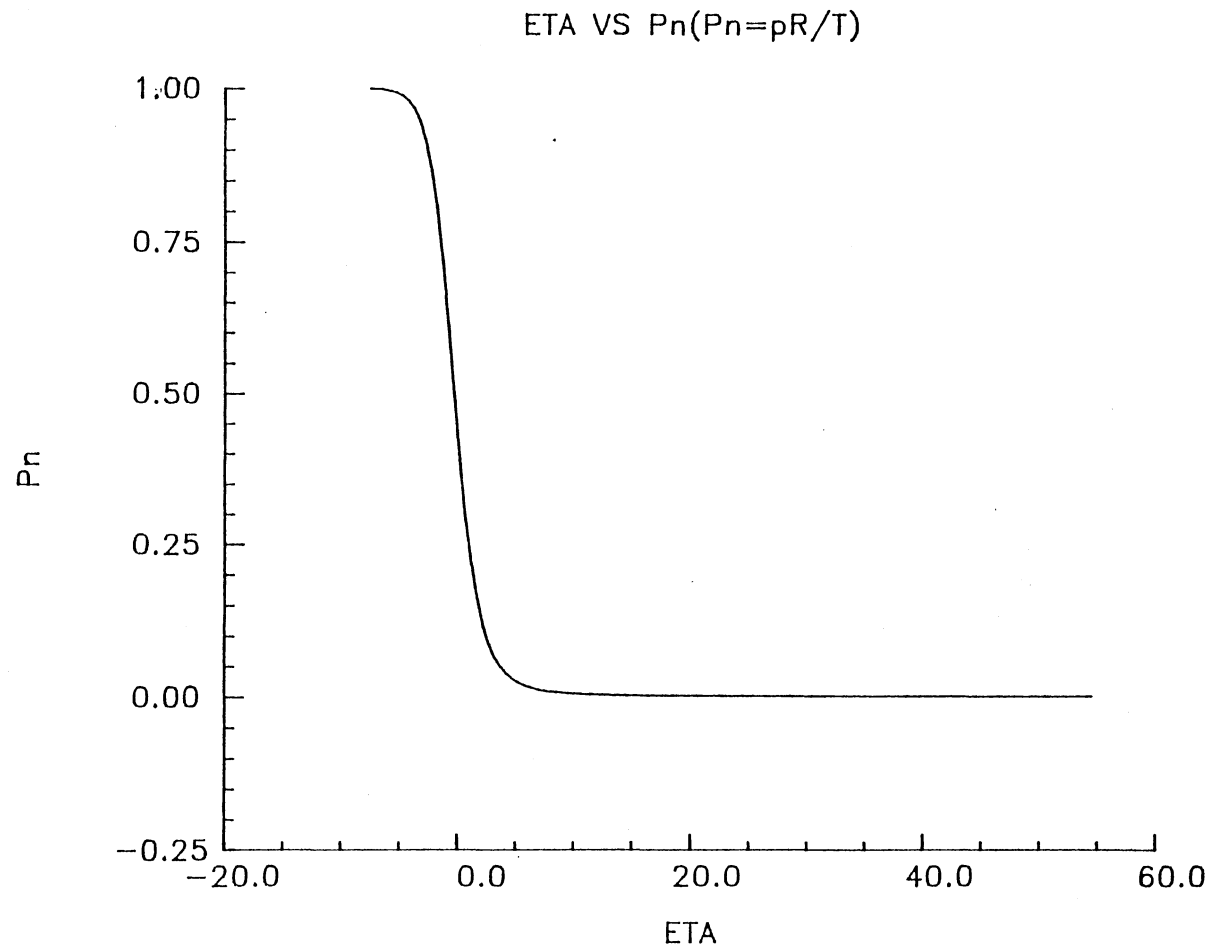


Figure 16. Air Film Pressure in the Inlet Region.

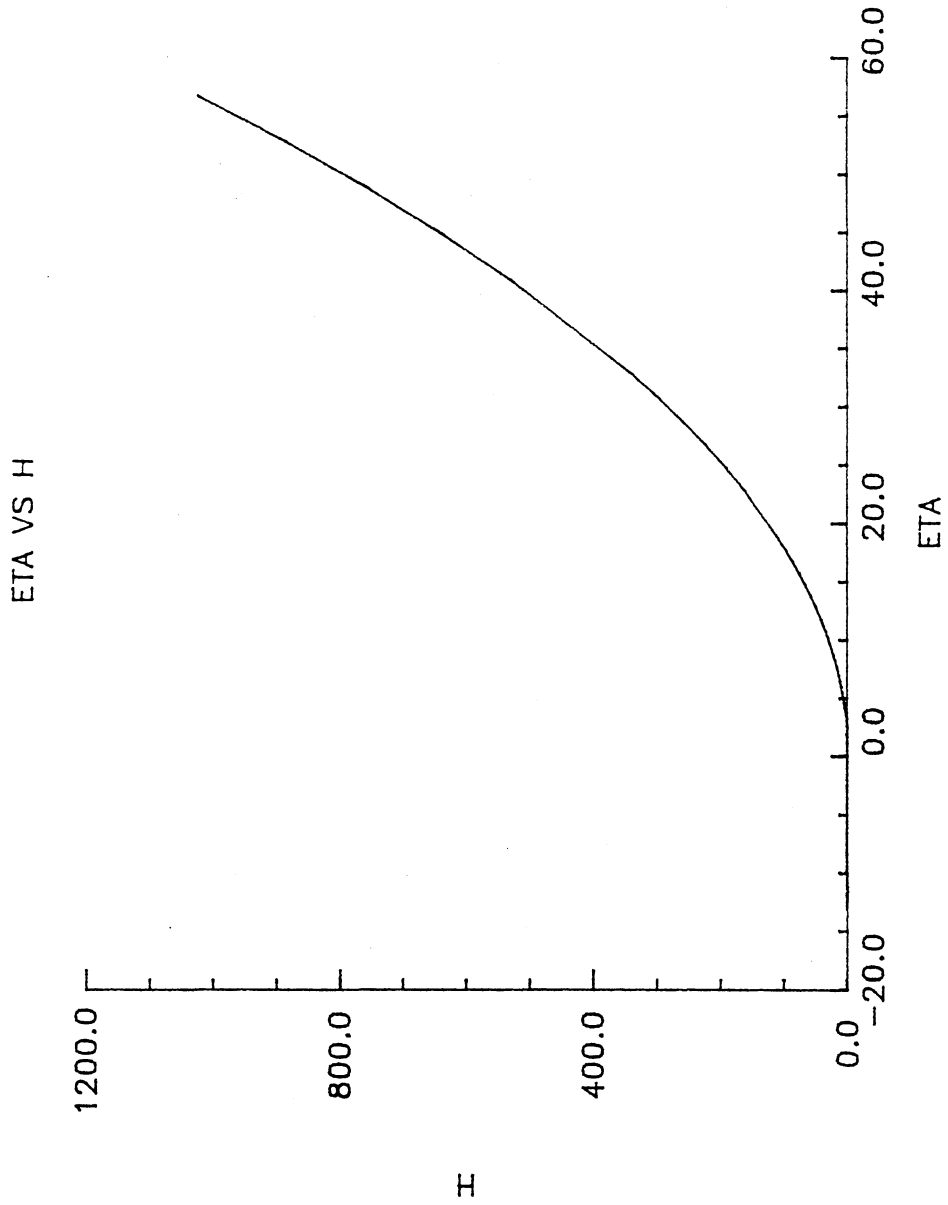


Figure 17. Air Film Thickness in the Exit Region

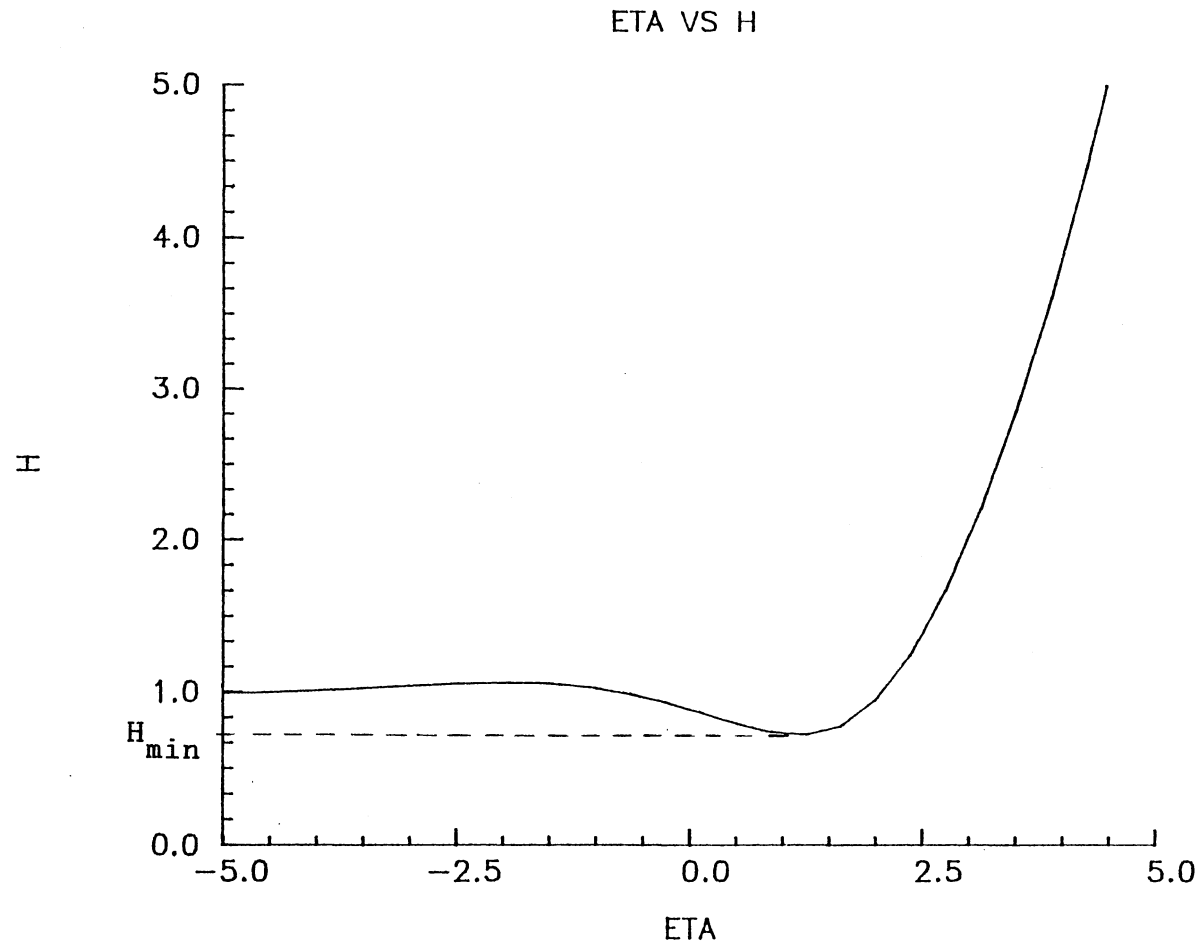


Figure 18. "Undulation" Near the Exit Transition Region

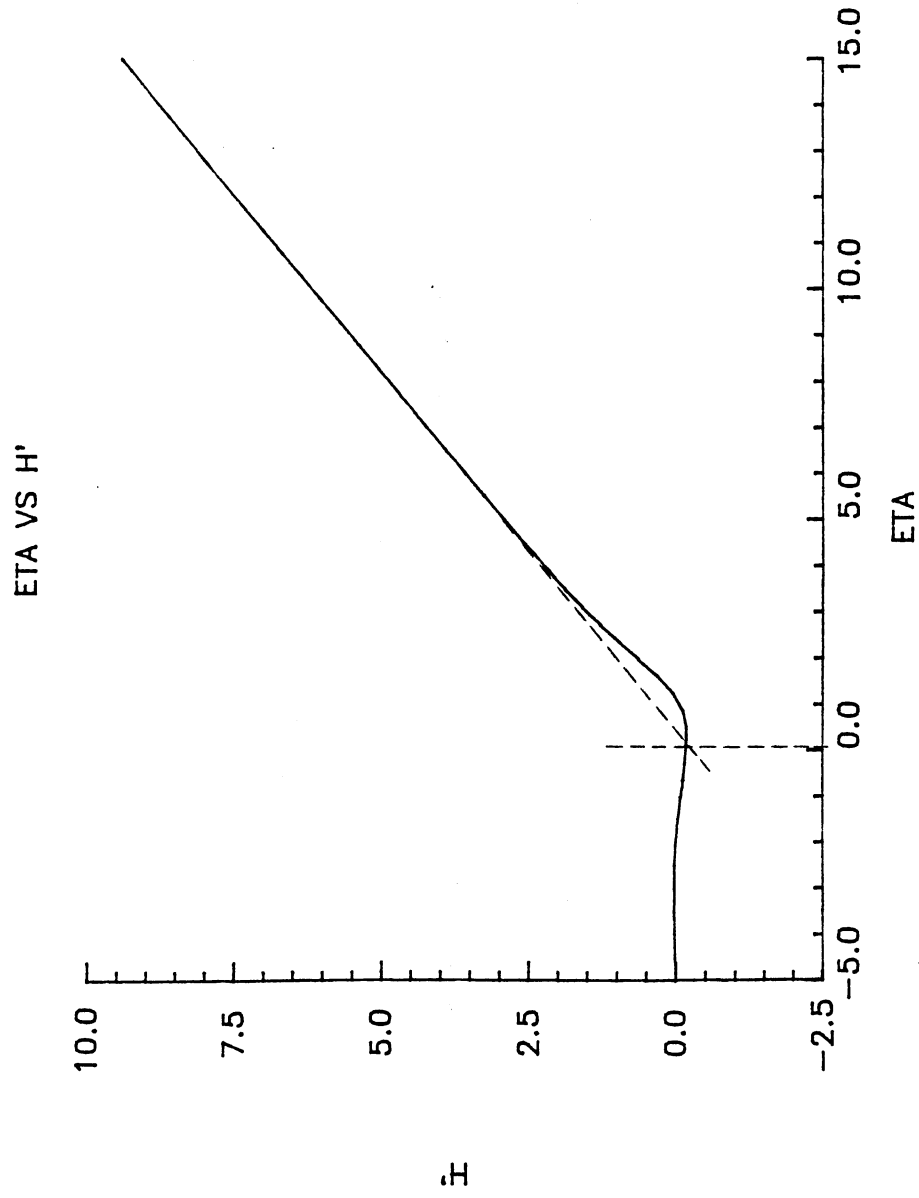


Figure 19. Plot of ETA VS H' - Exit Region

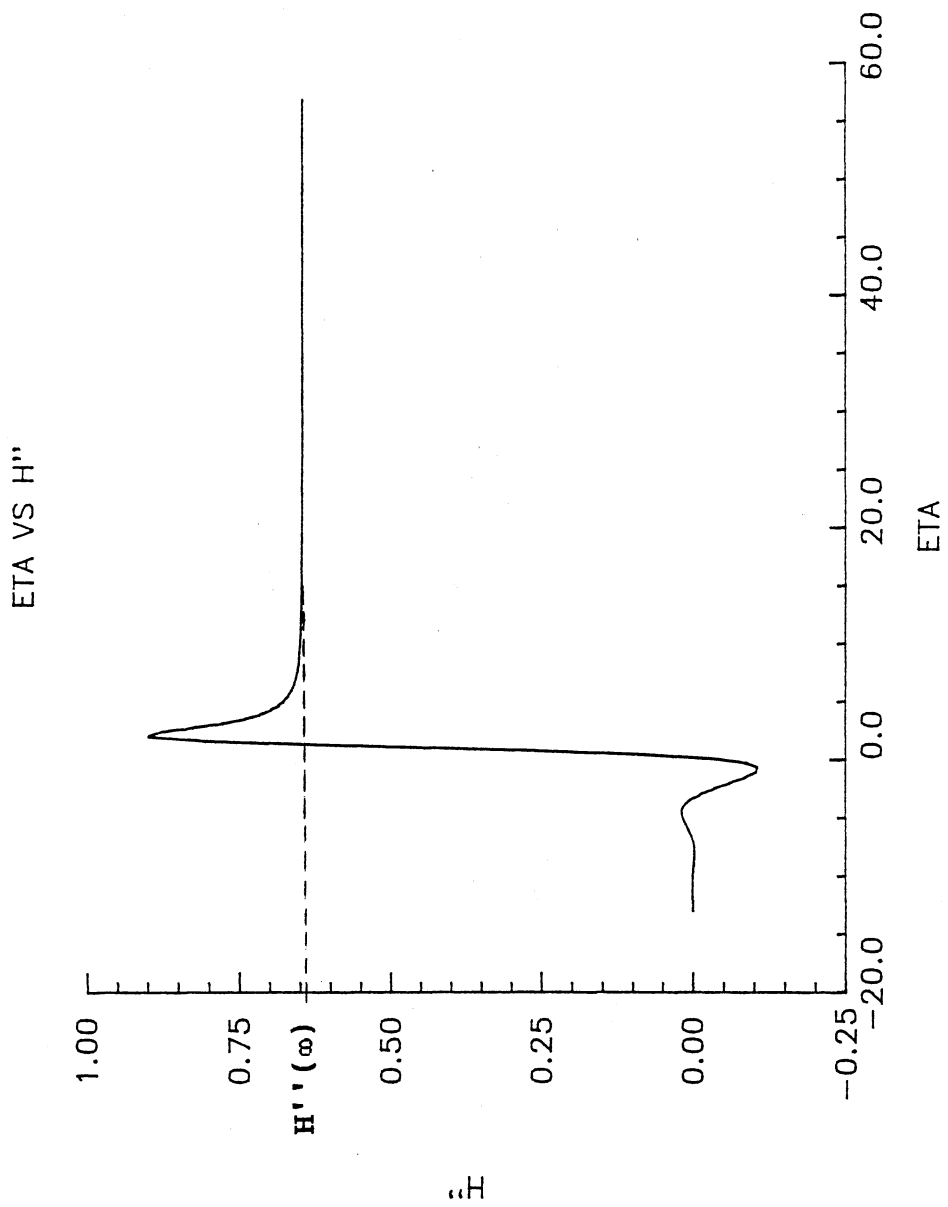


Figure 20. Plot of η VS H'' - Exit Region

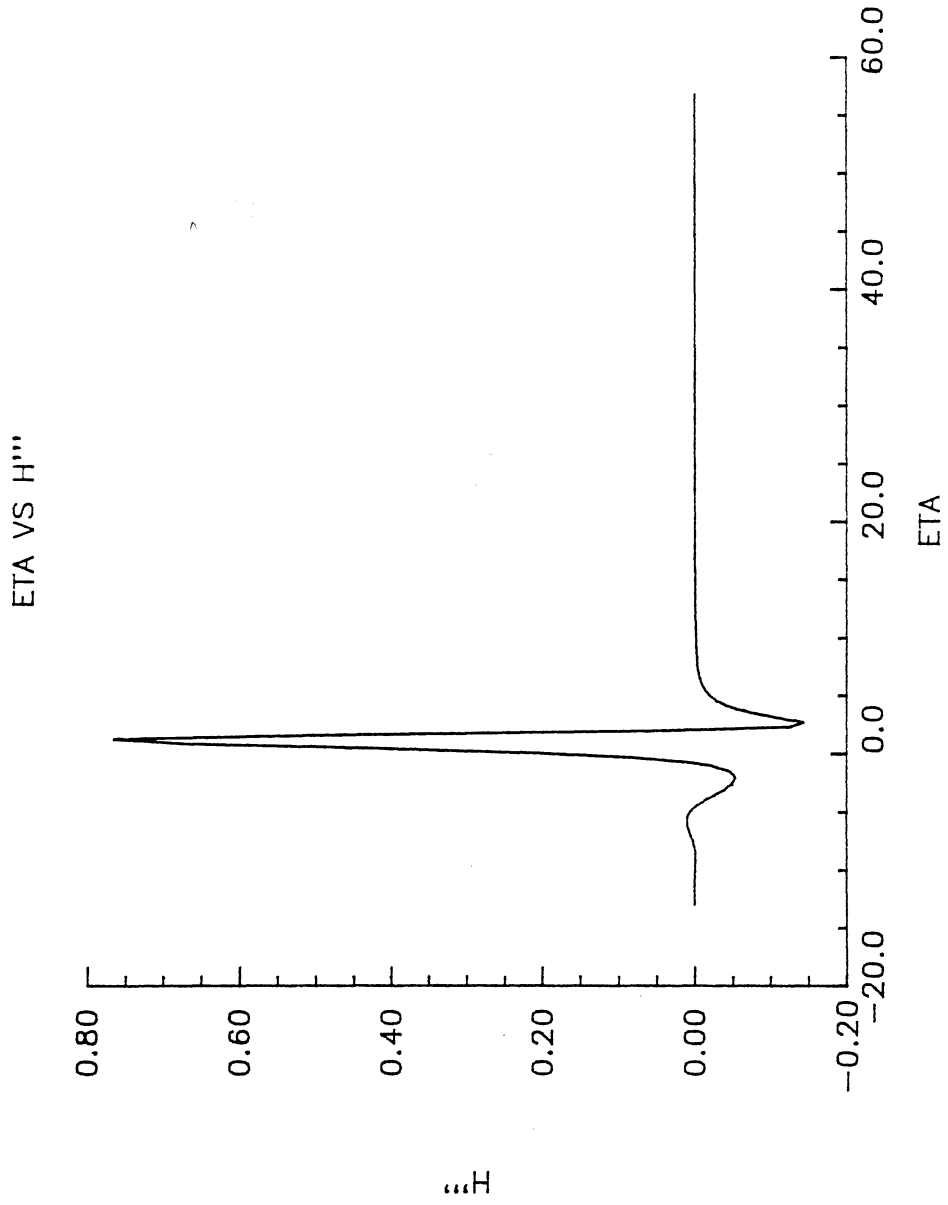


Figure 21. Plot of ETA VS H''' - Exit Region

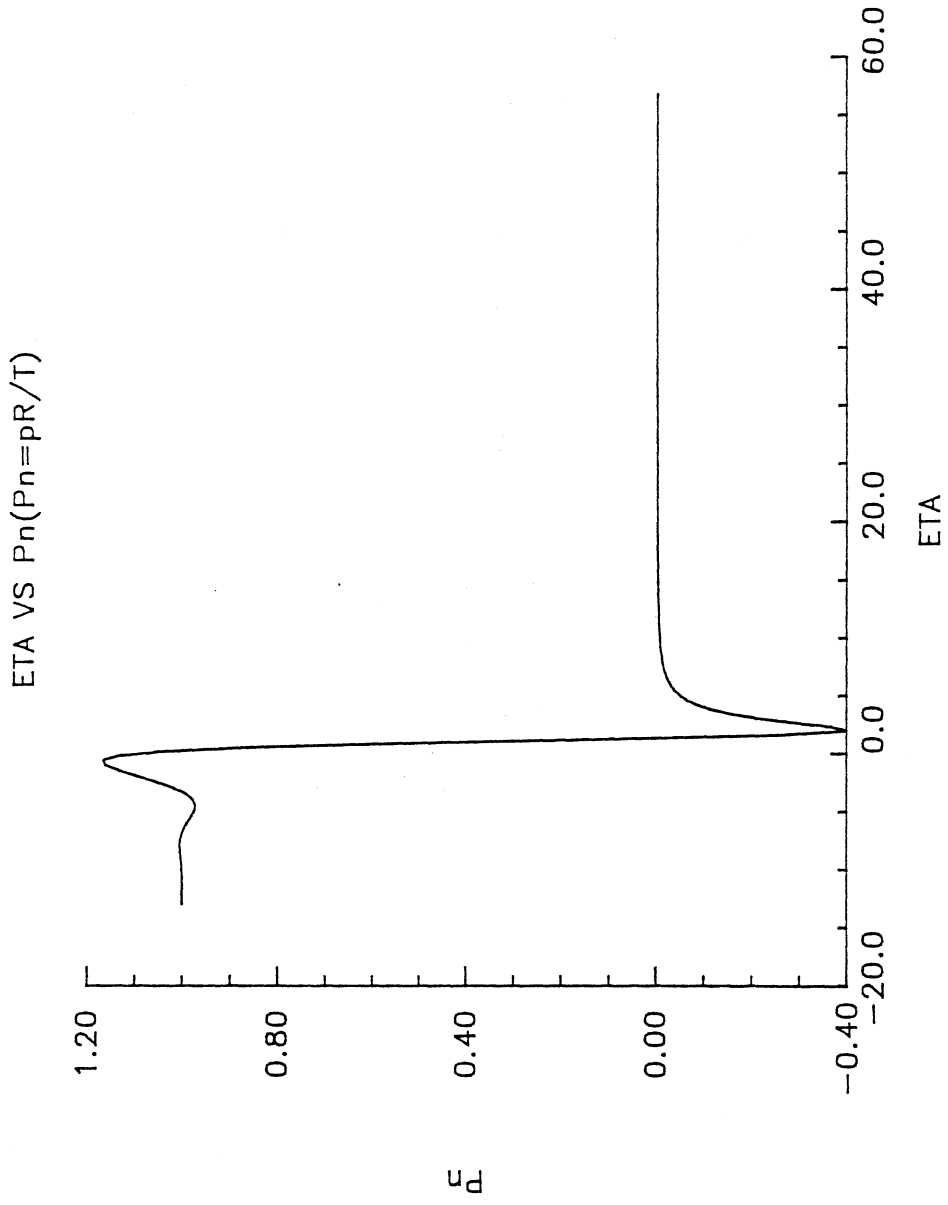


Figure 22. Air Film Pressure in the Exit Region

theoretical analysis (section 2.6). It can be seen from these two figures that the behavior of the pressure in the two regions is quite different. There is a gradual increase of pressure from ambient to a constant value corresponding to the uniformity region in case of inlet region (see Figure 16) while there is a sinusoidal pressure distribution in the exit region (see Figure 22), compatible with the undulation of the web noted in Figure 18. Both the inlet region and the exit region solutions give the same pressure in the uniformity region and according to equation (2.4.7) this pressure is given by

$$p = p_a + T/R \quad (3.4.3)$$

From equation (3.4.1) it is obvious that the sum of the web and supporting roller speed U and the reduced tension in the web T are important parameters in developing the air film thickness. The effect of these parameters on air film thickness is shown in Figures (23) & (24). In order to observe the effect of the speed U on the constant gap film thickness h_0 , the reduced tension T was kept at a constant value of 1 lb/in. And to observe the effect of the tension T on the constant gap film thickness, the speed U was kept at a constant value of 400 in/sec. These two plots are obtained for a roller of 36 inches in dia.

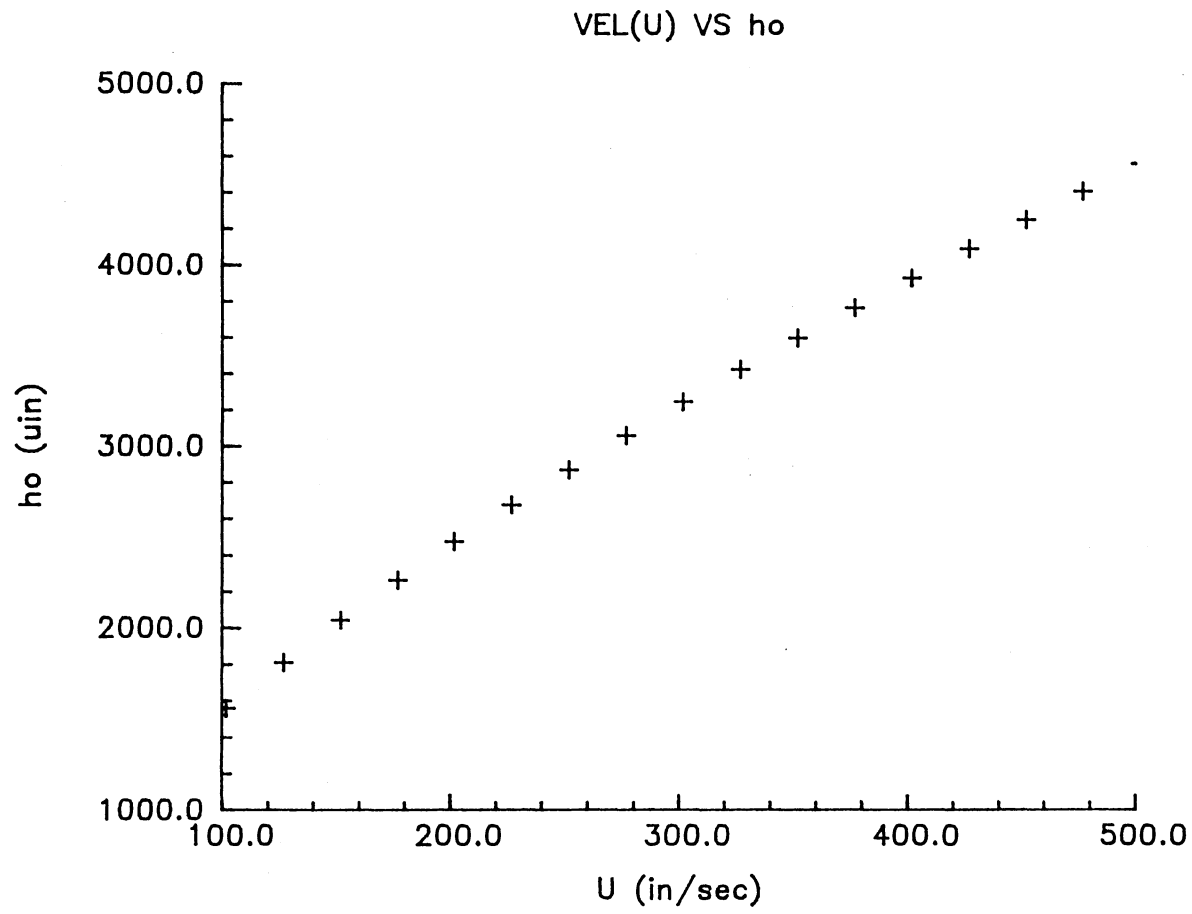


Figure 23. Effect of Relative Speed U on Constant Gap Film Thickness

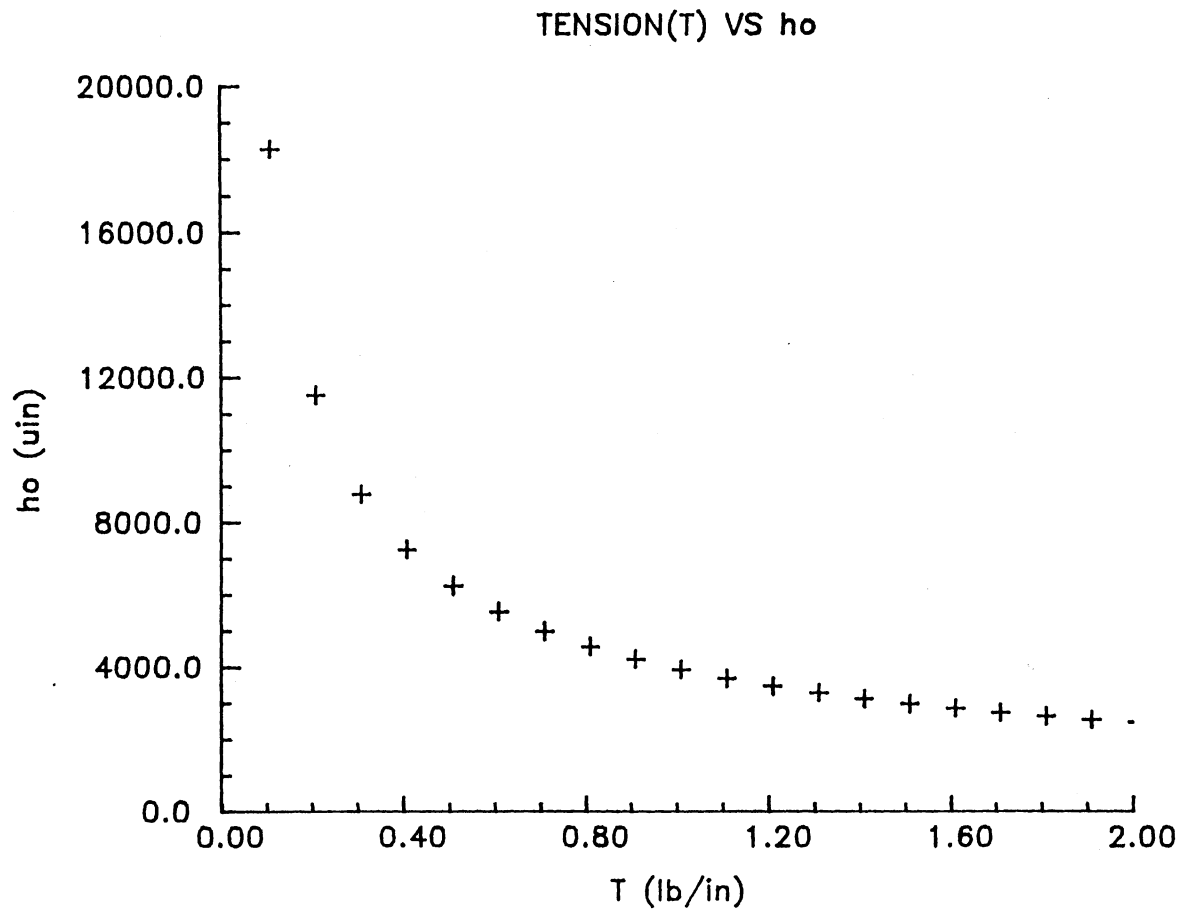


Figure 24. Effect of Tension T on Constant Gap Film Thickness

3.5 Constant Gap Film Thickness for Various Web Handling Applications

Numerical values of the constant gap film thickness h_0 and the length of the inlet region for three different sets of operating parameters are given in Table III. The first three columns show the operating parameters whereas, the last two are the calculated numerical values of constant gap film thickness h_0 and the length of the inlet region. The constant gap film thickness is calculated by using equation (3.4.1) whereas the length of the inlet region is calculated by using equation (2.3.10b). Observe from Figure 16 that the ambient pressure is achieved at approximately $\eta=8$. This value of η is used in equation (2.3.10b) to obtain the dimensional length of the inlet region.

TABLE III

NUMERICAL VALUES OF CONSTANT GAP FILM THICKNESS AND
LENGTH OF THE INLET REGION FOR DIFFERENT
OPERATING PARAMETERS

Radius of Roller (in)	Tension in Web (lb/in)	Speed $U_w + U_R$ (in/sec)	Constant Gap Film Thickness (μ in)	Length of Inlet Region (in)
0.5	0.5	50	43.50	0.0374
18.0	1.0	400	3943.0	2.1400
54.0	10.0	1600	6422.0	4.7200

CHAPTER IV

STRATEGY FOR CONTROLLING AIR

ENTRAINMENT

Since it is desirable to move webs at high speeds, it is important to be able to control the entrainment of the air in order to avoid related web handling problems. This is true not only for the present problem but for other related applications such as the winding process. In this chapter a strategy for controlling the air entrainment will be developed and modelled.

In the last three chapters a model was developed which enables the estimation of the air film clearance for the passage of a flexible web over a supporting roller. This clearance cannot usually be modified without changing any of the parameters given in equation (3.4.1). However, application of some external pressure on the web will enable the uniform clearance to be reduced considerably. One common method of reducing the air entrainment in most web handling applications is through the use of a "rider roller". A rider roller may be described as the roller which rides on the web at the web-supporting roller interaction. In case of winding process it is placed near the nip of the wound roll. However, such a practice is

based solely on physical intuition and, at present, no theory exists which analyzes the effects of placing a rider roller over the web. In the present chapter the model that has been developed will be modified to incorporate the effects of placing a rider roller in the inlet region of the web-supporting roller interaction. The new modified geometry is shown in Figure 25. The objective of this portion of the study will be to determine the effect of rider roller size, location, and imposed pressure on controlling air film thickness between the web and the supporting roller.

4.1 Modification of the Model

As for the supporting roller we assume that there is a negligible amount of friction on the rider roller surface (i.e. the surface is completely smooth). The general Reynolds lubrication equation for the air entrainment between the web and the supporting roller, as derived in chapter II, is found to be unchanged and is rewritten as

$$\nabla \cdot \left\{ (\rho h^3) / \mu \nabla p \right\} = 6 \left\{ \nabla \cdot (\rho h U) \right\} + 12 \frac{\partial}{\partial t} (\rho h) \quad (4.1.1)$$

where all the notations have the same definition as given for equation (2.2.21).

From the modified geometry, however, it is clear that

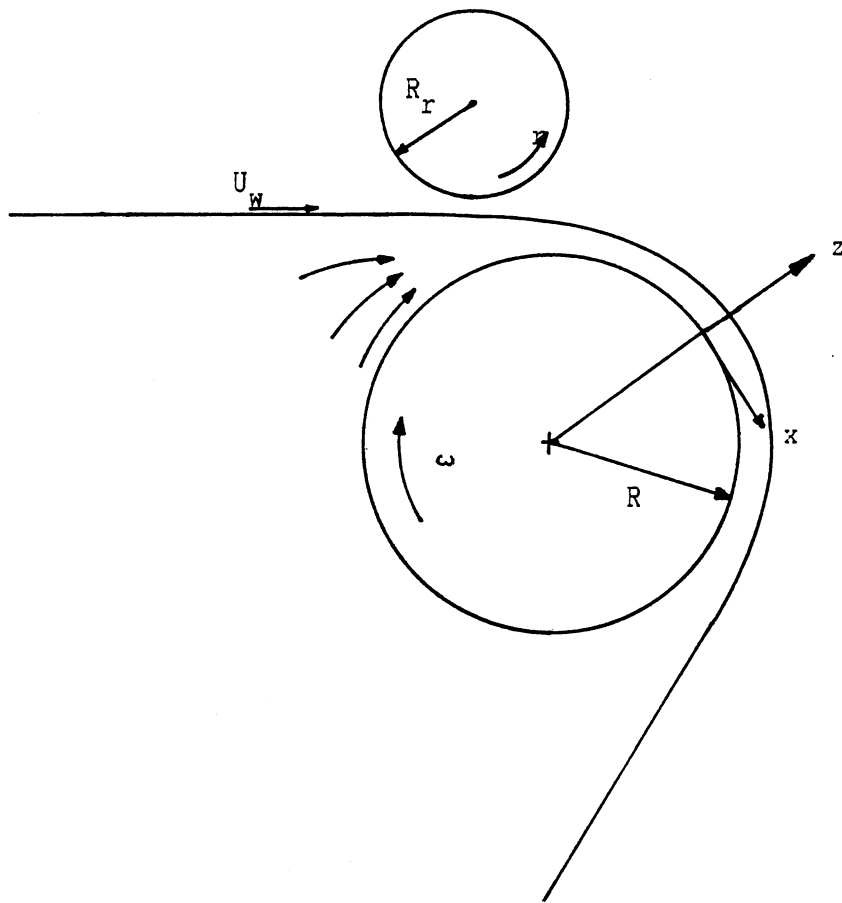


Figure 25. The Modified Geometry

the equilibrium equation must be changed. A new modified set of equilibrium equations is developed in an approach similar to the one given in section (2.2) and on the basis of Figure 26, which shows the action of forces on the web element. These equilibrium equations are

$$\frac{\partial N}{\partial X}x + \frac{\partial N}{\partial Y}yx + Q_x \frac{\partial^2 W}{\partial X^2} - \tau = 0 \quad (4.1.2)$$

$$\frac{\partial N}{\partial X}xy + \frac{\partial N}{\partial Y}y = 0 \quad (4.1.3)$$

$$\frac{\partial Q}{\partial X}x + \frac{\partial Q}{\partial Y}y - (p-p_a) + p_r + \sigma U_w \frac{\partial^2 W}{\partial X^2} - \frac{\partial^2 W}{\partial X^2} N_x = 0 \quad (4.1.4)$$

$$\frac{\partial M}{\partial X}x + \frac{\partial M}{\partial Y}yx - Q_x = 0 \quad (4.1.5)$$

$$\frac{\partial M}{\partial X}xy + \frac{\partial M}{\partial Y}y - Q_y = 0 \quad (4.1.6)$$

where all the notations have the same definition as given in section (2.2), except now τ is the sum of shear forces (per unit area) between the web and the roller and between the web and the rider roller (see Figure 26) and p_r is the external pressure on the web due to the rider roller.

Applying the same assumptions for the derivation of normal shear force and moment equations as previously, the equations governing the lateral deflection, bending and shearing action of the web are:

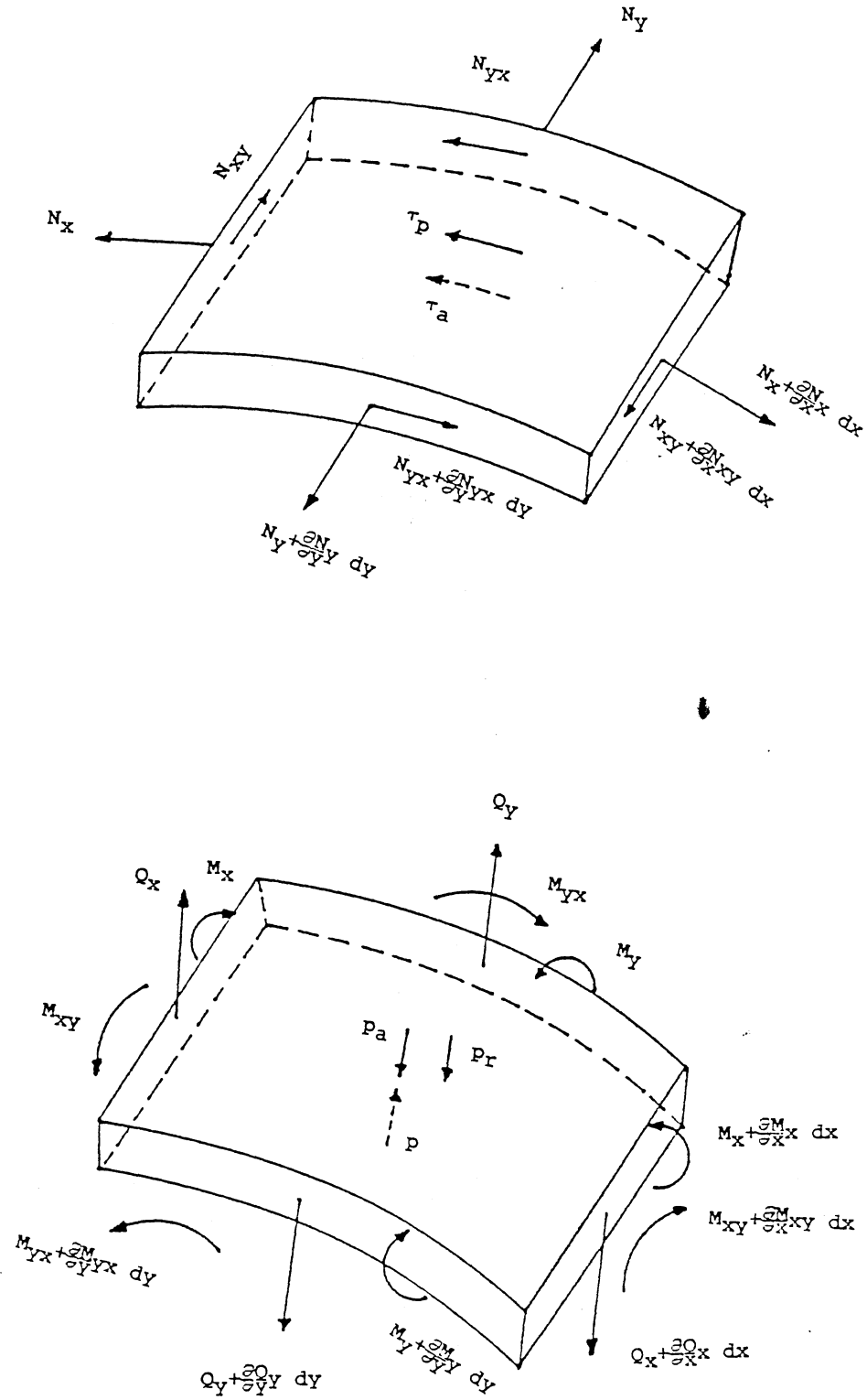


Figure 26. Web Element Under Various Forces and Moments

$$\frac{\partial M}{\partial X}x + \frac{\partial M}{\partial Y}Yx - Q_x = 0 \quad (4.1.7)$$

$$\frac{\partial M}{\partial X}xy + \frac{\partial M}{\partial Y}Y = 0 \quad (4.1.8)$$

$$\frac{\partial Q}{\partial X}x + \frac{\partial Q}{\partial Y}Y - (p-p_a) + p_r + \sigma U_w \frac{\partial^2}{\partial X^2} - \frac{\partial^2}{\partial X^2} N_x = 0 \quad (4.1.9)$$

$$M_x = D \left[\frac{\partial^2}{\partial X^2} + \nu \frac{\partial^2}{\partial Y^2} \right] \quad (4.1.10)$$

$$M_y = D \left[\frac{\partial^2}{\partial Y^2} + \nu \frac{\partial^2}{\partial X^2} \right] \quad (4.1.11)$$

$$M_{xy} = \left\{ (Et^3)/(12(1+\nu)) \right\} \frac{\partial^2}{\partial X \partial Y} W \quad (4.1.12)$$

where $D = \left\{ (Et^3)/(12(1-\nu^2)) \right\}$ is the flexure rigidity of the web material.

The equations governing the in-plane stress resultants and in-plane mid-surface displacements are:

$$\frac{\partial N}{\partial X}x + \frac{\partial N}{\partial Y}Yx + Q_x \frac{\partial^2}{\partial X^2} - \tau = 0 \quad (4.1.13)$$

$$\frac{\partial N}{\partial X}xy + \frac{\partial N}{\partial Y}Y = 0 \quad (4.1.14)$$

$$N_x = \left\{ (Et)/(1-\nu^2) \right\} \left[\frac{\partial u}{\partial X}o + \nu \frac{\partial v}{\partial Y}o \right] + T_o \quad (4.1.15)$$

$$N_Y = \left\{ (Et)/(1-\nu^2) \right\} \left[\frac{\partial v_0}{\partial y} + \nu \frac{\partial u_0}{\partial x} \right] + \nu T_0 \quad (4.1.16)$$

$$N_{XY} = \left\{ (Et)/(12(1+\nu)) \right\} \left[\frac{\partial u_0}{\partial y} + \frac{\partial v_0}{\partial x} \right] \quad (4.1.17)$$

By comparing above eleven equations with the pertinent equations of section (2.2) (equations (2.2.31) through (2.2.33), equations (2.2.48) through (2.2.50), equations (2.2.54) through (2.2.56), and equation (2.2.29) & (2.2.30)) it is clear that only two equations are modified; equation (4.1.9) and equation (4.1.13). Applying the same mathematical manipulation as in section (2.2) we get the following modified equilibrium equation:

$$\left\{ (Et^3)/(12(1-\nu^2)) \right\} \left\{ \nabla^2 \nabla^2 h \right\} - (p - p_a) + p_r + \left\{ \frac{\partial^2 h}{\partial x^2} - 1/R \right\} (\sigma U_w - T_0) = 0 \quad (4.1.18)$$

If the assumptions of constant viscosity and incompressibility hold true for this case also then equation (4.1.1) for a steady state case reduces to one dimensional form

$$\frac{d}{dx} \left\{ h^3/\mu \frac{dp}{dx} \right\} = 6U \frac{dh}{dx} \quad (4.1.19)$$

Integrating the above equation we get

$$\frac{dp}{dx} = 6\mu U \left\{ (h - h_0)/h^3 \right\} \quad (4.1.20)$$

where, again, h_0 is the constant of integration and is the constant gap film thickness (film thickness at the point where $\frac{dp}{dx} = 0$).

For a perfectly flexible web, equation (4.1.18) reduces to

$$-(p - p_a) + p_r - T \left\{ \frac{d^2 h}{dx^2} - 1/R \right\} = 0 \quad (4.1.21)$$

where T is the reduced tension defined by equation (2.3.3). The above equation may be written as

$$p - p_a = p_r + (T/R) \left\{ 1 - R \frac{d^2 h}{dx^2} \right\} \quad (4.1.22)$$

Differentiating equation (4.1.22) with respect to x , we get

$$\frac{dp}{dx} = \frac{dp_r}{dx} - T \frac{d^3 h}{dx^3} \quad (4.1.23)$$

Eliminating $\frac{dp}{dx}$ by combining equations (4.1.20) and (4.1.23), we have

$$\frac{d-h}{dx^3} = (6\mu U/T) \left\{ (h_0 - h)/h^3 \right\} + (1/T) \frac{dp}{dx} \quad (4.1.24)$$

Using normalized expressions from equations (2.3.8) and (2.3.10) we may write the above equation as

$$\frac{d-H}{dx^3} = \left\{ (1 - H)/H^3 \right\} + (h_0/T) \left\{ T/(6\mu U) \right\}^{2/3} \frac{dp}{dx} \quad (4.1.25)$$

Let us define a non-dimensional pad (external) pressure as

$$P_r = (h_0/T) \left\{ T/(6\mu U) \right\}^{2/3} p_r \quad (4.1.26)$$

Equation (4.1.25) is then written as

$$\frac{d-H}{dx^3} = \left\{ (1 - H)/H^3 \right\} + \frac{dP_r}{dx} \quad (4.1.27)$$

Since the air film clearance in the uniformity region is dependent on the amount of air entrained and since the exit region air film thickness variation is also dependent on the amount of air initially entrained in the inlet region, it is obvious that any control strategy will be most effective if applied in the entrance region. Consequently, the modified differential equation should be true for the inlet region. Equation (4.1.27) is based on a coordinate system as defined in Figure 25. For a

differential equation that governs the inlet region we need to define a coordinate system where the x-coordinate direction is positive in a direction opposite to the direction of web motion. From the analysis of Chapter II it is clear that for this new coordinate system only the Reynolds Lubrication equation is changed. Hence for the inlet region equation (4.1.27) may be written as

$$\frac{d}{dx} \left(\frac{H^3}{\eta} \right) = \left\{ (H - 1)/H^3 \right\} + \frac{dP}{dx} r \quad (4.1.28)$$

4.2 Controlling Air Entrainment

Via a Rider Roller

In this section the effects of applying an external pressure on the web through a rider roller will be studied. In this regard, an equation for the pressure due to the rider roller will be developed which may be incorporated in the modified differential equation (equation (4.1.28)). This pressure equation will be developed for the case where the pressure due to the rider roller is contained in both the inlet and the uniformity region (see Figure 27). The merit of analyzing this geometry is that it enables one to evaluate the pressure equation for the case where the pressure due to the rider roller is contained fully in the inlet region of the web-supporting roller interaction (as shown in Figure 28) along with the case where the pressure

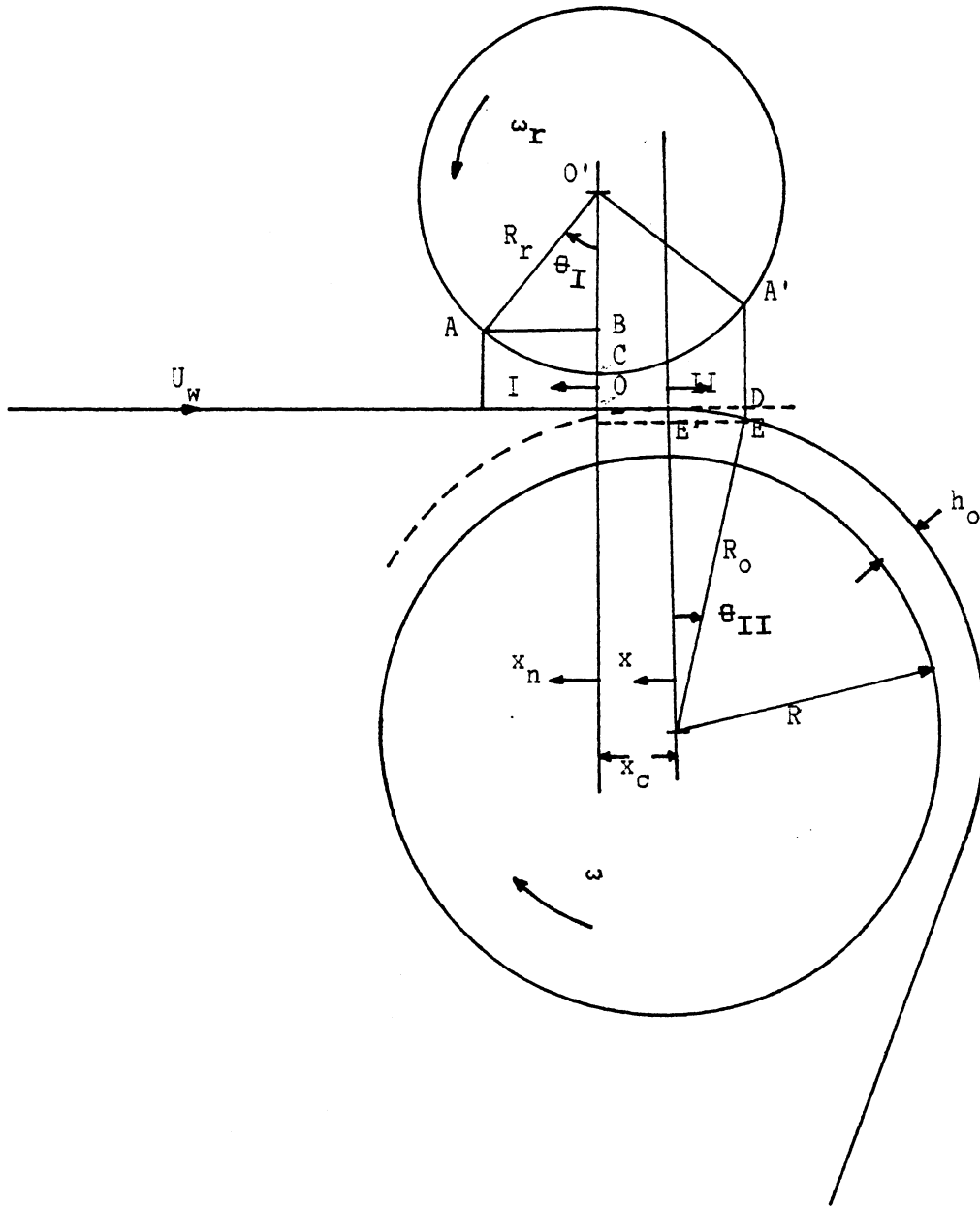


Figure 27. Pressure due to Rider Roller in Both the Inlet and Uniformity Region

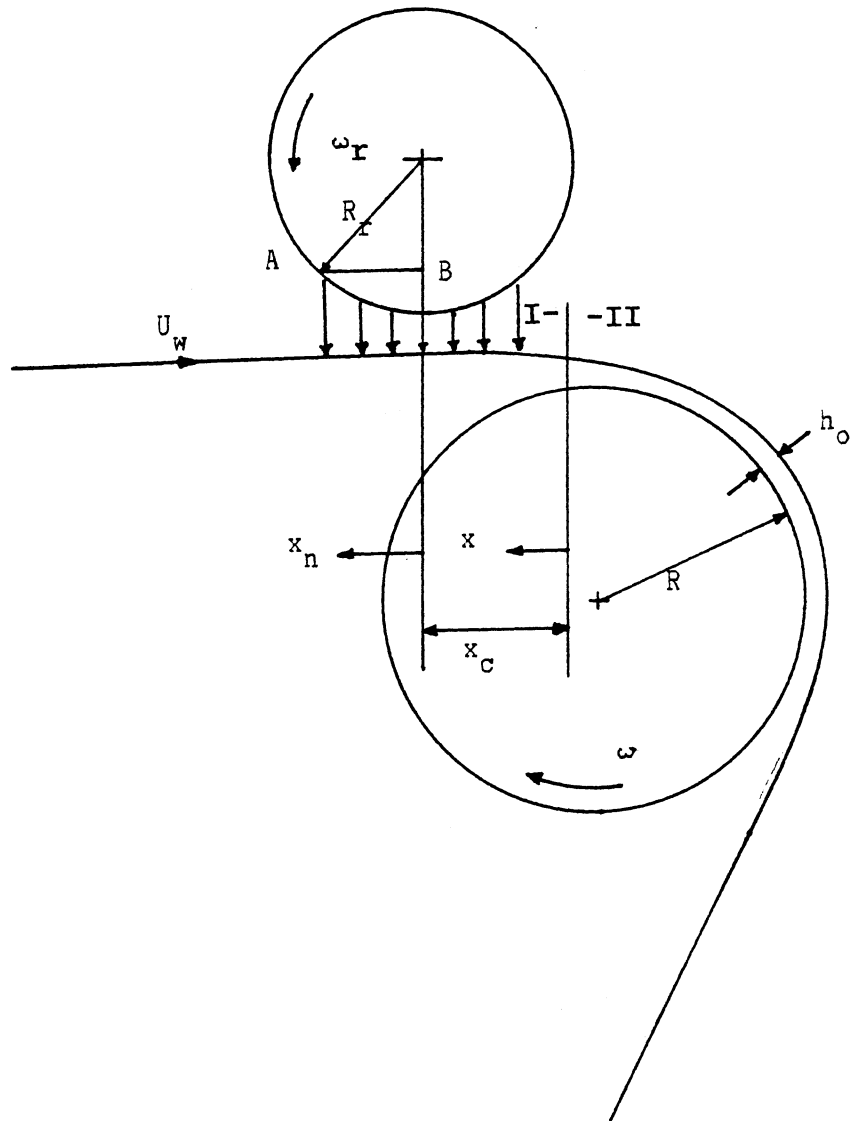


Figure 28. Rider Roller Pressure Fully in the Inlet Region

is partially contained in both the inlet region and the uniformity region. Since the modified differential equation is true for the inlet region where the air film thickness variation is assumed to be parabolic, the numerical solution will be obtained for the case where pressure due to the rider roller is within the inlet region.

Let us assume that the point of minimum clearance between the web and the rider roller (point O) lies somewhere in the inlet region such that the pressure developed on the web is in both the inlet and the uniformity region (see Figure 27). The clearance in the two regions are given by:

$$C_I = 1 + K_1 \{ \eta - \eta_c \}^2 \quad (4.2.1)$$

and,

$$C_{II} = 1 + K_2 \{ \eta \}^2 \quad (4.2.2)$$

where subscript I and II represent the clearance in the inlet region and in the uniformity region, respectively. In equation (4.2.1) η_c is the normalized distance of the point of minimum clearance from the point where $\eta=0$, C_I and C_{II} are the ratio of local clearance to the minimum clearance, i.e.

$$c_I = c_I / c_m \quad (4.2.3)$$

$$c_{II} = c_{II} / c_m \quad (4.2.4)$$

and K_1 and K_2 are given by

$$K_1 = 0.45467 R / \sqrt{(R_R c_m)} \left\{ (6\mu U) / T \right\}^{1/3} \quad (4.2.5)$$

$$K_2 = 0.45467 R / \sqrt{(R_C c_m)} \left\{ (6\mu U) / T \right\}^{1/3} \quad (4.2.6)$$

where R_C is the combination of radii R_R and R_O and may be defined from equation $1/R_C = 1/R_R + 1/R_O$.

A detailed derivation of equations (4.2.1) & (4.2.2) along with the expressions of K_1 and K_2 is given in Appendix H. From equations (4.2.5) and (4.2.6) we may write

$$K_1 / K_2 = \left\{ R_C / R_R \right\}^{1/2} \quad (4.2.7b)$$

A relationship between K_1 and K_2 may be obtained as

$$K_2 = K_1 \left\{ 1 + R_R / R_O \right\}^{1/2} \quad (4.2.7b)$$

For a coordinate system, whose origin is defined at the point of minimum clearance, we may write the one

dimensional Reynolds equation for the air entrained between the web and the rider roller as

$$\frac{dp}{dx}_n = -6\mu U_n \left\{ (c - c^*)/c^3 \right\} \quad (4.2.8)$$

where c^* is the constant of integration and is the clearance at the point where $\frac{dp}{dx} = 0$, U_n is the relative speed between the web and the rider roller. The negative sign on the right hand side of equation (4.2.8) is due to the fact that the velocity of the web is in a direction opposite to the x_n -coordinate direction.

The above equation may be written as

$$\frac{dp}{dx}_n = -(6\mu U_n)/c_m^2 \left\{ (c - c^*)/c^3 \right\} \quad (4.2.9)$$

Referring to Figure 27 we may write

$$x_n = x - x_c \quad (4.2.10)$$

where x_c is the dimensional distance corresponding to the normalized distance η_c . Substituting equation (4.2.10) in equation (4.2.9) we get

$$\frac{dp}{dx}_n = -(6\mu U_n)/c_m^2 \left\{ (c - c^*)/c^3 \right\}$$

substituting the normalized expressions from equations (2.3.10a) and (4.1.26) in the above equation we get

$$\frac{dP}{d\eta} r = - \left\{ 6\mu U_n / c_m^2 \right\} \left\{ (h_o^2 / T) (T / 6\mu U)^{1/3} / (6\mu U / T)^{2/3} \right\} \left\{ (C - C^*) / C^3 \right\} \quad (4.2.11)$$

which may be written as

$$\frac{dP}{d\eta} r = -\Lambda \left\{ (C - C^*) / C^3 \right\} \quad (4.2.12)$$

where,

$$\Lambda = 0.41345 (R / c_m)^2 (U_n / U) \left\{ (6\mu U) / T \right\}^{4/3} \quad (4.2.13)$$

The above expression for Λ is obtained by substituting the expression for h_o from equation (3.4.1) in the dimensional term of equation (4.2.11). It is important to note the difference between U and U_n ; U is the sum of the web and supporting roller speed while U_n is the sum of the web and rider roller speed.

The equation (4.2.12) for the two zones may be written as

$$\left. \frac{dP}{d\eta} r \right]_I = -\Lambda \left\{ (C - C^*) / C^3 \right\}_I \quad (4.2.14)$$

$$\frac{dP}{d\eta} \Big|_{II} = -\Lambda \left\{ (C - C^*) / C^3 \right\} \Big|_{II} \quad (4.2.15)$$

The pressure developed by the rider roller can be determined by integrating equations (4.2.14) and (4.2.15). Let us define the following transformation

$$\tan \psi_I = \left\{ x_n / \sqrt{(2R_I C_m)} \right\} \quad (4.2.16)$$

$$\tan \psi_{II} = \left\{ x / \sqrt{(2R_C C_m)} \right\} \quad (4.2.17)$$

Such a transformation has been used for the solution of many lubrication problems. A better understanding of these transformed angles may be obtained from Figure 29. In a normalized form these transformed equations may be written as

$$\tan \psi_I = K_1 (\eta - \eta_C) \quad (4.2.18)$$

and,

$$\tan \psi_{II} = K_2 (\eta) \quad (4.2.19)$$

Equations (4.2.1) & (4.2.2) are then written as

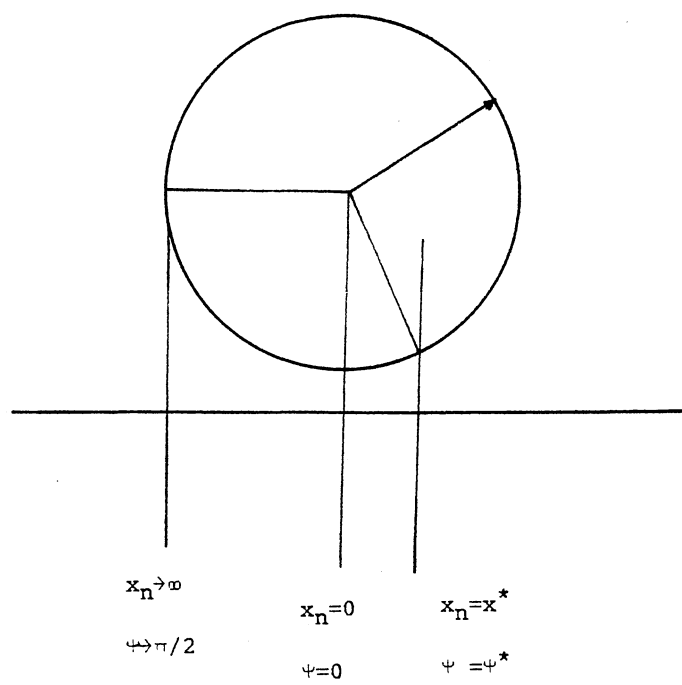


Figure 29. Definition of the Transformed Angle

$$C_I = 1 + \tan^2 \psi_I \quad (4.2.20)$$

or,

$$C_I = \sec^2 \psi_I \quad (4.2.21)$$

and,

$$C_{II} = 1 + \tan^2 \psi_{II} \quad (4.2.22)$$

or,

$$C_{II} = \sec^2 \psi_{II} \quad (4.2.23)$$

Using the last six equations, we may write equation (4.2.11) for the two regions as

$$dp_{rI} = -(6\mu U_n) / c_m^2 \left\{ (\sec^2 \psi_I - \sec^2 \psi_I^*) / \sec^6 \psi_I \right\} \sqrt{2R_r c_m} \sec^2 \psi_I d\psi_I$$

which may be simplified to

$$\left\{ c_m^2 / (6\mu U_n \sqrt{2R_r c_m}) \right\} dp_{rI} = \left\{ (\cos^4 \psi_I / \cos^2 \psi_I^*) - \cos^2 \psi_I \right\} d\psi_I \quad (4.2.24)$$

Similarly, for the second region we may write

$$\left\{ c_m^2 / (6\mu U_n \sqrt{2R_o c_m}) \right\} dp_{rII} = \left\{ (\cos^4 \psi_{II} / \cos^2 \psi_{II}^*) - \cos^2 \psi_{II} \right\} d\psi_{II} \quad (4.2.25)$$

where ψ_I^* and ψ_{II}^* are the angles corresponding to the point where $C_I=C_I^*$ and $C_{II}=C_{II}^*$, respectively.

Integrating the last two equations

$$\left\{ \frac{c_m^2}{(6\mu U_n \sqrt{2R_I c_m})} \right\} \int dp_r = (1/\cos^2 \psi_I^*) \int \cos^4 \psi_I d\psi_I - \int \cos^2 \psi_I d\psi_I \quad (4.2.26)$$

$$\left\{ \frac{c_m^2}{(6\mu U_n \sqrt{2R_O c_m})} \right\} \int dp_r = (1/\cos^2 \psi_{II}^*) \int \cos^4 \psi_{II} d\psi_{II} - \int \cos^2 \psi_{II} d\psi_{II} \quad (4.2.27)$$

Applying the following integral expressions

$$\int \cos^2 \psi d\psi = \sin 2\psi/4 + \psi/2 + C_1$$

$$\int \cos^4 \psi d\psi = \sin 4\psi/32 + \sin 2\psi/4 + 3\psi/8 + C_2$$

the last two equations may be written as

$$\left\{ \frac{c_m^2}{(6\mu U_n \sqrt{2R_I c_m})} \right\} p_r = (1/\cos^2 \psi_I^*) \left[\frac{\sin 4\psi_I}{32} + \frac{\sin 2\psi_I}{4} + \frac{3\psi_I}{8} \right] - \frac{\sin 2\psi_I}{4} - \frac{\psi_I}{2} + C_1 \quad (4.2.28)$$

and,

$$\left\{ \frac{c_m^2}{(6\mu U_n \sqrt{2R_o c_m})} \right\} p_{r, II} = (1/\cos^2 \psi_{II}^*) \left[\sin^4 \psi_{II}/32 + \sin^2 \psi_{II}/4 + 3\psi_{II}/8 \right] - \sin^2 \psi_{II}/4 - \psi_{II}/2 + C_2 \quad (4.2.29)$$

Applying the boundary conditions

$$\text{at } x_n \rightarrow \infty \quad p_{r, I} \rightarrow 0 \quad (\text{ambient})$$

i.e.

$$\text{at } \psi \rightarrow \pi/2 \quad p_{r, I} \rightarrow 0$$

with this condition equation (4.2.28) gives

$$C_1 = \pi/4 - (1/\cos^2 \psi_I^*) [3\pi/16]$$

Substituting the above expression of C_1 in equation

(4.2.28) we get

$$\left\{ \frac{c_m^2}{(6\mu U_n \sqrt{2R_r c_m})} \right\} p_{r, I} = (1/\cos^2 \psi_I^*) \left[\sin^4 \psi_I/32 + \sin^2 \psi_I/4 + 3\psi_I/8 - 3\pi/16 \right] - \sin^2 \psi_I/4 - \psi_I/2 + \pi/4 \quad (4.2.30)$$

The other boundary condition is

$$\left. \begin{aligned} \text{e} \quad \psi_{II} &= \psi_{II}^* \\ p_r \end{aligned} \right]_{II} = 0$$

Substituting the above condition in equation (4.2.29) we get

$$C_2 = \sin 2\psi_{II}^*/2 + \psi_{II}^*/2 - (1/\cos^2\psi_{II}^*) [\sin 4\psi_{II}^*/32 + \sin 2\psi_{II}^*/4 + 3\psi_{II}^*/8]$$

Substituting this expression for C_2 in equation (4.2.29) we get

$$\begin{aligned} \left. \left\{ c_m^2 / (6\mu U \sqrt{2R_0 c_m}) \right\} p_r \right]_{II} &= (1/\cos^2\psi_{II}^*) [\sin 4\psi_{II}^*/32 + \sin 2\psi_{II}^*/4 \\ &+ 3\psi_{II}^*/8] - \sin 2\psi_{II}^*/4 - \psi_{II}^*/2 + \sin 2\psi_{II}^*/4 + \psi_{II}^*/2 - \\ &(1/\cos^2\psi_{II}^*) [\sin 4\psi_{II}^*/32 + \sin 2\psi_{II}^*/4 + 3\psi_{II}^*/8] \end{aligned} \quad (4.2.31)$$

Since the connection between the two regions is continuous, we have $C_I^* = C_{II}^*$; from which we may write

$$\psi_I^* = \psi_{II}^* \quad (4.2.32)$$

Let ψ_{I0} be defined as the transformed angle that corresponds to the distance of the point of minimum

clearance (point O in Figure 27) from the inlet transition point where $\eta=0$ (i.e. transformed angle corresponding to normalized length η_c). This angle may be determined from equation (4.2.18) and is written as

$$\psi_{I0} = \tan^{-1}(-K_1 \eta_c) \quad (4.2.33)$$

The importance of this angle is that for a particular combination of rider roller size and its location, it enables one to determine whether the pressure developed by the rider roller is within the inlet region or is partially in the inlet region and partially in the uniformity region (for the latter case this angle may be further used in determining the point where $\psi=\psi^*$ by solving equation (4.2.34)). This fact may be determined by first assuming that the whole pressure development is within the inlet region (refer Figure 28). For this case the angle ψ^* is determined (the angle corresponding to $c=c^*$). This angle may be determined by applying the condition that at $\psi_I=\psi^*$; $p_I = 0$ in equation (4.2.30) and is calculated to be -25.415° . If ψ_{I0} is less than -25.415° the pressure developed is within the inlet region. And if it is greater than -25.415° the pressure developed is partially in the inlet region and partially in the uniformity region.

Let us now develop a pressure equation for the latter

case where pressure is partially in the inlet region and partially in the uniformity region. We then have a condition

$$\text{e} \quad \psi_{II} = 0 ; \quad \psi_I = \psi_{I0} ; \quad p_{rI} = p_{rII}$$

With this condition equations (4.2.30) and (4.2.31) combine to give

$$\begin{aligned} \left\{ K_2/K_1 \right\} \left[(1/\cos^2\psi^*) \left\{ \sin^4\psi_{I0}/32 + \sin^2\psi_{I0}/4 + 3\psi_{I0}/8 - \right. \right. \\ \left. \left. 3\pi/16 \right\} - \sin^2\psi_{I0}/4 - \psi_{I0}/2 + \pi/4 \right] = \\ \left[\sin^2\psi^*/4 + \psi^*/2 - (1/\cos^2\psi^*) \left\{ \sin^4\psi^*/32 + \right. \right. \\ \left. \left. \sin^2\psi^*/4 + 3\psi^*/8 \right\} \right] \end{aligned} \quad (4.3.34)$$

This equation may be solved to obtain the value of ψ^* for particular values of K_1 and K_2 ; from which we may determine C^* .

Using the following trigonometric relations

$$\sin 2\psi = 2 \left\{ \tan\psi / \sec^2\psi \right\}$$

and,

$$\sin^4\psi = 4 \left\{ \tan\psi / \sec^2\psi \right\} \left\{ 2/\sec^2\psi - 1 \right\}$$

we may write equation (4.2.30) as

$$\begin{aligned}
\left\{ \frac{c_m^2}{(6\mu U_n \sqrt{2R_r c_m})} \right\} P_{R_I} &= (C^*/8) \{2/\sec^2 \psi_I - 1\} \{2/\sec^2 \psi_I - 1\} \\
&+ (1/2) \{ \tan \psi_I / \sec^2 \psi_I \} (C^* - 1) + (\psi_I/2) \{3C^*/4 - 1\} \\
&- (\pi/4) \{3C^*/4 - 1\}
\end{aligned} \tag{4.2.35}$$

Using equations (4.2.5), (4.2.18) and (4.2.21) the above equation may be written in a normalized pressure form as

$$\begin{aligned}
P_{R_I} &= (\Lambda/K_1) \left[(C^*/8) \{K_1(\eta - \eta_C)/C_I\} \{2/C_I - 1\} \right. \\
&+ (1/2) \{K_1(\eta - \eta_C)/C_I\} (C^* - 1) + \tan^{-1} \{K_1(\eta - \eta_C)\} \{3C^*/4 - 1\} / 2 \\
&\left. - (\pi/4) \{3\psi^*/4 - 1\} \right]
\end{aligned} \tag{4.2.36}$$

In an approach similar to that used above, equation (4.2.31) may be reduced to

$$\begin{aligned}
P_{R_{II}} &= (\Lambda/K_2) \left[(C^*/8) \{K_2(\eta - \eta_C)\} \{2/C_{II} - 1\} \right. \\
&+ (1/2) \{K_2(\eta - \eta_C)/C_{II}\} (C^* - 1) + \tan^{-1} \{K_2(\eta - \eta_C)\} \{3C^*/4 - 1\} / 2 \\
&- (\tan \psi^*/8) \{2/C^* - 1\} - (1/2) (\tan \psi^*/C^*) (C^* - 1) \\
&\left. - (\psi^*/2) \{3C^*/4 - 1\} \right]
\end{aligned} \tag{4.2.37}$$

The load w developed by the rider roller on the web at the inlet region may be determined by integrating the pressure developed within the inlet region of the web-supporting roller interaction. Such a load in an integral form is given by

$$w = \int_{\infty}^{\psi^*} p_r dx \quad (4.2.38)$$

which may be written as

$$w = \int_{\pi/2}^{\psi^*} p_r \frac{2R_r c_m}{\sec^2 \psi} d\psi \quad (4.2.39)$$

Using the expression of p_r from equation (4.2.36) and substituting $\psi^* = -25.415^\circ = -0.44355$ rad (for the case of pressure within the inlet region) in the above equation and performing the integration we get

$$w = 2.44752 \left\{ (\mu U_n R_r) / c_m \right\} \quad \text{lb/in} \quad (4.2.40)$$

Substituting the above relation in equation (4.2.13) we get

$$\Lambda = 0.41412 \left\{ w^2 / (\mu U_n T) \right\} \left\{ 6\mu U / T \right\}^{1/3} (R/R_r)^2 \quad (4.2.41)$$

4.3 Modification of the Computer Code to Account for Rider Roller Effects

The same coupled numerical technique of a Runge-Kutta method and a Milne predictor-corrector method (as used for

the solution of the governing differential equation (3.1.1)) is used for the solution of the modified differential equation (4.1.28). The essential difference between these two equations is the additional pressure term in the modified differential equation due to the external pressure. This term for the case of a rider roller has been developed in the previous section (see equation (4.2.12)). The analysis of the previous section is based on Figure 27 which depicts the partial distribution of pressure in both the inlet and uniformity region. The modification in the computer code is done on the basis of this analysis. However, as discussed earlier, since the modified differential equation is essentially true for the inlet region, numerical solutions will be obtained for the case when the pressure due to the rider roller is within the inlet region (with reference to Figure 28 for such a case the applied pressure development is confined within the region I).

Before starting the numerical solution it is important first to determine the angle ψ_{I0} produced by a given combination of K_1 and η_c (using equation (4.2.33)). As discussed in the previous section, for the rider roller pressure to be within the inlet region $|\psi_{I0}|$ should be greater than 25.415° . A solution cannot be obtained for the case when $|\psi_{I0}| < 25.415^\circ$ (because then some of the pressure due to the rider roller will be in the uniformity

region). Once the above condition is satisfied the numerical solution of the modified differential equation can be proceed. In order to incorporate the pressure term (equation (4.2.12)) in the modified differential equation we need three quantities; Λ , C^* , and C . Λ is the normalized quantity which relates to the minimum clearance between the web and rider roller (the significance of this quantity and those associated with C is discussed in the next section). C^* is the normalized clearance at the point where $\frac{dP}{dr} = P_r = 0$ and may be determined by using $C^* = \sec^2 \psi^*$ (see equation (4.2.21)). C is the local normalized clearance between the web and rider roller (for the case where pressure due to the rider roller is within the inlet region this local clearance is given by equation (4.2.1)).

Three subprograms have been added to the computer code in order to obtain the numerical solution of the modified differential equation. This modified computer program is listed in Appendix I. In this program the purpose of the subroutine "SEARCH" is to determine the value to ψ^* for the given parameters which satisfies equation (4.2.34). Note that the parameter K_2 relates to the region II of Figure 27. For the case where pressure is within the inlet region $K_2 = K_1$ (see equations (4.2.5) and (4.2.6)). The local clearance C for the case where pressure is within the inlet region may be determined for each value of η by using equation (4.2.1). Note that there are two normalized

quantities in the equation C; K_1 and η_c . The significance of these quantities will be discussed in the next section. Functions "EQN1" and "EQN2" may be used for calculating the pressure due to rider roller for the two regions I and II (see Figure 27) by the use of equations (4.2.36) and (4.2.37), respectively. Each set of these three quantities (Λ , C^* , and C) are substituted in the equation of pressure (equation (4.2.12)) which finally is incorporated in the solution of the modified differential equation (equation (4.1.28)).

4.4 Significance of the Normalized Quantities and Discussion of Results

The significance of H'' was obvious from chapter III where it was shown that its asymptotic value allows one to determine the constant gap film thickness. The governing dimensional expression between the asymptotic value of H'' and the constant gap film thickness h_0 is given by equation (3.4.1). The significance of the other normalized quantities, developed in this chapter, will be discussed in this section along with the discussion of the numerical results.

As discussed earlier, the essential difference between the governing differential equation (equation (3.1.1)) and the modified differential equation (equation (4.1.28)) is

the term due to the pressure developed via the rider roller. This term will be incorporated from the analysis of the previous section (equation (4.2.12)). The effect of this term may be observed by varying the size of the rider roller, by varying its location, or by varying the amount of load on the web due to the rider roller. The normalized expressions that may be used in order to examine the effects of varying these three quantities are given by equations (4.2.5), (4.2.18), and (4.2.13), respectively. The variation in these three quantities will enable us to determine the effect of the rider roller size, its location, and the imposed pressure on the constant gap film thickness.

Observe from equation (4.2.40) that the load w due to the rider roller depends on both the radius of the rider roller R_r and the amount of minimum clearance c_m . In other words, the effect of imposed pressure and the size of the rider roller are interrelated. An increase in the rider roller size will always be associated with an increase in the pressure even when c_m is kept the same. However, since Λ may be considered as a function of c_m for a particular set of operating parameters (see equation (4.2.13)), this normalized quantity may be used to vary the amount of imposed pressure by varying the minimum clearance c_m . For a particular rider roller size R_r this variation in c_m will result in different values of K_1 . Thus in order to examine

the effect of varying imposed pressure by changing c_m it is necessary to modify both the normalized quantities K_1 and Δ . However, keeping K_1 constant (see equation (4.2.5)) while varying Δ means that the amount of the imposed pressure (or load) is varied by changing both the radius of the rider roller and the minimum clearance. Physically, this is shown in Figure 30. Let us now discuss the significance of the above mentioned normalized quantities in detail and relate their effects on the numerical results.

First consider the significance of the normalized quantity K_1 . This quantity relates to the size of rider roller for a particular set of operating parameters (i.e. radius of supporting roller, tension in the web, sum of the web and supporting roller speed and the clearance between the web and rider roller), see equation (4.2.5). It can be seen from this equation that as the normalized quantity K_1 is increased the dimensional radius of the rider roller decreases and vice versa. Thus the effect of rider roller size may be obtained by varying the parameter K_1 (a normalized quantity) and substituting that value of K_1 into equation (4.2.1) which finally appears in the pressure equation (4.2.12). In obtaining the numerical solution Δ is kept constant (i.e. c_m constant) while K_1 is changed by varying R_r . This phenomenon of changing R_r

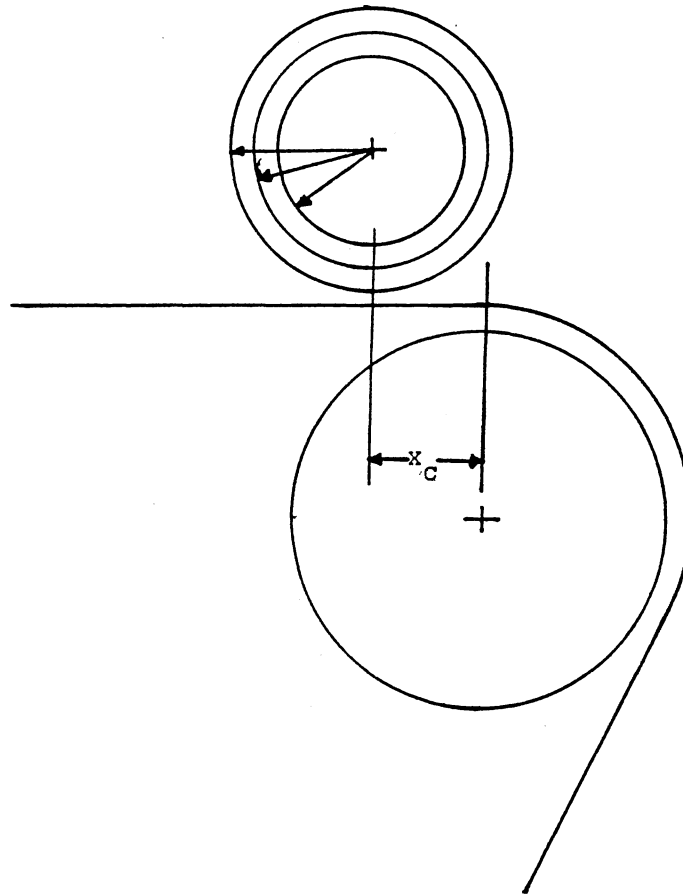


Figure 30. Sketch Illustrating Method of Increasing Rider Roller Pressure

while keeping c_m constant along with the location of the rider roller is shown in Figure 31. Note from equation (4.2.40) that the change in R_r is associated with a change in load w or pressure due to the rider roller. Figure 32, which is obtained from the numerical solution of the modified differential equation and by keeping $\Lambda=5$ and $\eta_c=1$ (these values of Λ and η_c are arbitrarily chosen), shows the effect of the rider roller size on the constant gap film thickness. In this and the subsequent figures the term BN and ETC represent the normalized quantities Λ and η_c , respectively. This figure basically shows the asymptotic values of H'' (i.e. $H''(\infty)$) for a range of K_1 values. It can be seen that as the value of K_1 is decreased (i.e. rider roller size is increased) the constant gap film thickness decreases. Note that the numerical solution has not been obtained for K_1 lower than 0.4. This is due to the limitation on the numerical value of the product of K_1 and η_c which should not be lower than 0.475156. Note that this numerical value has been obtained by substituting the limiting value of ψ_{I0} (i.e. 25.415°) in equation (4.2.33). It is obvious that if K_1 is reduced below 0.4 then $K_1\eta_c$ (since $\eta_c=1.0$) will be significantly lower than the limiting value of 0.475156 and thus a large amount of pressure will be developed in the uniformity region for which the modified differential equation is not

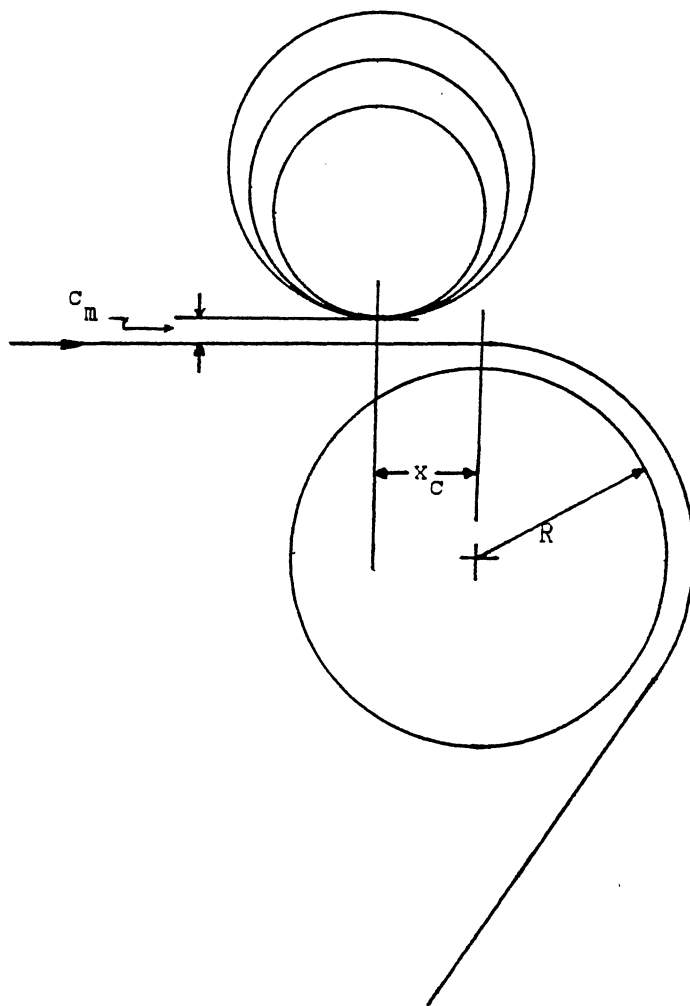


Figure 31. Sketch Illustrating Method of Varying Rider Roller Size

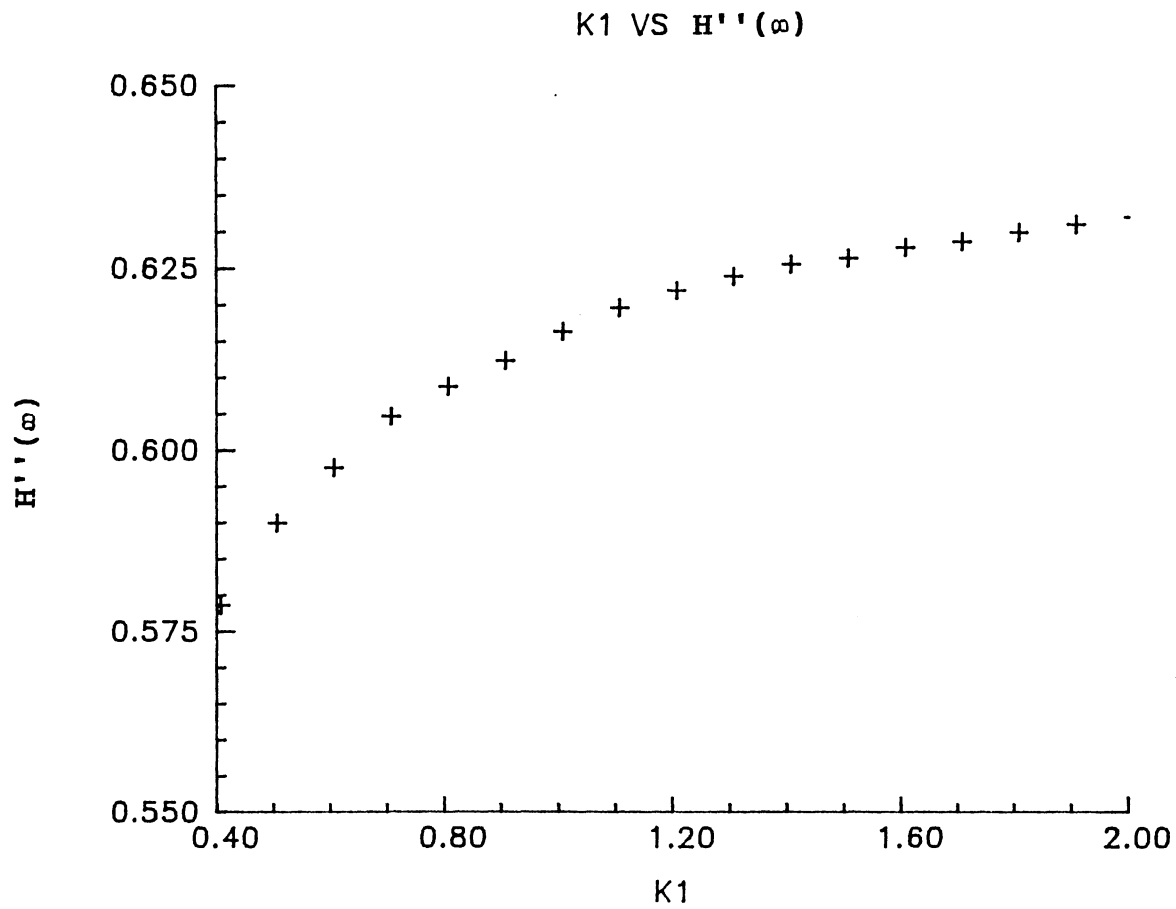


Figure 32. Effect of Rider Roller Size on Constant Gap Film Thickness - Normalized

valid. This limitation was discussed in detail in the last two sections. Observe from Figure 32 that there is a continuous reduction in $H''(\infty)$ which is due to the fact that as K_1 is decreased the amount of pressure development within the inlet region (which is of small length $5\eta - 8\eta$) increases. This higher amount of pressure due to the rider roller within the inlet region is basically responsible for the greater reduction in the film thickness as the value of K_1 is decreased (i.e. as the size of the rider roller is increased). This increment in the amount of the imposed pressure due to the rider roller for different values of K_1 is shown in Figure 33. It can be seen that as the value of K_1 is decreased (rider roller size is increased) the pressure development increases. It is interesting to note that increasing the rider roller size results in an increase of pressure development area (i.e. η range). This physically explains why the product of $K_1\eta_C$ has to be kept within a limit so that the pressure due to the rider roller remains within the inlet region (as discussed earlier). The pressure distribution in the air film beneath the web is shown in Figure 34 for three different values of K_1 (this and the subsequent pressure curves are obtained for a normalized pressure defined by equation (2.4.7)). It can be observed that there is almost no effect of the rider roller on the pressure in the air film since the pressure due to the rider roller only affects the

ETA VS Pr

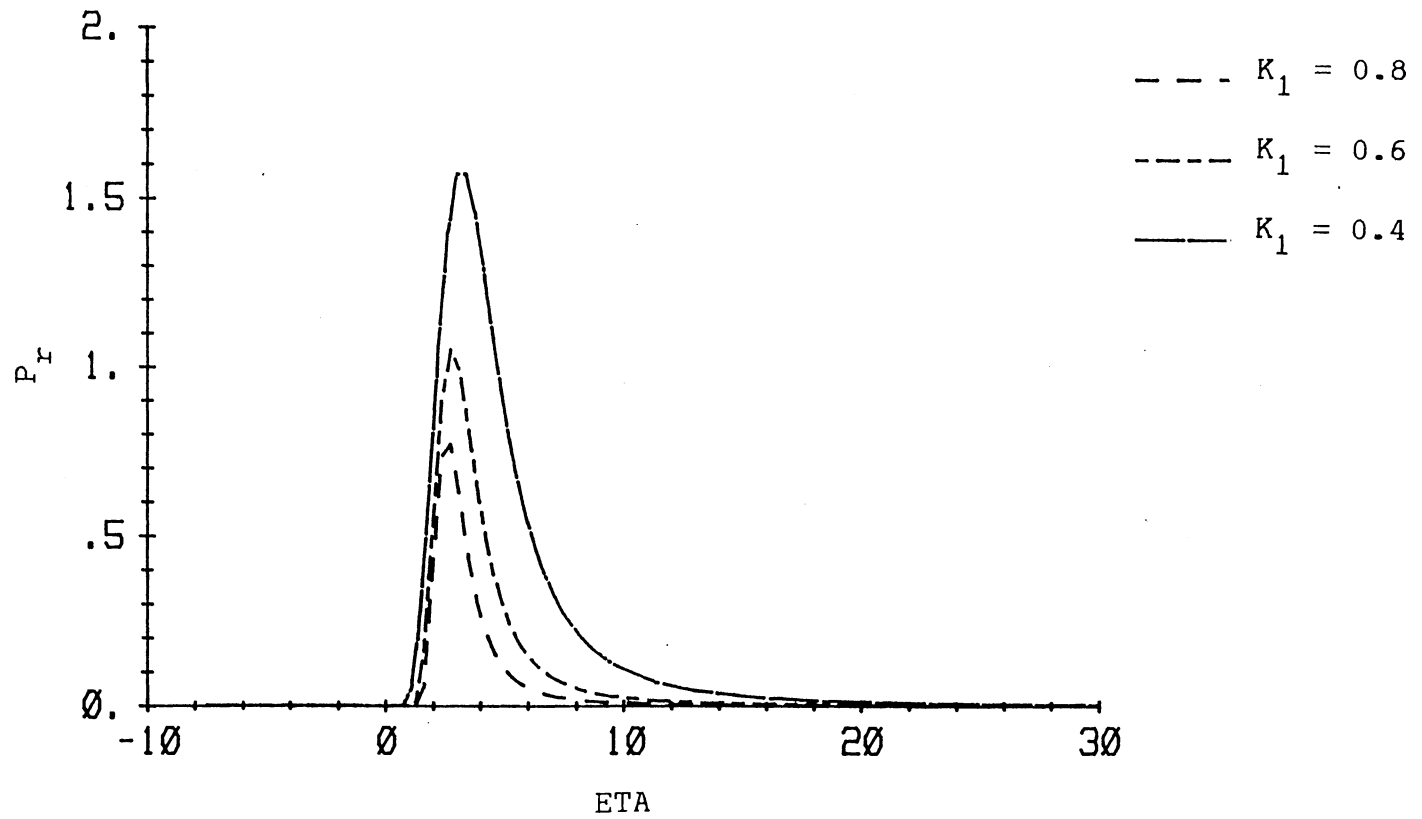


Figure 33. Rider Roller Pressure for Three Different K_1 Values (BN=5.0, ETC=1.0)

ETA VS Pn(Pn=pR/T)

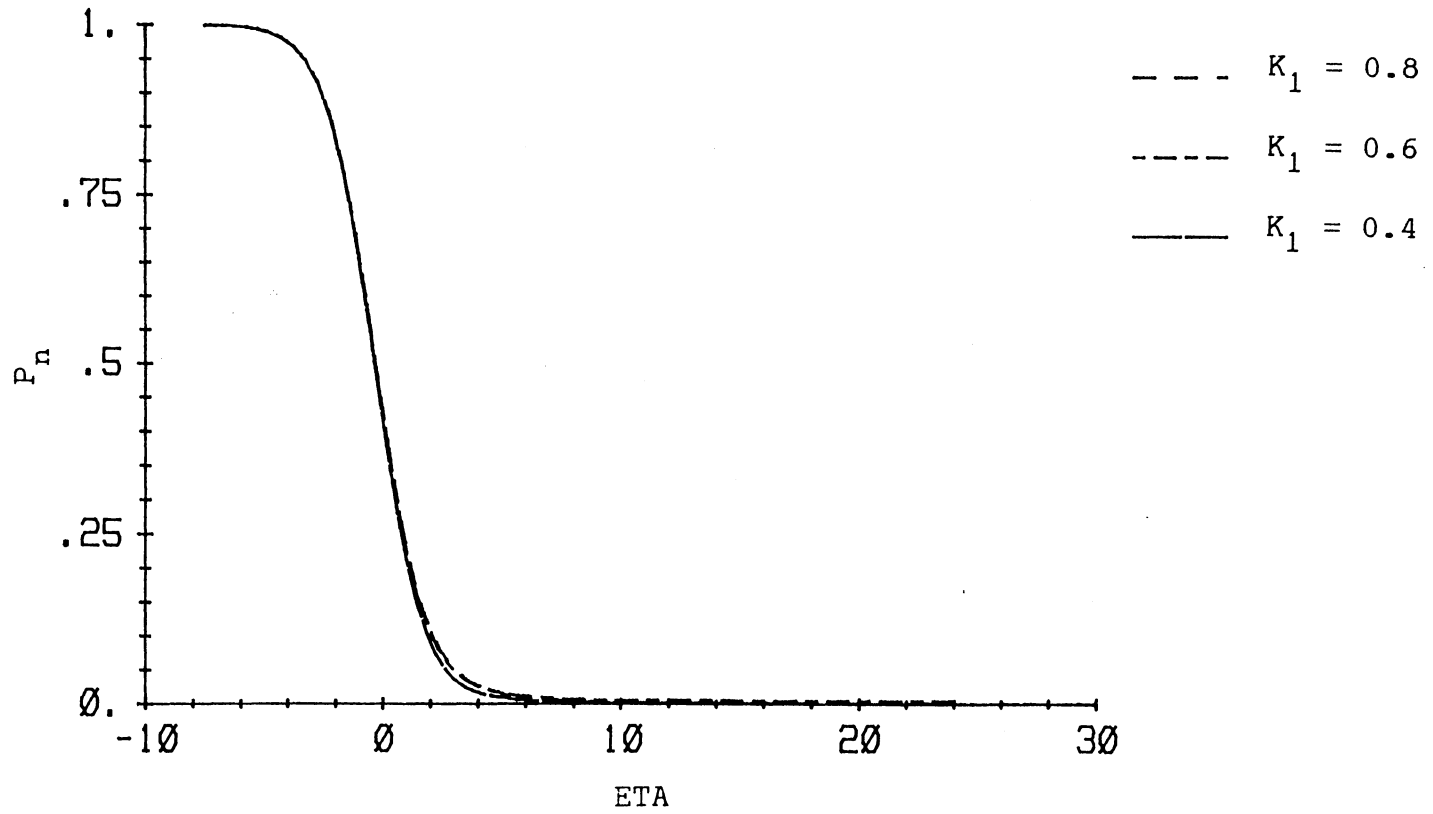


Figure 34. Pressure in the Air Film for Three Different K_1 Values (BN=5.0, ETC=1.0)

equilibrium of the web. Note that these last two plots for three different values of K_1 are obtained for $BN=5$ and $\eta_C=1.0$. As mentioned earlier, keeping Λ constant means that the minimum clearance is kept same for all value of K_1 . In other words, the radius of the rider roller is changed while the minimum clearance is kept same for all sizes of the rider roller (see Figure 31).

Let us now discuss the significance of the normalized quantity η_C . Recall that η_C is the normalized distance of the minimum clearance point from the inlet transition point i.e. from the point where $\eta=0$ (see Figure 28). Thus this quantity may be used to observe the effect of the rider roller location. The rider roller location may be varied by changing η_C within the inlet region; i.e. between $\eta=0$ to $\eta=\infty$ (where ∞ corresponds to the point where $p \rightarrow p_a$). In order to observe the effect of rider roller location, the rider roller size and the minimum clearance (the normalized quantities Λ and K_1) should be kept constant while the value of η_C is varied within the inlet region. Physically this is shown in Figure 35. Note that by keeping Λ and K_1 constant we are keeping the amount of imposed pressure due to the rider roller constant. The dimensional quantity x_C corresponding to η_C may be obtained from equation (2.3.10b). The numerical solution for observing the effect of rider roller location has been obtained for constant

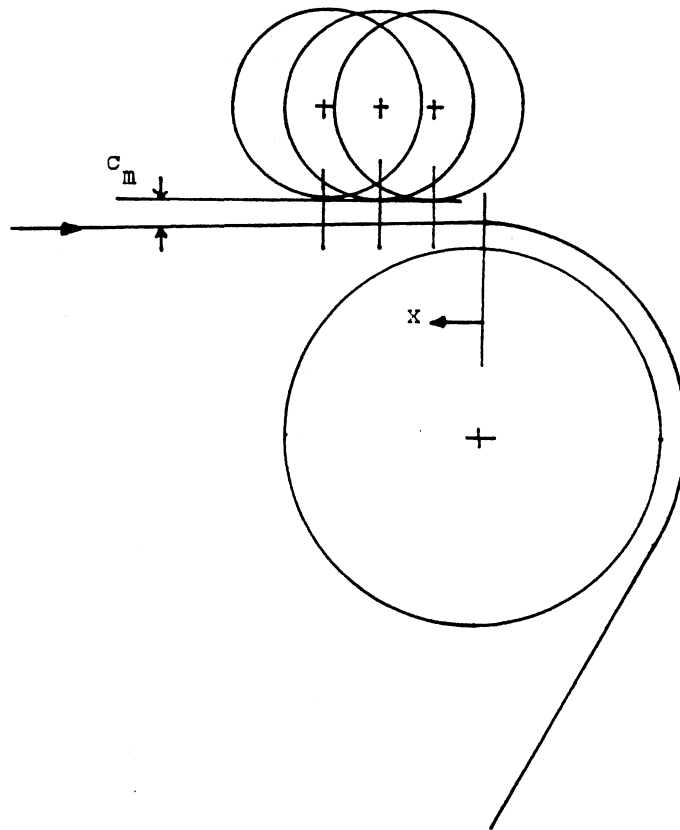


Figure 35. Sketch Illustrating Method of Varying Rider Roller Location

values of $BN=5.0$ and $K_1=0.50$ (i.e same value of both c_m and R_r). Figure 36 shows the effect of rider roller location on the constant gap film thickness. The reduction in the asymptotic value of H'' can be seen as the rider roller is moved towards the inlet transition region. It can be seen that as the rider roller is moved away from the inlet transition region the value of $H''(\infty)$ increases. A rider roller located near the inlet transition region develops most of the pressure within the inlet region and thus is most effective in reducing $H''(\infty)$ (i.e. constant gap film thickness). This pressure distribution due to the rider roller for three different positions is shown in Figure 37. Since the rider roller size (R_r) and the minimum clearance c_m are kept the same (i.e the same values of K_1 and Λ) for the three different positions of the rider roller, the amount of pressure development is constant (i.e the area under the curve is the same). The only effective parameter is the location of the rider roller. The pressure in the air film beneath the web (see Figure 38) is again observed to be almost the same except that the length of the inlet region decreases slightly as the rider roller moves away from the inlet transition region (since the asymptotic value of P_n is reached at small η range). Observe that at infinity the pressure is not exactly zero. Physically, this is because of the presence of a certain amount of rider roller pressure at infinity (see Figure 37). Mathematically, this

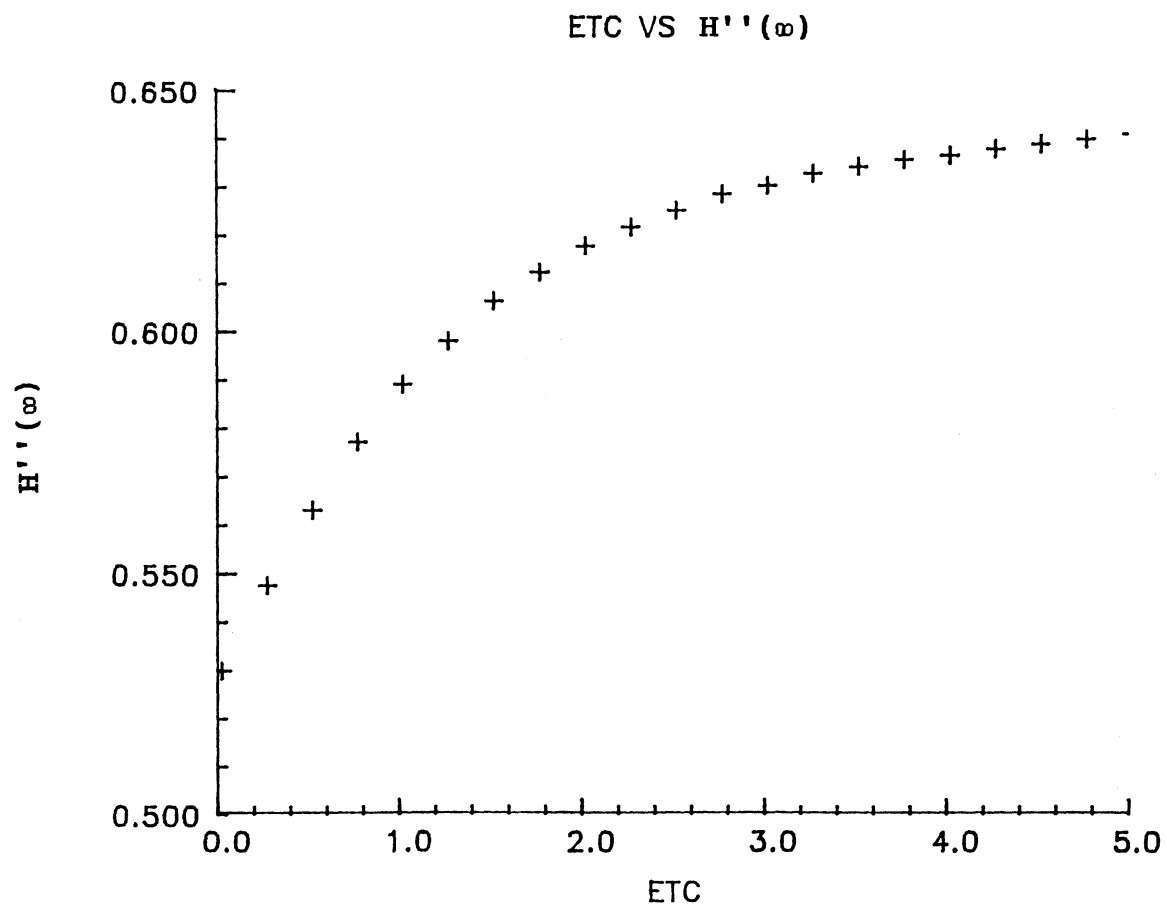


Figure 36. Effect of Rider Roller Location on Constant Gap Film Thickness - Normalized

ETA VS Pr

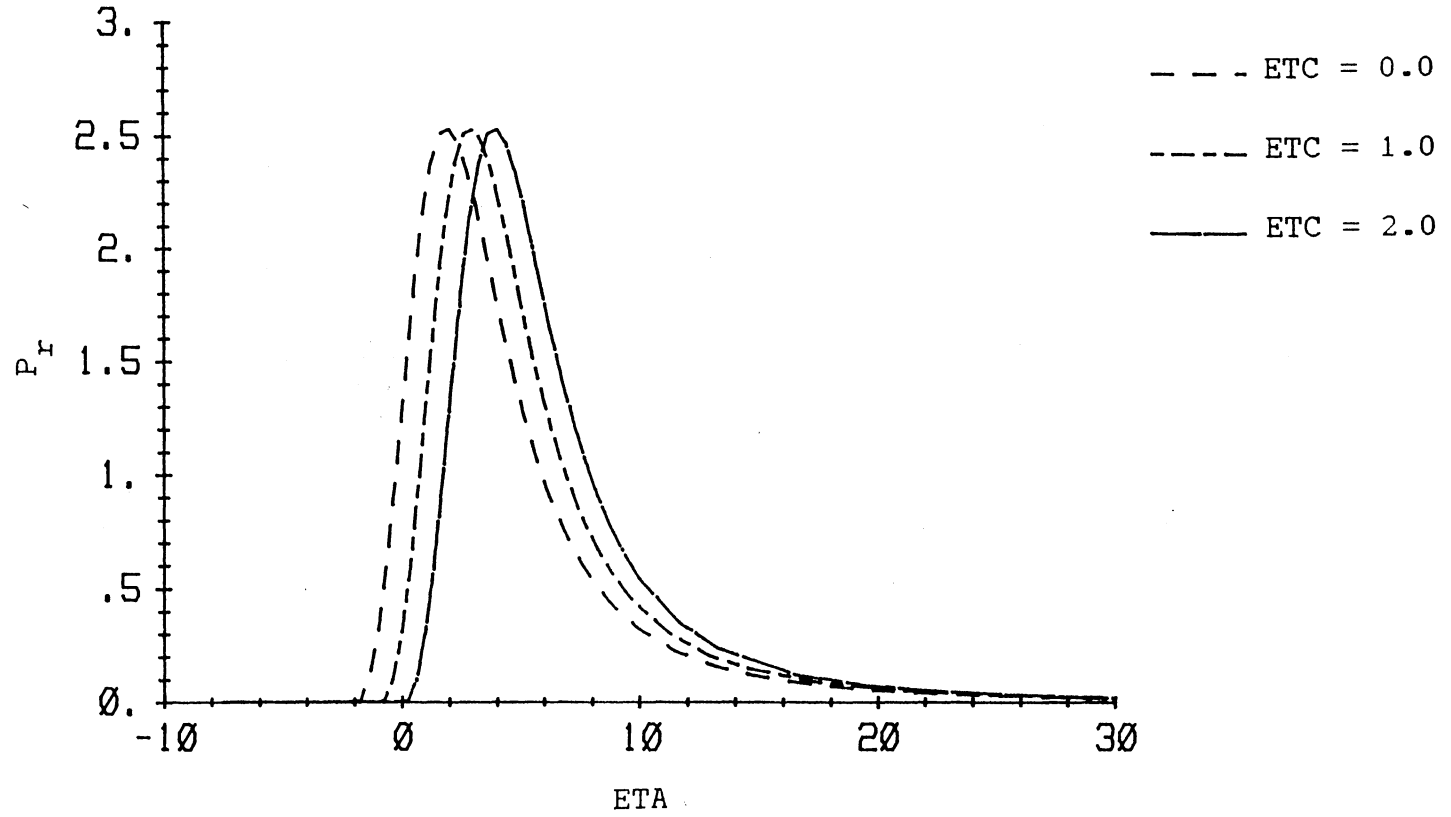


Figure 37. Rider Roller Pressure for Three Different η_c Values (BN=5.0, $K_1=0.5$)

ETA VS Pn(Pn=pR/T)

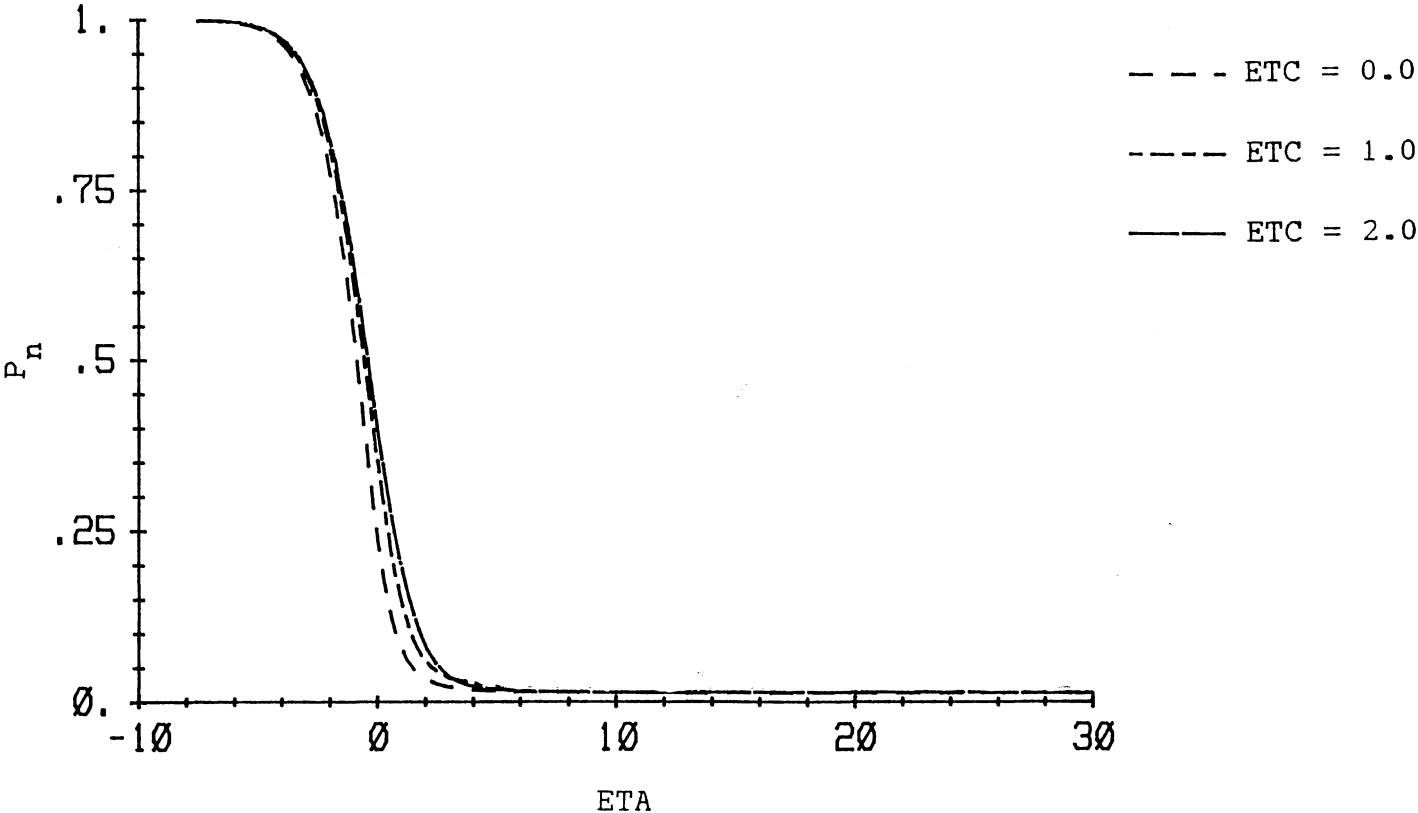


Figure 38. Pressure in the Air Film for Three Different η_c Values (BN=5.0, $K_1=0.5$)

may be justified from equation (4.1.21) which indicates that if the rider roller pressure exists at infinity then the pressure in the air film will not be ambient but a sum of ambient and rider roller pressure (since at infinity the last term of equation (4.1.21) becomes zero).

The effect of varying the amount of imposed pressure due to a rider roller located somewhere in the inlet region may be seen from the expression of Λ given by equation (4.2.13) which appears in the pressure equation. For a rider roller this relates to the amount of load developed on the web (see equation (4.2.41)). It is clear that an increase in load w will increase the value of this normalized quantity. The effect of the imposed pressure may thus be seen by varying the dimensional quantity w (lb/in). Note that the variation in load w is possible by changing the radius of the rider roller R_r and by changing the minimum clearance c_m (see equation (4.2.40)). To observe the effect of the imposed pressure, K_1 will be kept constant along with η_c while Λ is varied. This combination of the normalized quantities has already been discussed earlier in this section with the help of Figure 30. The effect of varying the normalized quantity Λ for $K_1 = 0.5$ and $\eta_c = 1.0$ is shown in Figure 39. This figure shows the effect of imposed pressure on the constant gap film thickness (note BN represents Λ). The reduction in the asymptotic value of H'' is clear as the amount of imposed

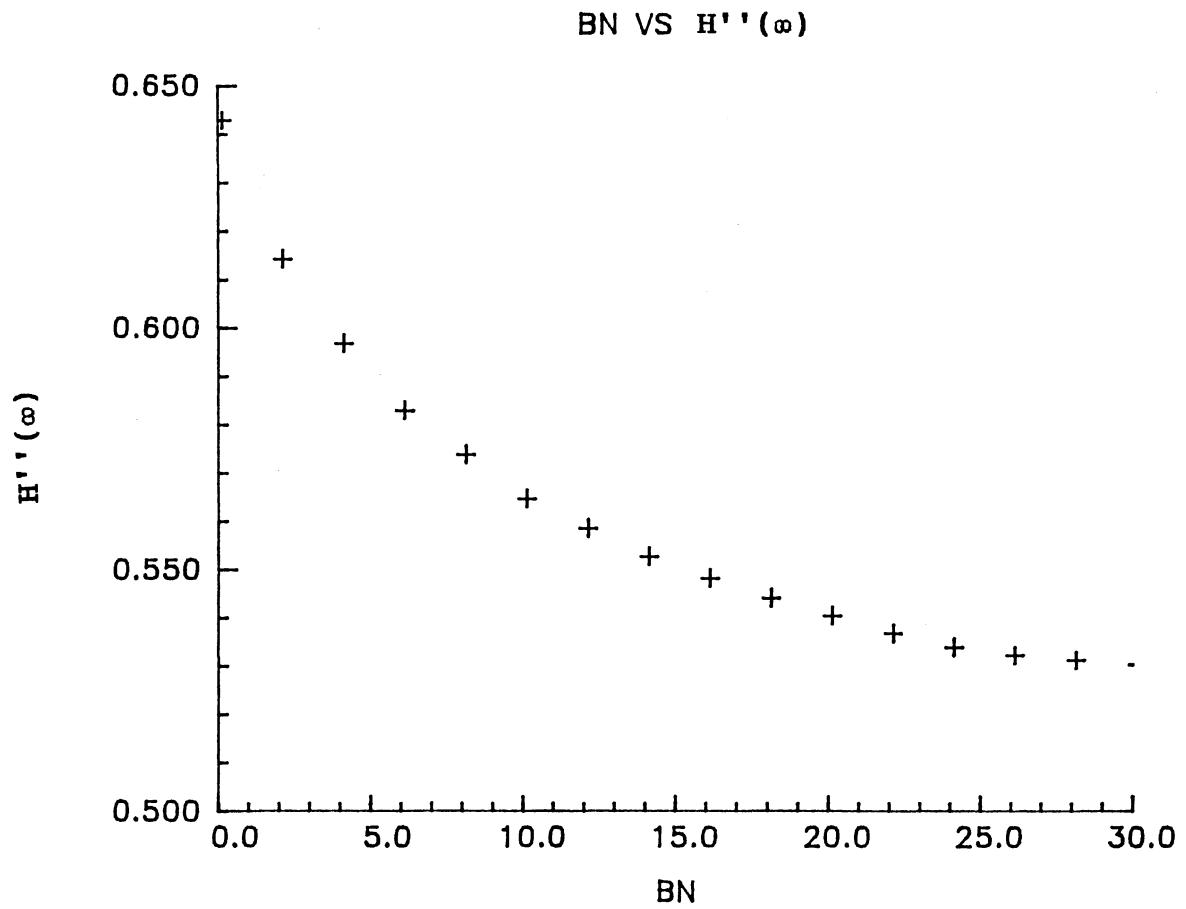


Figure 39. Effect of Imposed Pressure on Constant Gap Film Thickness - Normalized

pressure (i.e. BN) is increased. It may be observed from this curve that a limit is approached beyond which the increment in BN will not be effective in reducing the air film thickness. This is due to the fact that the derivation of the rider roller pressure (equation (4.2.12)) is based on the entrainment of the air (which is assumed to be incompressible) between the web and rider roller. In other words, the pressure on the web due to the rider roller is assumed to be the pressure which is developed in the air film between the web and the rider roller. Such an analysis is the basis of many lubrication problems (like slider bearings, gear teeth meshing, lubricating channel between two discs, etc). In such problems the increment in the bearing number (for the present problem the bearing number is Δ) after a certain limit is not effective in reducing the air film thickness. In the case of the present problem this behaviour is shown in Figure 39 where it can be seen that after a certain limit of BN (i.e. Δ) the increment in BN (or Δ) is not effective in reducing the constant gap film thickness. Note that in the development of the rider roller pressure the effects of the flexibility of the web were not considered (the consideration of the flexibility of the web in the development of the rider roller pressure requires a consideration of a web element under a complex state of bending moments and middle-plane forces due to both the wrapping of the web around the supporting roller and pressure on the web due to the rider

roller). Due to this simplification the present work has the limitation on the amount of external pressure applied. In the actual problem due to the flexibility of the web, after a certain amount of pressure the web will bend by wrapping around the rider roller, a situation which the present model cannot handle.

The increment in the amount of pressure due to rider roller is obvious from Figure 40, as BN is increased. Again note that the increment in the amount of pressure is due to the combined effect of varying rider roller size R_r and minimum clearance c_m . The pressure in the air film beneath the web is same as can be seen from Figure 41. The only difference occurs in the range of η at which the pressure approaches the ambient. It can be observed that as the load is increased the length of the inlet region is slightly decreased (i.e ambient pressure is achieved in a smaller η range).

4.5 An Example of Air Film

Thickness Control

In this section the effect of the rider roller on the constant gap film thickness will be examined for the dimensional parameters by considering the following operating parameters as an example

Radius of the supporting roller	=18 in
Reduced tension in the web	=1 lb/in

ETA VS Pr

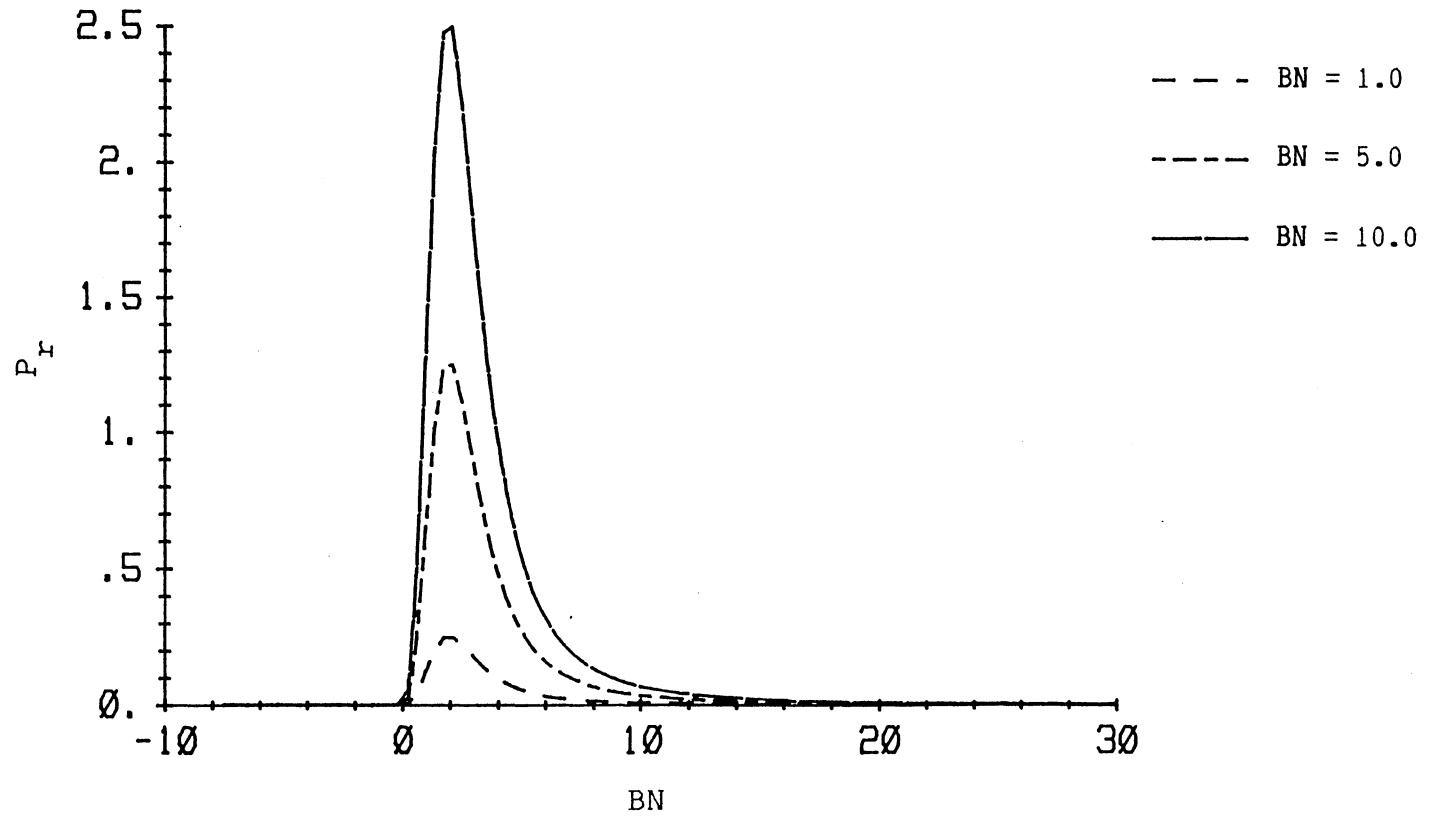


Figure 40. Rider Roller Pressure for Three Different BN Values (ETC=1.0, $K_1=0.5$)

ETA VS Pn(Pn=P_r/T)

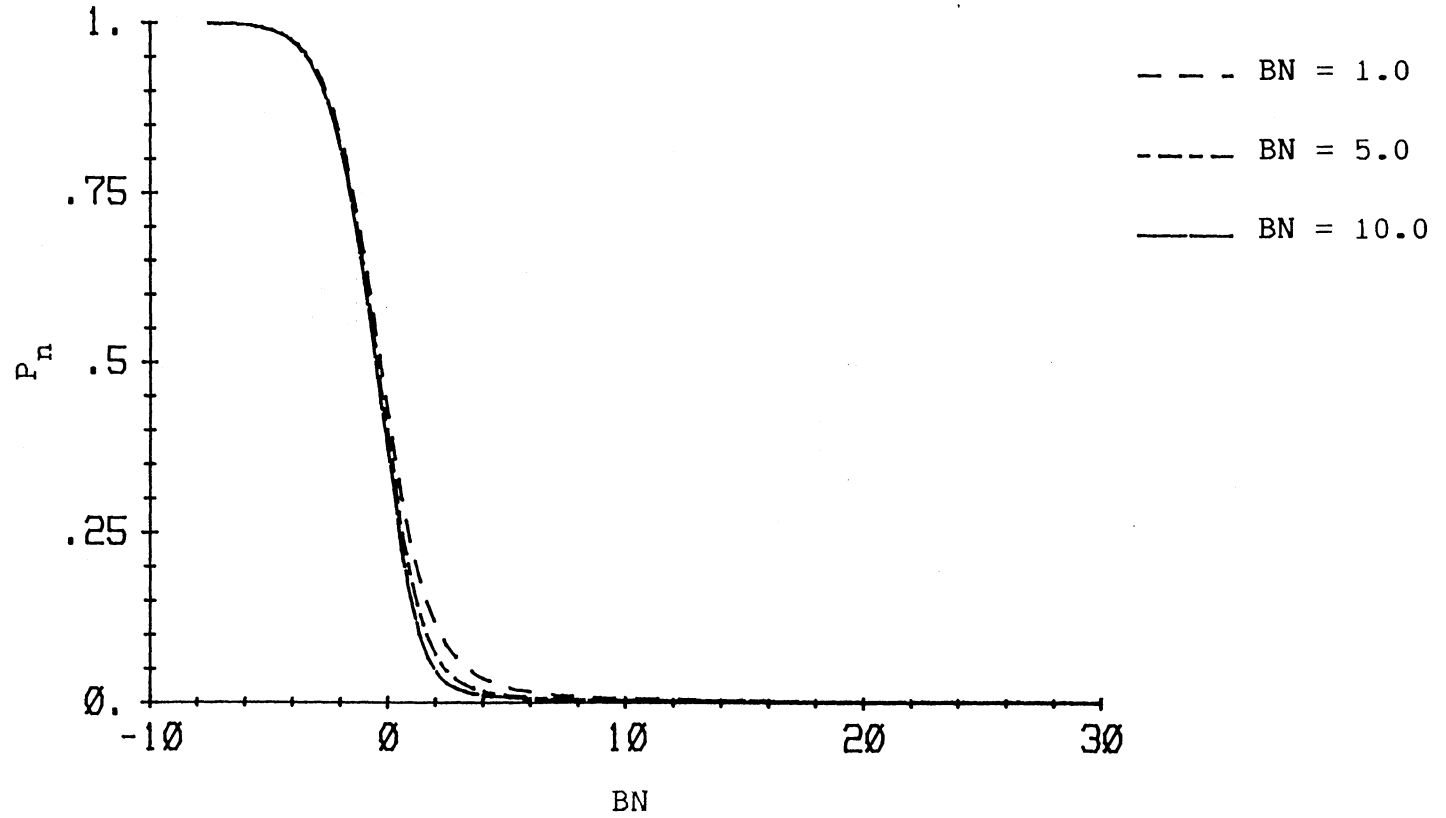


Figure 41. Pressure in the Air Film for Three Different BN Values (ETC=1.0, $K_1=0.5$)

Sum of the web and supporting roller speed =400 in/sec

Sum of the web and rider roller speed =400 in/sec

As discussed in the last section, the dimensional quantities corresponding to the three normalized quantities Λ , K_1 and η_c are the minimum clearance between the web and rider roller c_m , the radius of the rider roller R_r , and the dimensional location of the rider roller x_c . The effect of these three dimensional parameters will be obtained for the above mentioned operating parameters on the constant gap film thickness.

Figure 42 shows the effect of rider roller size (R_r) on the constant gap film thickness (h_0). This result has been obtained for the case where rider roller size is increasing while the minimum clearance and the location of the rider roller are kept same for all sizes of the rider roller (see Figure 31) so that the normalized quantities Λ and η_c remain constant while the radius of the rider roller is varied (i.e K_1 is varied). These constant values of x_c and c_m are 0.20 in and 1500 μ in, respectively. Compare this figure with Figure 32 which shows the effect of K_1 (normalized quantity which relates the radius of rider roller). A reduction in constant gap film thickness is observed as the radius of rider roller is increased.

Figure 43 shows the effect of rider roller location x_c (in dimensional form) on the constant gap film thickness

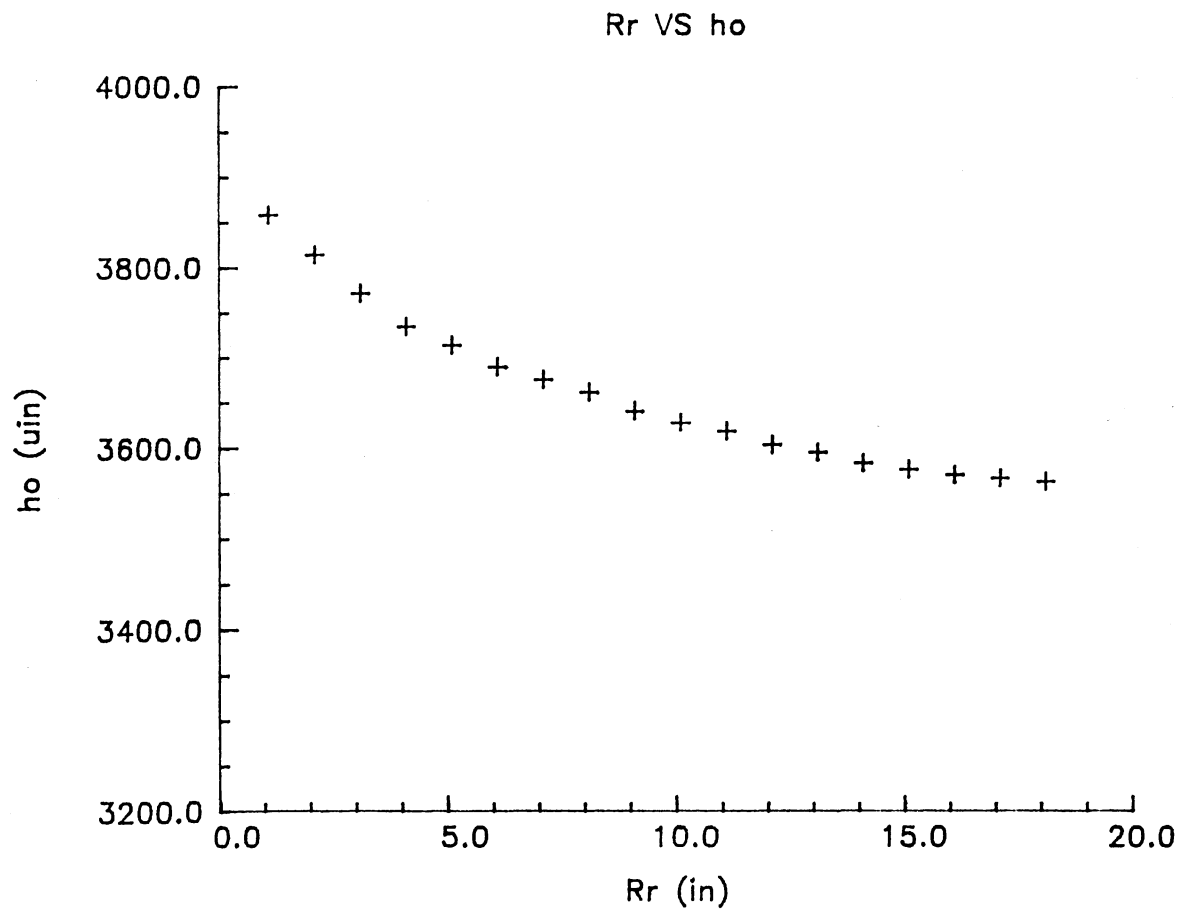


Figure 42. Effect of Rider Roller Size on Constant Gap Film Thickness - Dimensional

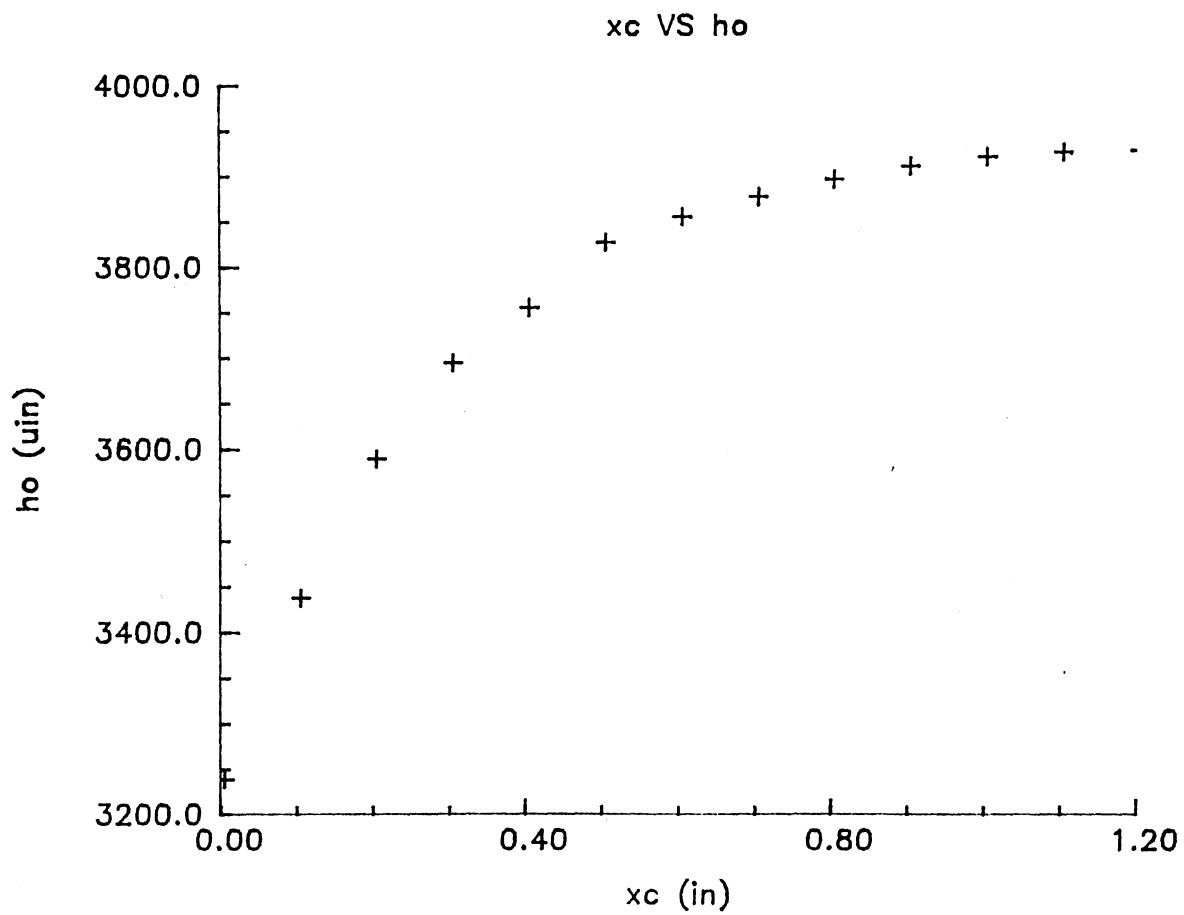


Figure 43. Effect of Rider Roller Location on constant Gap Film Thickness - Dimensional

h_0 . This plot has been obtained for a constant value of both $c_m = 1500 \mu\text{in}$ and $R_r = 6 \text{ in}$. Since η_c is the normalized value of x_c , a curve similar to the one shown in Figure 36 is obtained. Again observe that as the rider roller is moved towards the inlet transition region the reduction in the constant gap film thickness h_0 increases.

The effect of imposed pressure (in dimensional form) on constant gap film thickness is shown in Figure 44. Note that the relation expressing the load w is given by equation (4.2.40). As mentioned earlier, the load may be varied by changing the size of the rider roller R_r and by changing the amount of minimum clearance between the web and the rider roller (see Figure 30). It can be seen from Figure 44 that as the amount of load is increased (which may be due to change in both c_m and R_r) the constant gap film thickness h_0 is decreased. Comparing this figure with Figure 39 it can be seen that both curves (i.e. dimensional and dimensionless results) give the identical behavior. This curve has been obtained for a constant value of $x_c = 0.2 \text{ in}$

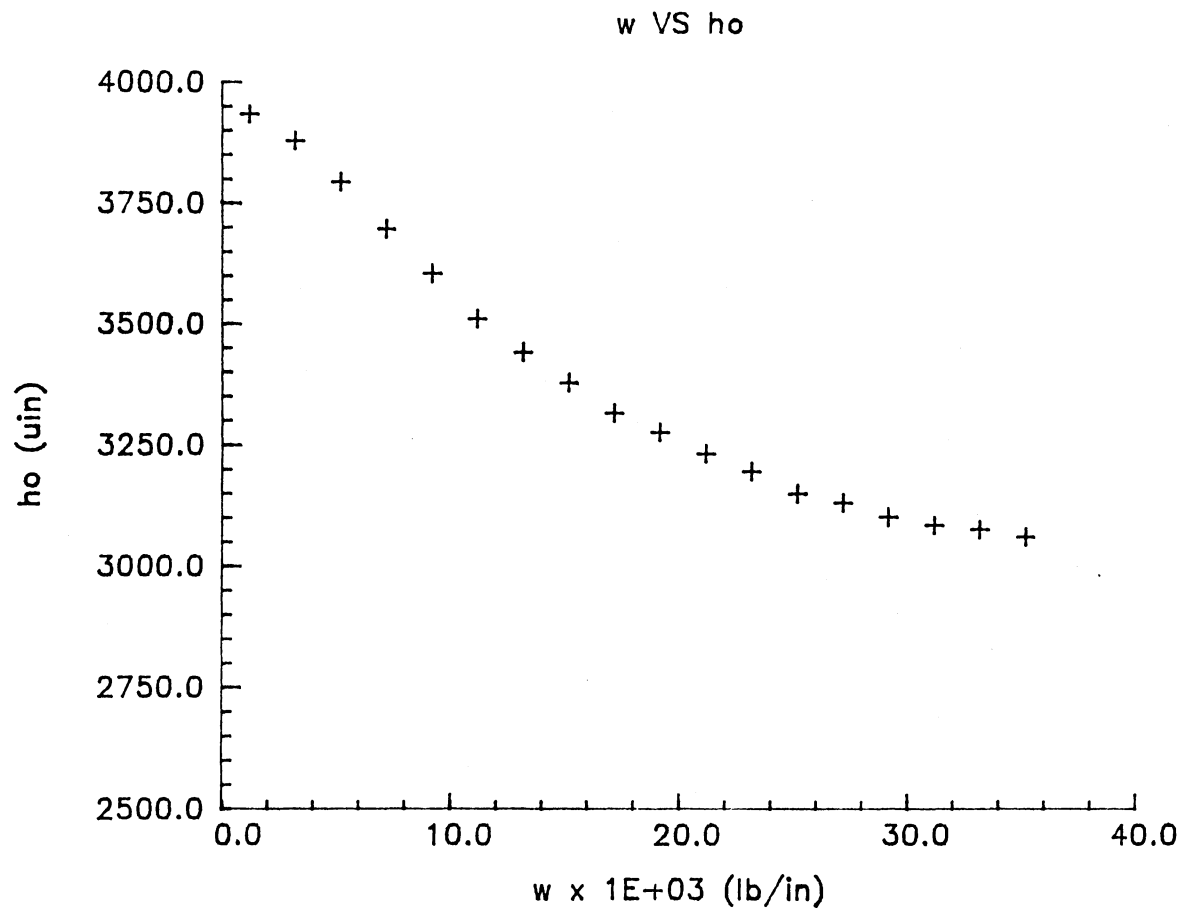


Figure 44. Effect of Imposed Pressure on Constant Gap Film Thickness - Dimensional

CHAPTER V

CONCLUSIONS AND RECOMMENDATIONS

5.1 Conclusions

The following conclusions are drawn from both the qualitative analysis and the numerical solution of the differential equations. Reference is made to the section or figure of the thesis where the details corresponding to each conclusion is laid down.

1. In the passage of a web over a supporting roller three regions exist; the entrance region where pressure increases from ambient to some value corresponding to the constant gap region, uniformity region in which both the air film thickness and the pressure are constant, and the exit region where the web undulates in order to adjust to the decreasing pressure from the constant gap region value to the ambient. (Ref. Section 2.6).

2. Constant gap air film thickness is dependent upon viscosity of air, sum of the web and supporting roller speed, radius of the roller, and the reduced tension in the web. This film thickness is given by equation (3.4.1).

$$h_0 = 0.643 R \left\{ (6\mu U) / T \right\}^{2/3}$$

3. Pressure in the constant gap region is given by equation (3.4.3).

$$p = p_a + T/R$$

From the above equation it is clear that the increase in air film pressure from ambient to constant gap region is T/R . This ratio for most web handling applications is small compared to ambient pressure. Thus the assumption of incompressibility should be appropriate (Ref. Section 3.4).

4. The length of the inlet region for most web handling applications is very small. This fact may be corroborated from Table III where it can be seen that for a roller of 18 in. radius the length of the inlet region is 2.14 inches, which is very small compared to the radius of the roller.

5. The constant gap film thickness is not the minimum film thickness, in fact, minimum film thickness occurs somewhere in the exit region and is approximately 71.6% of the constant gap film thickness. (Ref. Section 3.4 and Figure 18).

6. The modification of the mathematical formulation for the modified geometry, in which external pressure is applied on the web, results in a new modified equilibrium equation. The hydrodynamic lubrication equation is not affected. Since the constant gap air film thickness is dependent on the amount of air entrained through the inlet

region, the strategy for controlling air entrainment will be effective in the inlet region. (Ref. Section 4.2).

7. Increase in pressure on the web due to the rider roller results in a decrease in the constant gap film thickness. (Ref. Section 4.4).

✓8. It has been found numerically that a rider roller closer to the inlet transition point is most effective in reducing the air entrainment. (Ref. Section 4.4).

9. Since an increase in the rider roller size is associated with an increase in the pressure due to the rider roller, a reduction in the constant gap film thickness has been observed as the rider roller size is increased. (Ref. Section 4.4).

5.2 Recommendations for Future Work

The following points are recommended as the areas for the further investigations.

1. The model that has been developed is based on many assumptions. Before the study of this model is further extended it seems very appropriate to have an experimental verification of the model. The experimental phase will provide a reliable data base by which the present model may be tested (an experimental work in this regard is already underway under the guidance of principal investigator of this project).

The recommendations for extending the analytical model are described in the following points:

2. The transformation of the coordinate system to the transition regions lead to a solution which is independent of the length of the constant gap region (i.e. wrap angle). This approximation is true as long as a sufficient length of the uniformity region separates the inlet and exit regions and as long as the web is close to the roller. However, when the length of the uniformity region (i.e. wrap angle) approaches zero, the gap is expected to approach infinity because no radial component of tension is present to keep the web near the roller. On the basis of these arguments it seems important to obtain a formulation by considering the origin of the coordinate system at the center of the uniformity region. Such a formulation will enable one to obtain a solution dependent on the length of the uniformity region (i.e. wrap angle). Such a formulation will also be appropriate for examining the effects of applying external pressure in the uniformity region.

3. The present model will not give a true picture of air film thickness variation for web handling applications where porous materials are processed. It is recommended for future work to take into account the porosity effects. This will involve modification of the hydrodynamic equation and a one dimensional Reynolds equation will not be applicable for such a problem.

4. As mentioned earlier in the report, the neglect of the bending term in the web equilibrium equation leads to a solution valid for a perfectly flexible web. A perfectly

flexible web, thus, by our analysis is the one in which the resistance to bending is negligible and the tension term is the dominating one in the equilibrium equation. This idealization is very useful to get insight into the air entrainment mechanism for tension-dominated web handling applications. However, even a very thin web when bent over a small roller can produce substantial resistance to the bending thereby affecting the equilibrium equation. It is recommended that future work examines the effects of the resistance to bending of the web material in the development of air film thickness. For such a study one needs to consider the flexure rigidity of the web. The one dimensional hydrodynamic equation will still remain applicable, but in the web equilibrium equation the bending term should not be disregarded so that the effects of plane strain, plate type bending are included. The consideration of web rigidity is very important for the study of control strategy. The inclusion of this term will enable to examine the effects of applying load to the extent beyond which the web material will elastically deform.

5. We know that the entrance region is all important as far as the development of air film thickness is concerned. Any change in this region will ultimately affect the film thickness behavior. A change in pressure in the inlet region can be caused at high line speeds due to fluid inertial effects. The inertial effects create a pressure component given by $\rho U^2/2$. If the line speed is high the

pressure due to this term will be comparable to the pressure due to tension. Since today most webs are processed at high speeds, it is felt necessary also to study the effect of fluid inertia on the overall air film development.

✓ 6. The limitation of the modified model is that it does not take into account the effects of the flexibility of the web material (since in the derivation of the equation of the rider roller pressure we did not consider the flexibility of the web). Due to this limitation the application of external pressure beyond a certain limit does not show any reduction in the constant gap film thickness. It is recommended that in future work, the flexibility effects of the web should be considered in the derivation of the equation of the rider roller pressure. The inclusion of this effect will enable us to determine the true reduction in the constant gap film thickness, particularly at large loads (the range beyond which the present model does not show any reduction in the constant gap film thickness).

7. The conclusion drawn that the rise in pressure in the air film is much smaller than the ambient pressure is true as long as there is no external pressure applied on the web. However, application of a significant amount of pressure on the web is expected to cause the rise in air film pressure to be comparable with the ambient pressure. In such case the incompressibility assumption will not be

true and it becomes necessary to modify the model by treating air to be compressible. Such a treatment is expected to show a higher reduction in constant gap film thickness. This will be due to the smaller volume flow rate at a given mass flow for higher pressure.

A SELECTED BIBLIOGRAPHY

1. Knox, K. L., and Sweeney, T. L., "Fluid EFFECTS Associated with Web Handling." Ind. Eng. Chem. Process, 10, 201-205 (1971).
2. Block, H., and Van Rossum, J. J., " The Foil Bearing - A New Departure." Lub. Eng., 9, 316-320 (1953).
3. Gross, W. A., Gas Film Lubrication, John Willey and Sons, Inc., New York, 1962.
4. Langlois, W. E., "The Lightly Loaded Foil Bearing at Zero Angle of Wrap." IBM J. of Res. & Dev., 7, 112-116 (1963).
5. Baumeister, H. K., "Nominal Clearance of the Foil Bearing." IBM J. of Res. & Dev., 7, 153-154 (1963).
6. Eshel, A., and Elrod, H. G., "The Theory of Infinitely Wide, Perfectly Flexible, Self-Acting Foil Bearing." J. of Basic Eng., 87, 831-836 (1965).
7. Barlow, E. J., "Self-Acting Foil Bearing of Infinite Width." J. of Lub. Tech., 89, 341-345 (1967).
8. Flugge, W., Stresses in Shells, Springer-Verlag, Berlin, 1960.
9. Barlow, E. J., "Derivation of Governing Equations for Self-Acting Foil Bearing." J. of Lub. Tech., 89, 334-340 (1967).
10. Timoshenko, S., Theory of Plates and Shells, McGraw-Hill Book Company, Inc., New York, 1940.
11. James, M. L., Smith, G. M., and Delford, J. C., Applied Numerical Methods for Digital Computation with ForTran, Int. Textbood Comp., Pennsylvania, 1967.

APPENDICES

APPENDIX A

NORMALIZATION FOR THE DERIVATION OF THE
REYNOLDS LUBRICATION EQUATION

Let us first assume the following normalizations

$$\bar{x} = x/l$$

$$U = \bar{u}/U_i$$

$$\bar{y} = y/b$$

$$V = \bar{v}/V'$$

Now the continuity equation for a steady two dimensional case is

$$\frac{\partial \bar{u}}{\partial \bar{x}} + \frac{\partial \bar{v}}{\partial \bar{y}} = 0$$

Substituting above normalizations

$$(U_i/l) \frac{\partial U}{\partial \bar{x}} + (V'/b) \frac{\partial V}{\partial \bar{y}} = 0$$

$$\frac{\partial U}{\partial \bar{x}} + (V'l)/(U_i b) \frac{\partial V}{\partial \bar{y}} = 0$$

Since the continuity equation must not change, hence we may write

$$(V'l)/(U_i b) = 1$$

or

$$V' = (U_i b)/l$$

Thus the new normalized velocity component for y-coordinate direction is

$$\psi = \bar{v}/V' = (v'l)/(U_i b)$$

Similarly we may write z-coordinate direction normalized

velocity as

$$\omega = (\bar{\omega}l)/(U_i h)$$

APPENDIX B

COMPARISON OF THE ORDER OF MAGNITUDE IN
THE DERIVATION OF REYNOLDS EQUATION

Consider x-coordinate momentum equation for a steady state case

$$\bar{u} \frac{\partial \bar{u}}{\partial x} + \bar{v} \frac{\partial \bar{u}}{\partial y} + \bar{w} \frac{\partial \bar{u}}{\partial z} = - (1/\rho) \frac{\partial p}{\partial x} + \nu \left[\frac{\partial^2 \bar{u}}{\partial x^2} + \frac{\partial^2 \bar{u}}{\partial y^2} + \frac{\partial^2 \bar{u}}{\partial z^2} \right]$$

Substituting the normalized expressions from equation (2.2.8) we get

$$U_i \mu (U_i/l) \frac{\partial \psi}{\partial x} + (U_i b/l) \mu (U_i/b) \frac{\partial \psi}{\partial y} = p_a / (\rho l) \frac{\partial p}{\partial x} + \nu \left[(U_i/l^2) \frac{\partial^2 \psi}{\partial x^2} + (U_i/b^2) \frac{\partial^2 \psi}{\partial y^2} + (U_i/h^2) \frac{\partial^2 \psi}{\partial z^2} \right]$$

or,

$$(U_i^2/l) \left[\mu \frac{\partial \psi}{\partial x} + \mu \frac{\partial \psi}{\partial y} + \mu \frac{\partial \psi}{\partial z} \right] = - p_a / (\rho l) \frac{\partial p}{\partial x} + \nu (U_i/h^2) \left[(h/l)^2 \frac{\partial^2 \psi}{\partial x^2} + (h/b)^2 \frac{\partial^2 \psi}{\partial y^2} + \frac{\partial^2 \psi}{\partial z^2} \right]$$

which may be written as

$$Re(h/l)^2 \left[\mu \frac{\partial \psi}{\partial x} + \mu \frac{\partial \psi}{\partial y} + \mu \frac{\partial \psi}{\partial z} \right] = - (p_a h^2) / (\mu l U_i) \frac{\partial p}{\partial x} + \left[(h/l)^2 \frac{\partial^2 \psi}{\partial x^2} + (h/b)^2 \frac{\partial^2 \psi}{\partial y^2} + \frac{\partial^2 \psi}{\partial z^2} \right]$$

Since $h \lll 1$ and $h \lll b$, we may neglect the higher order terms of (h/l) & (h/b) .

$$(p_a h^2) / (\mu U_i l) \frac{\partial p}{\partial x} = \frac{\partial^2 \psi}{\partial z^2}$$

APPENDIX C
SIMPLIFYING STEPS IN THE DERIVATION
OF REYNOLDS EQUATION

We have from equation (2.2.19)

$$\int_0^h \frac{\partial}{\partial x} (\rho \bar{u}) dz + \int_0^h \frac{\partial}{\partial y} (\rho \bar{v}) dz + \frac{\partial}{\partial t} (\rho h) = 0 \quad (i)$$

Applying Leibnitz's rule

$$\frac{\partial}{\partial x} \int_0^h (\rho \bar{u}) dz + \frac{\partial}{\partial y} \int_0^h (\rho \bar{v}) dz + \frac{\partial}{\partial t} (\rho h) = 0$$

Assuming that density of air is constant along the thickness of the air film (i.e. $\rho \neq \rho(z)$)

$$\frac{\partial}{\partial x} \left\{ \rho \int_0^h \bar{u} dz \right\} + \frac{\partial}{\partial y} \left\{ \rho \int_0^h \bar{v} dz \right\} + \frac{\partial}{\partial t} (\rho h) = 0 \quad (ii)$$

Substituting \bar{u} & \bar{v} from equations (2.2.16a) & (2.2.16b) we get, for the integral terms

$$\int_0^h \bar{u} dz = - (1/12) (h^3/\mu) \frac{\partial p}{\partial x} + (U_w h)/2$$

$$\int_0^h \bar{v} dz = - (1/12) (h^3/\mu) \frac{\partial p}{\partial y} + (V_w h)/2$$

Substituting the above integrals in equation (ii) we get

$$\begin{aligned} \frac{\partial}{\partial x} \left[\rho \left\{ - (1/12) (h^3/\mu) + U_w h/2 \right\} \right] + \frac{\partial}{\partial y} \left[\rho \left\{ - (1/12) (h^3/\mu) + V_w h/2 \right\} \right] \\ + \frac{\partial}{\partial t} [\rho h] = 0 \end{aligned}$$

which may be simplified to ^{the} a form

$$\frac{\partial}{\partial x} \left[(\rho h^3) / \mu \frac{\partial p}{\partial x} \right] + \frac{\partial}{\partial y} \left[(\rho h^3) / \mu \frac{\partial p}{\partial y} \right] = 6 \frac{\partial}{\partial x} [\rho U_w h] + 6 \frac{\partial}{\partial y} [\rho V_w h] +$$

$$12 \frac{\partial}{\partial t} [\rho h]$$

APPENDIX D

FORCE AND MOMENT EQUATIONS FOR
THE WEB ELEMENT

$$N_x = \int_{-t/2}^{t/2} \sigma_x(r_y + z)/r_y dz$$

$$N_y = \int_{-t/2}^{t/2} \sigma_y(r_x + z)/r_x dz$$

$$N_{xy} = \int_{-t/2}^{t/2} \tau_{xy}(r_y + z)/r_y dz$$

$$N_{yx} = \int_{-t/2}^{t/2} \tau_{yx}(r_x + z)/r_x dz$$

$$Q_x = - \int_{-t/2}^{t/2} \tau_{xz}(r_y + z)/r_y dz$$

$$Q_y = - \int_{-t/2}^{t/2} \tau_{yz}(r_x + z)/r_x dz$$

$$M_x = - \int_{-t/2}^{t/2} \sigma_x(r_y + z)/r_y z dz$$

$$M_y = - \int_{-t/2}^{t/2} \sigma_y(r_x + z)/r_x z dz$$

$$M_{xy} = - \int_{-t/2}^{t/2} \tau_{xy}(r_y + z)/r_y z dz$$

$$M_{yx} = - \int_{-t/2}^{t/2} \tau_{yx}(r_x + z)/r_x z dz$$

APPENDIX E

SIMPLIFIED FORCE AND MOMENT EQUATIONS
FOR THE WEB ELEMENT

$$N_x = \int_{-t/2}^{t/2} \sigma_x dz$$

$$N_y = \int_{-t/2}^{t/2} \sigma_y(r_x + z)/r_x dz$$

$$N_{xy} = \int_{-t/2}^{t/2} \tau_{xy} dz$$

$$N_{yx} = \int_{-t/2}^{t/2} \tau_{yx}(r_x + z)/r_x dz$$

$$Q_x = - \int_{-t/2}^{t/2} \tau_{xz} dz$$

$$Q_y = - \int_{-t/2}^{t/2} \tau_{yz}(r_x + z)/r_x dz$$

$$M_x = - \int_{-t/2}^{t/2} \sigma_x z \, dz$$

$$M_y = - \int_{-t/2}^{t/2} \sigma_y (r_x + z) / r_x \, z \, dz$$

$$M_{xy} = - \int_{-t/2}^{t/2} \tau_{xy} z \, dz$$

$$M_{yx} = - \int_{-t/2}^{t/2} \tau_{yx} (r_x + z) / r_x \, z \, dz$$

APPENDIX F

DERIVATION OF THE FORCE EQUILIBRIUM EQUATION

Multiplying equation (2.2.25) with dz and then integrating between the limits $-t/2$ to $t/2$ we get

$$\int_{-t/2}^{t/2} \frac{\partial \tau}{\partial X} xy \, dz + \int_{-t/2}^{t/2} \frac{\partial \sigma}{\partial Y} \left\{ (r_x + z)/r_x \right\} dz = 0$$

Applying Leibnitz's rule

$$\frac{\partial}{\partial X} \int_{-t/2}^{t/2} \tau_{xy} \, dz + \frac{\partial}{\partial Y} \int_{-t/2}^{t/2} \sigma_Y \left\{ (r_x + z)/r_x \right\} dz = 0$$

Referring to the equations given in the Section II, Appendix B the above equation may be written as

$$\frac{\partial N}{\partial X} xy + \frac{\partial N}{\partial Y} = 0$$

APPENDIX G

COUPLED NUMERICAL PROCEDURE OF RUNGE-KUTTA
AND MILNE PREDICTOR-CORRECTOR METHODS

The computer code that has been written for the purpose of solving the governing differential equation uses a coupled numerical procedure of Runge-Kutta method and Milne predictor-corrector method. The starting values required for the Milne method are computed by the use of fourth-order Runge-Kutta method, which is in its most general form written as

$$H_{i+1} = H_i + (k_1 + 2k_2 + 2k_3 + k_4)/6$$

where K's are given by

$$k_1 = (\Delta\eta)f(\eta_i, H_i)$$

$$k_2 = (\Delta\eta)f(\eta_i + \Delta\eta/2, H_i + k_1/2)$$

$$k_3 = (\Delta\eta)f(\eta_i + \Delta\eta/2, H_i + k_2/2)$$

$$k_4 = (\Delta\eta)f(\eta_i + \Delta\eta, H_i + k_3)$$

With the starting procedure established, the following predictor-corrector equations of the Milne method are used in further integration of the differential equation.

(Predictor)

$$P(H_{i+1}) = H_{i-3} + (4/3)\Delta\eta[2H_i - H_{i-1} + 2H_{i-2}] \quad (i)$$

$$P(H_{i+1}^I) = H_{i-3}^{I'} + (4/3)\Delta\eta [2H_{i-1}^{I'} - H_{i-1}^{I'} + 2H_{i-2}^{I'}] \quad (\text{ii})$$

$$P(H_{i+1}^{II}) = H_{i-3}^{II'} + (4/3)\Delta\eta [2H_{i-1}^{II'} - H_{i-1}^{II'} + 2H_{i-2}^{II'}] \quad (\text{iii})$$

$$P(H_{i+1}^{III}) = \pm \{P(H_{i+1}) - 1\} / P(H_{i+1})^3 \quad (\text{iv})$$

(Corrector)

$$C(H_{i+1}) = H_{i-1}^I + \Delta\eta/3 [H_{i-1}^I + 4H_i^I + P(H_{i+1}^I)] \quad (\text{v})$$

$$C(H_{i+1}^{II}) = H_{i-1}^{II} + \Delta\eta/3 [H_{i-1}^{II} + 4H_i^{II} + P(H_{i+1}^{II})] \quad (\text{vi})$$

$$C(H_{i+1}^{III}) = H_{i-1}^{III} + \Delta\eta/3 [H_{i-1}^{III} + 4H_i^{III} + P(H_{i+1}^{III})] \quad (\text{vii})$$

$$C(H_{i+1}^{IV}) = \pm \{C(H_{i+1}) - 1\} / C(H_{i+1})^3 \quad (\text{viii})$$

From equations (i) through (iv) we obtain predicted values. These values are then substituted in equations (v) through (viii) to obtain the corrected values. Since both $P(H_{i+1})$ and $C(H_{i+1})$ are determined in each step of the calculation, it is a trivial amount of work to determine the error at each step. Once the error has been determined we may easily change the step size. To change the step size at any point we must restart the solution at that point with four new starting values of each H and its derivatives corresponding to new step size. An easy approach in this regard is to double or halve the step size, since in that way we can use values of H and its

derivatives already available. This approach requires seven values of each H and its derivatives computed at the old step size

APPENDIX H

EQUATION FOR WEB-RIDER ROLLER CLEARANCE

From Figure 27 we can write

$$c_I = OB = OC + CB$$

where

$$CB = O'C - O'B$$

or,

$$CB = R_r(1 - \cos\theta_I)$$

and,

$$OC = c_m$$

then,

$$c_I = c_m + R_r(1 - \cos\theta_I)$$

Generally, the pressure development in such a case is within a small region; i.e. within a small angle, thus the expansion of $\cos\theta_I$ is

$$\cos\theta_I = 1 - \theta_I^2/2! + \text{----- neglected}$$

Also for small angle,

$$\theta_I \approx x_n/R_r$$

This gives the expansion of $\cos\theta_I$ as

$$\cos\theta_I = 1 - x_n^2/(2R_r^2)$$

Thus

$$c_I = c_m + x_n^2/(2R_r)$$

or,

$$c_I = c_m \left\{ 1 + x_n^2 / (2R_r c_m) \right\}$$

which may be written as

$$C_I = 1 + x_n^2 / (2R_r c_m)$$

where

$$C_I = c_I / c_m$$

From Figure 27 we may write

$$x_n = x - x_c$$

then,

$$C_I = 1 + (x - x_c)^2 / (2R_r c_m)$$

Using the normalized form of x from equation (2.3.10) the above equation may be written as

$$C_I = 1 + \left[h_0^2 \left\{ T / (6\mu U) \right\}^{2/3} (\eta - \eta_c)^2 / (2R_r c_m) \right]$$

or,

$$C = 1 + K_1^2 (\eta - \eta_c)^2$$

where

$$K_1 = \left\{ h_0 / \sqrt{2R_r c_m} \right\} \left\{ T / (6\mu U) \right\}^{1/3}$$

or,

$$K_1 = \left\{ 0.45467R / \sqrt{R_r c_m} \right\} \left\{ (6\mu U) / T \right\}^{1/3}$$

The clearance equation to the right of the inlet transition point may be determined in a similar approach. Now the length DE due to the curvature of the web in the uniformity region must be considered.

$$c_{II} = c_m + x^2/2R_r + DE$$

Since the pressure is developed within a small range we may write

$$DE = x^2/2R_o$$

$$\text{where } R_o = R + h_o$$

$$c_{II} = c_m + (x^2/2) \left\{ 1/R_r + 1/R_o \right\}$$

Let us define

$$1/R_c = 1/R_r + 1/R_o$$

$$c_{II} = c_m \left\{ 1 + x^2/2R_c \right\}$$

which may be simplified to

$$C_{II} = 1 + K_2^2 (\eta)^2$$

where,

$$K_2 = \left\{ 0.45467R / \sqrt{(R_c C_m)} \right\} \left\{ (6\mu U) / T \right\}^{1/3}$$

APPENDIX I

COMPUTER PROGRAM LISTINGS

```

C      INLET REGION SOLUTION
C
C      DIMENSION ET(6)
C      DIMENSION F(6),FD(6),FDD(6),FDDD(6),H(7),HD(7),HDD(7),HDDD(7),
1      Q(3),QD(3),QDD(3),QDDD(3),PR(7),PRN(7),PRD(7),R(3),RD(3)
C
C      DATA D,EPS,ERR/.25,1.0E-06,1.0E-06/
C      OPEN(UNIT=122,FILE='ENT1')
C      HDDINF=0.643
C
C      INITIAL VALUES
C
C      I=1
C      ET(I)=-7.5 ✓
C      F(I)=0.0005
C      FD(I)=0.0005 = F'
C      FDD(I)=0.0005 = F''
C      FDDD(I)=0.0005 = F'''
C      PR(I)=1.0
C      PRN(I)=1.0
C      PRD(I)=-FDDD(I)
C
C      SIX REQUIRED STARTING VALUES THROUGH RUNGE-KUTTA METHOD
C
111  IF(I .GT. 5) GOTO 112
      D1F=D*FD(I)
      D1P=D*FDD(I)
      D1Q=D*F(I)
      D1R=D*(-FDDD(I))
      D2F=D*(FD(I)+D1P/2.)
      D2P=D*(FDD(I)+D1Q/2.)
      D2Q=D*(F(I)+D1F/2.)
      D2R=D*(-FDDD(I)+D1R/2.)
      D3F=D*(FD(I)+D2P/2.)
      D3P=D*(FDD(I)+D2Q/2.)
      D3Q=D*(F(I)+D2F/2.)
      D3R=D*(-FDDD(I)+D2R/2.)
      D4F=D*(FD(I)+D3P)
      D4P=D*(FDD(I)+D3Q)
      D4Q=D*(F(I)+D3F)
      D4R=D*(-FDDD(I)+D3R)
      F(I+1)=F(I)+(D1F+2.*D2F+2.*D3F+D4F)/6.0
      FD(I+1)=FD(I)+(D1P+2.*D2P+2.*D3P+D4P)/6.0
      FDD(I+1)=FDD(I)+(D1Q+2.*D2Q+2.*D3Q+D4Q)/6.0
      FDDD(I+1)=F(I+1)
      PR(I+1)=PR(I)+(D1R+2.*D2R+2.*D3R+D4R)/6.
      PRN(I+1)=1.-FDD(I+1)/HDDINF
      PRD(I+1)=-FDDD(I+1)
      ET(I+1)=ET(I)+D
      I=I+1
      GOTO 111
112  DO 113 I=1,6
      H(I)=F(I)+1.0

```

```

      HD(I)=FD(I)
      HDD(I)=FDD(I)
113  HDDD(I)=FDDD(I)
      WRITE(122,97)
97   FORMAT(1H , '                                TABLE I',//)
      WRITE(122,98)
98   FORMAT(1H , '                                NUMERICAL RESULTS OF INLET '
1     'REGION SOLUTION',///)
      WRITE(122,99)
99   FORMAT(1H , '          ETA          H          H'          H''')
1     '          H''          P',//)
      DO 114 I=1,6
114  WRITE(122,100) ET(I),H(I),HD(I),HDD(I),HDDD(I),PRN(I)
C
C   MILNE PREDICTOR CORRECTOR METHOD
C
      ETA=ET(6)
      ETOLD=ETA
      ETAM=10000.0
      DETA=D
      ERR=1.0E-06
      EPS=1.0E-06
      ERP=29.0*ERR
      ERG=.01*ERP
10   A=4./3.*DETA
      B=1./3.*DETA
      K=1
1   HDD(7)=HDD(3)+A*(2.*HDDD(4)-HDDD(5)+2.*HDDD(6))
      ETA=ETA+DETA
      HDDP=HDD(7)
      HD(7)=HD(3)+A*(2.*HDD(4)-HDD(5)+2.*HDD(6))
      HDP=HD(7)
      H(7)=H(3)+A*(2.*HD(4)-HD(5)+2.*HD(6))
      HP=H(7)
      HDDD(7)=(HP-1.0)/(HP**3)
      HDDDP=HDDD(7)
      PR(7)=PR(3)+A*(2.*PRD(4)-PRD(5)+2.*PRD(6))
      PRN(7)=1.0-HDDP/HDDINF
      PRD(7)=-HDDDP
3   HDD(7)=HDD(5)+B*(HDDD(5)+4.*HDDD(6)+HDDD(7))
      HDDC=HDD(7)
      HD(7)=HD(5)+B*(HDD(5)+4.*HDD(6)+HDD(7))
      HDC=HD(7)
      H(7)=H(5)+B*(HD(5)+4.*HD(6)+HD(7))
      HC=H(7)
      HDDD(7)=(HC-1.)/(HC**3)
      HDDDC=HDDD(7)
      PR(7)=PR(5)+B*(PRD(5)+4.*PRD(6)+PRD(7))
      PRN(7)=1.0-HDDC/HDDINF
      PRD(7)=-HDDDC
C
C   LOCAL ERROR EVALUATION
C
26  IF(ABS(HC-HP)-1.0E-04)26,26,4
      IF((ETA-ETOLD)-0.320)4,4,27

```

```

27  WRITE(3,*) ETA,H(7),HD(7),HDD(7),HDDD(7)
    WRITE(122,100) ETA,H(7),HD(7),HDD(7),HDDD(7),PRN(7)
100 FORMAT(1H ,F10.4,5E13.4)
    ETOLD=ETA
4   C=ABS(HC-HP)
    IF(C-ERP*HC) 20,20,21
20  IF((ETA .GT. 3.) .AND. (HDDDC .LE. 1.E-06)) GOTO 40
5   IF(C-ERG*HC) 7,7,30
30  K=1
16  DO 31 I=1,6
    H(I)=H(I+1)
    HD(I)=HD(I+1)
    HDD(I)=HDD(I+1)
    PR(I)=PR(I+1)
    PRD(I)=PRD(I+1)
31  HDDD(I)=HDDD(I+1)
    GOTO 1
7   GOTO(11,12,13,14,15),K
11  W1=H(1)
    WD1=HD(1)
    WDD1=HDD(1)
    WDDD1=HDDD(1)
    P1=PR(1)
    PD1=PRD(1)
    K=2
    GOTO 16
12  K=3
    GOTO 16
13  W2=H(1)
    WD2=HD(1)
    WDD2=HDD(1)
    WDDD2=HDDD(1)
    P2=PR(1)
    PD2=PRD(1)
    K=4
    GOTO 16
14  K=5
    GOTO 16
15  H(6)=H(7)
    H(4)=H(3)
    H(3)=H(1)
    H(2)=W2
    H(1)=W1
    PR(6)=PR(7)
    PR(4)=PR(3)
    PR(3)=PR(1)
    PR(2)=P2
    PR(1)=P1
    HD(6)=HD(7)
    HD(4)=HD(3)
    HD(3)=HD(1)
    HD(2)=WD2
    HD(1)=WD1
    HDD(6)=HDD(7)
    HDD(4)=HDD(3)

```

```

HDD(3)=HDD(1)
HDD(2)=WDD2
HDD(1)=WDD1
PRD(6)=PRD(7)
PRD(4)=PRD(3)
PRD(3)=PRD(1)
PRD(2)=PD2
PRD(1)=PD1
HDDD(6)=HDDD(7)
HDDD(4)=HDDD(3)
HDDD(3)=HDDD(1)
HDDD(2)=WDDD2
HDDD(1)=WDDD1
DETA=DETA+DETA
GOTO 10
21 IF(DETA-0.00000001)40,40,41
41 DO 42 I=1,3
   Q(I)=.5*(H(5-I)+H(6-I))-0.0625*(H(7-I)-H(6-I)-H(5-I)+H(4-I))
   R(I)=.5*(PR(5-I)+PR(6-I))-0.0625*(PR(7-I)-PR(6-I)-PR(5-I)
     +PR(4-I))
1   QD(I)=.5*(HD(5-I)+HD(6-I))-0.0625*(HD(7-I)-HD(6-I)-HD(5-I)
1     +HD(4-I))
   RD(I)=.5*(PRD(5-I)+PRD(6-I))-0.0625*(PRD(7-I)-PRD(6-I)-
1     PRD(5-I)+PRD(4-I))
   QDD(I)=.5*(HDD(5-I)+HDD(6-I))-0.0625*(HDD(7-I)-HDD(6-I)-
1     HDD(5-I)+HDD(4-I))
42  QDDD(I)=.5*(HDDD(5-I)+HDDD(6-I))-0.0625*(HDDD(7-I)-HDDD(6-I)
1     -HDDD(5-I)+HDDD(4-I))
   H(6)=H(5)
   H(2)=H(3)
   H(5)=Q(1)
   H(3)=Q(2)
   H(1)=Q(3)
   PR(6)=PR(5)
   PR(2)=PR(3)
   PR(5)=R(1)
   PR(3)=R(2)
   PR(1)=R(3)
   HD(6)=HD(5)
   HD(2)=HD(3)
   HD(5)=QD(1)
   HD(3)=QD(2)
   HD(1)=QD(3)
   PRD(6)=PRD(5)
   PRD(2)=PRD(3)
   PRD(5)=RD(1)
   PRD(3)=RD(2)
   PRD(1)=RD(3)
   HDD(6)=HDD(5)
   HDD(2)=HDD(3)
   HDD(5)=QDD(1)
   HDD(3)=QDD(2)
   HDD(1)=QDD(3)
   HDDD(6)=HDDD(5)
   HDDD(2)=HDDD(3)

```

```
HDDD(5)=QDDD(1)
HDDD(3)=QDDD(2)
HDDD(1)=QDDD(3)
ETA=ETA-2.*DETA
DETA=0.5*DETA
GOTO 10
40 STOP
END
```

```

C      EXIT REGION SOLUTION
C
C
      DIMENSION ET(6)
      DIMENSION F(6),FD(6),FDD(6),FDDD(6),H(7),HD(7),HDD(7),HDDD(7),
1      Q(3),QD(3),QDD(3),QDDD(3),PR(7),PRD(7),R(7),RD(7),PRN(7)
C
C
      DATA D,EPS,ERR/.25,1.0E-06,1.0E-06/
      OPEN(UNIT=122,FILE='EXT1')
      HDDINF=0.643
C
C      INITIAL VALUES
C
      I=1
      ET(I)=-13.0
      F(I)=-0.000272
      FD(I)=0.0000046
      FDD(I)=0.000260
      FDDD(I)=0.00026
      PR(I)=1.0
      PRN(I)=1.0
      PRD(I)=-FDDD(I)
C
C      USE OF RUNGE-KUTTA METHOD FOR SIX STARTING VALUES
C
111  IF(I .GT. 5) GOTO 112
      D1F=D*FD(I)
      D1P=D*FDD(I)
      D1Q=-D*F(I)
      D1R=D*(-FDDD(I))
      D2F=D*(FD(I)+D1P/2.)
      D2P=D*(FDD(I)+D1Q/2.)
      D2Q=-D*(F(I)+D1F/2.)
      D2R=D*(-FDDD(I)+D1R/2.)
      D3F=D*(FD(I)+D2P/2.)
      D3P=D*(FDD(I)+D2Q/2.)
      D3Q=-D*(F(I)+D2F/2.)
      D3R=D*(-FDDD(I)+D2R/2.)
      D4F=D*(FD(I)+D3P)
      D4P=D*(FDD(I)+D3Q)
      D4Q=-D*(F(I)+D3F)
      D4R=D*(-FDDD(I)+D3R)
      F(I+1)=F(I)+(D1F+2.*D2F+2.*D3F+D4F)/6.0
      FD(I+1)=FD(I)+(D1P+2.*D2P+2.*D3P+D4P)/6.0
      FDD(I+1)=FDD(I)+(D1Q+2.*D2Q+2.*D3Q+D4Q)/6.0
      FDDD(I+1)=-F(I+1)
      PR(I+1)=PR(I)+(D1R+2.*D2R+2.*D3R+D4R)/6.0
      PRN(I+1)=1.0-FDD(I+1)/HDDINF
      PRD(I+1)=-FDDD(I+1)
      ET(I+1)=ET(I)+D
      I=I+1
      GOTO 111
112  DO 113 I=1,6
      H(I)=F(I)+1.0

```

```

      HD(I)=FD(I)
      HDD(I)=FDD(I)
113  HDDD(I)=FDDD(I)
      WRITE(122,97)
97   FORMAT(1H , '                                TABLE II',//)
      WRITE(122,98)
98   FORMAT(1H , '                                NUMERICAL RESULTS OF EXIT'
1     ' REGION SOLUTION',///)
      WRITE(122,99)
99   FORMAT(1H , '          ETA          H          H'          H''')
1     '          H''          P',//)
      DO 114 I=1,6
114  WRITE(122,100) ET(I),H(I),HD(I),HDD(I),HDDD(I),PRN(I)
C
C   MILNE PREDICTOR-CORRECTOR METHOD
C
      ETA=ET(6)
      ETOLD=ETA
      ETAM=10000.0
      DETA=D
      ERR=1.0E-06
      EPS=1.0E-06
      ERP=29.0*ERR
      ERG=.01*ERP
10   A=4./3.*DETA
      B=1./3.*DETA
      K=1
1    HDD(7)=HDD(3)+A*(2.*HDDD(4)-HDDD(5)+2.*HDDD(6))
      ETA=ETA+DETA
      HDDP=HDD(7)
      HD(7)=HD(3)+A*(2.*HDD(4)-HDD(5)+2.*HDD(6))
      HDP=HD(7)
      H(7)=H(3)+A*(2.*HD(4)-HD(5)+2.*HD(6))
      HP=H(7)
      HDDD(7)=(1.0-HP)/(HP**3)
      HDDDP=HDDD(7)
      PR(7)=PR(3)+A*(2.*PRD(4)-PRD(5)+2.*PRD(6))
      PRN(7)=1.0-HDDP/HDDINF
      PRD(7)=-HDDDP
3    HDD(7)=HDD(5)+B*(HDDD(5)+4.*HDDD(6)+HDDD(7))
      HDDC=HDD(7)
      HD(7)=HD(5)+B*(HDD(5)+4.*HDD(6)+HDD(7))
      HDC=HD(7)
      H(7)=H(5)+B*(HD(5)+4.*HD(6)+HD(7))
      HC=H(7)
      HDDD(7)=(1.-HC)/(HC**3)
      HDDDC=HDDD(7)
      PR(7)=PR(5)+B*(PRD(5)+4.*PRD(6)+PRD(7))
      PRN(7)=1.0-HDDC/HDDINF
      PRD(7)=-HDDDC
C
C   LOCAL ERROR EVALUATION
C
      IF(ABS(HC-HP)-1.0E-04)26,26,4
26   IF((ETA-ETOLD)-0.520) 4,4,27

```



```

27  WRITE(3,*) ETA,H(7),HDD(7),HDDD(7),PRN(7)
    WRITE(122,100) ETA,H(7),HD(7),HDD(7),HDDD(7),PRN(7)
100  FORMAT(1H ,F10.4,5E13.4)
    ETOLD=ETA
4    C=ABS(HC-HP)
    IF(C-ERP*HC) 20,20,21
20   IF((ETA .GT. 3.) .AND. (ABS(HDDDC) .LE.1.E-6)) GOTO 40
5    IF(C-ERG*HC) 7,7,30
30   K=1
16   DO 31 I=1,6
      H(I)=H(I+1)
      HD(I)=HD(I+1)
      HDD(I)=HDD(I+1)
      PR(I)=PR(I+1)
      PRD(I)=PRD(I+1)
31   HDDD(I)=HDDD(I+1)
      GOTO 1
7    GOTO(11,12,13,14,15),K
11   W1=H(1)
      WD1=HD(1)
      WDD1=HDD(1)
      WDDD1=HDDD(1)
      P1=PR(1)
      PD1=PRD(1)
      K=2
      GOTO 16
12   K=3
      GOTO 16
13   W2=H(1)
      WD2=HD(1)
      WDD2=HDD(1)
      WDDD2=HDDD(1)
      P2=PR(1)
      PD2=PRD(1)
      K=4
      GOTO 16
14   K=5
      GOTO 16
15   H(6)=H(7)
      H(4)=H(3)
      H(3)=H(1)
      H(2)=W2
      H(1)=W1
      PR(6)=PR(7)
      PR(4)=PR(3)
      PR(3)=PR(1)
      PR(2)=P2
      PR(1)=P1
      HD(6)=HD(7)
      HD(4)=HD(3)
      HD(3)=HD(1)
      HD(2)=WD2
      HD(1)=WD1
      PRD(6)=PRD(7)
      PRD(4)=PRD(3)

```

```
HDDD(3)=QDDD(2)
HDDD(1)=QDDD(3)
ETA=ETA-2.*DETA
DETA=0.5*DETA
40  GOTO 10
STOP
END
```

```

C   THE MODIFIED COMPUTER PROGRAM
C
C   DIMENSION ET(6)
C   DIMENSION F(6),FD(6),FDD(6),FDDD(6),H(7),HD(7),HDD(7),HDDD(7),
1     Q(3),QD(3),QDD(3),QDDD(3),PR(7),PRN(7),PRD(7),R(3),RD(3),
1     PPR(7),PPRD(7),S(3),SD(3)
C   LOGICAL FLAG
C
C   PARAMETER (PI=3.141593)
C   DATA D,EPS,ERR,VIS/.25,1.0E-06,1.0E-06,2.62E-09/
C   OPEN(UNIT=122,FILE='VWRR')
C
C   INPUT OPERATING PARAMETERS
C
C   U=400.0
C   UN=400.0
C   RS=18.0
C   T=1.0
C   CONSTANT GAP FILM THICKNESS W/O RIDER ROLLER
C   HO=0.643*RS*((6.*VIS*U/T)**0.6667)
C   RO=RS+HO
C   XC=0.2136
C   RR=1.0
C   CM=1500E-06
C   WLOD=2.44752*VIS*UN*RR/CM
C   CO=0.45467*RS*((6.*VIS*U/(T))**0.3333)/(SQRT(CM))
C   C1=CO*SQRT(1/RR)
C   C2=CO*SQRT(1/RR+1/RO)
C   BN=0.41345*((RS/CM)**2)*(U/UN)*((6*VIS*U/T)**1.33333)
C   ETC=1.55521*XC*(T/(6.*VIS*U))**0.3333/RS
C   WRITE(3,*)BN,C1,ETC
C
C   PSII0=ATAN(-C1*ETC)
C   FLAG=.FALSE.
C   IF((ETC*C1) .LT. 0.475156) FLAG=.TRUE.
C
C   FOR INLET REGION SOLUTION SET FLAG = FALSE
C
C   FLAG=.FALSE.
C   CALL SEARCH(C1,C2,FLAG,PSII0,PSIS)
C   CS=(1/COS(PSIS))**2
C   HDDINF=0.593
C
C   INITIAL VALUES
C
C   91  I=1
C       ET(I)=-7.5
C       F(I)=0.0005
C       FD(I)=0.0005
C       FDD(I)=0.0005
C       CI=C2
C       IF(ET(I) .GE. 0.) CI=C1
C   FOR INLET REGION SOLUTION USE C1

```

```

CI=C1
XP=CI*(ET(I)-ETC)
C=1.+(XP**2)
IF(ET(I) .GE. 0.) THEN
  PPR(I)=EQN1(C1,C2,BN,XP,C,CS,PSIS)
ELSE
  PPR(I)=EQN2(C1,C2,BN,XP,C,CS,PSIS)
END IF
C FOR INLET REGION SOLUTION USE FIRST EQUATION
PPR(I)=EQN1(C1,C2,BN,XP,C,CS,PSIS)
IF(XP .LT. TAN(PSIS)) PPR(I)=0.0
PPRD(I)=BN*(CS-C)/(C**3)
IF(XP .LT. TAN(PSIS)) PPRD(I)=0.0
FDDD(I)=F(I)+PPRD(I)
PR(I)=1.0
PRN(I)=1.0+(PPR(I)-FDD(I))/HDDINF
PRD(I)=PPRD(I)-FDDD(I)
111 IF(I .GT. 5) GOTO 112
D1F=D*FD(I)
D1P=D*FDD(I)
D1Q=D*F(I)
D1R=D*(-FDDD(I))
D2F=D*(FD(I)+D1P/2.)
D2P=D*(FDD(I)+D1Q/2.)
D2Q=D*(F(I)+D1F/2.)
D2R=D*(-FDDD(I)+D1R/2.)
D3F=D*(FD(I)+D2P/2.)
D3P=D*(FDD(I)+D2Q/2.)
D3Q=D*(F(I)+D2F/2.)
D3R=D*(-FDDD(I)+D2R/2.)
D4F=D*(FD(I)+D3P)
D4P=D*(FDD(I)+D3Q)
D4Q=D*(F(I)+D3F)
D4R=D*(-FDDD(I)+D3R)
F(I+1)=F(I)+(D1F+2.*D2F+2.*D3F+D4F)/6.0
FD(I+1)=FD(I)+(D1P+2.*D2P+2.*D3P+D4P)/6.0
FDD(I+1)=FDD(I)+(D1Q+2.*D2Q+2.*D3Q+D4Q)/6.0
ET(I+1)=ET(I)+D
CI=C2
IF(ET(I+1) .GE. 0.) CI=C1
C USE C1 FOR INLET REGION SOLUTION
CI=C1
XP=CI*(ET(I+1)-ETC)
C=1.+(XP**2)
IF(ET(I+1) .GE. 0.) THEN
  PPR(I+1)=EQN1(C1,C2,BN,XP,C,CS,PSIS)
ELSE
  PPR(I+1)=EQN2(C1,C2,BN,XP,C,CS,PSIS)
END IF
C USE FIRST EQUATION FOR INLET REGION SOLUTION
PPR(I+1)=EQN1(C1,C2,BN,XP,C,CS,PSIS)
IF(XP .LT. TAN(PSIS)) PPR(I+1)=0.0
PPRD(I+1)=BN*(CS-C)/(C**3)
IF(XP .LT. TAN(PSIS)) PPRD(I+1)=0.0
FDDD(I+1)=F(I+1)+PPRD(I+1)

```

```

PR(I+1)=PR(I)+(D1R+2.*D2R+2.*D3R+D4R)/6.0
PRN(I+1)=1.0+(PPR(I+1)-FDDD(I+1))/HDDINF
PRD(I+1)=PPRD(I+1)-FDDD(I+1)
I=I+1
GOTO 111
112 DO 113 I=1,6
    H(I)=F(I)+1.0
    HD(I)=FD(I)
    HDD(I)=FDD(I)
113 HDDD(I)=FDDD(I)
C DO 114 I=1,6
C 114 WRITE(122,100) ET(I),H(I),HD(I),HDD(I),HDDD(I),PRN(I),PPR(I)
    ETA=ET(6)
    ETOLD=ETA
    ETAM=10000.0
    DETA=D
    ERP=29.0*ERR
    ERG=.01*ERP
10  A=4./3.*DETA
    B=1./3.*DETA
    K=1
1   HDD(7)=HDD(3)+A*(2.*HDDD(4)-HDDD(5)+2.*HDDD(6))
    ETA=ETA+DETA
    HDDP=HDD(7)
    HD(7)=HD(3)+A*(2.*HDD(4)-HDD(5)+2.*HDD(6))
    HDP=HD(7)
    H(7)=H(3)+A*(2.*HD(4)-HD(5)+2.*HD(6))
    HP=H(7)
    CI=C2
    IF(ETA .GE. 0.) CI=C1
C USE C1
    CI=C1
    XP=CI*(ETA-ETC)
    C=1.+(XP**2)
C   PPR(7)=PPR(3)+A*(2.*PPRD(4)-PPRD(5)+2.*PPRD(6))
    IF(ETA .GE. 0.) THEN
        PPR(7)=EQN1(C1,C2,BN,XP,C,CS,PSIS)
    ELSE
        PPR(7)=EQN2(C1,C2,BN,XP,C,CS,PSIS)
    END IF
C USE FIRST EQUATION
    PPR(7)=EQN1(C1,C2,BN,XP,C,CS,PSIS)
    IF(XP .LT. TAN(PSIS)) PPR(7)=0.0
    PPRP=PPR(7)
    PPRD(7)=BN*(CS-C)/(C**3)
    IF(XP .LT. TAN(PSIS)) PPRD(7)=0.0
    PPRDP=PPRD(7)
    HDDD(7)=(HP-1.0)/(HP**3)+PPRDP
    HDDDP=HDDD(7)
    PR(7)=PR(3)+A*(2.*PRD(4)-PRD(5)+2.*PRD(6))
    PRN(7)=1.0+(PPRP-HDDP)/HDDINF
    PRD(7)=PPRDP-HDDDP
3   HDD(7)=HDD(5)+B*(HDDD(5)+4.*HDDD(6)+HDDD(7))
    HDDC=HDD(7)
    HD(7)=HD(5)+B*(HDD(5)+4.*HDD(6)+HDD(7))

```

```

HDC=HD(7)
H(7)=H(5)+B*(HD(5)+4.*HD(6)+HD(7))
HC=H(7)
CI=C2
IF(ETA .GE. 0.) CI=C1
C USE C1
  CI=C1
  XP=CI*(ETA-ETC)
  C=1.+(XP**2)
C   PPR(7)=PPR(5)+B*(PPRD(5)+4.*PPRD(6)+PPRD(7))
  IF(ETA .GE. 0.) THEN
    PPR(7)=EQN1(C1,C2,BN,XP,C,CS,PSIS)
  ELSE
    PPR(7)=EQN2(C1,C2,BN,XP,C,CS,PSIS)
  END IF
C USE FIRST EQUATION
  PPR(7)=EQN1(C1,C2,BN,XP,C,CS,PSIS)
  IF(XP .LT. TAN(PSIS)) PPR(7)=0.0
  PPRC=PPR(7)
  PPRD(7)=BN*(CS-C)/(C**3)
  IF(XP .LT. TAN(PSIS)) PPRD(7)=0.0
  PPRDC=PPRD(7)
  HDDD(7)=(HC-1.)/(HC**3)+PPRDC
  HDDDC=HDDD(7)
  PR(7)=PR(5)+B*(PRD(5)+4.*PRD(6)+PRD(7))
  PRN(7)=1.0+(PPRC-HDDC)/HDDINF
  PRD(7)=PPRDC-HDDDC
C
C   LOCAL ERROR EVALUATION
C
C   DO NOT WRITE FOR OBTAINING Rr OR cm OR xc VS ho
C
C   DWGIT=0.35
C   IF(ETA .GT. 10.) DWGIT=1.5
C
C   IF(ABS(HC-HP)-9.99E-04)26,26,4
C 26 IF((ETA-ETOLD)-DWGIT) 4,4,27
C 27 WRITE(3,*) ETA,HDD(7),HDDD(7),PPR(7),PPR(7)
C   WRITE(122,100) ETA,H(I),HD(7),HDD(7),HDDD(7),PRN(7),PPR(7)
C 100 FORMAT(1H ,F10.4,6E11.3)
C   ETOLD=ETA
C   4 CL=ABS(HC-HP)
  IF(CL-ERP*HC) 20,20,21
C 20 IF((ETA .GT. 3.).AND.(ABS(HDDDC) .LE. 1.0E-09)) GOTO 92
C   5 IF(CL-ERG*HC) 7,7,30
C 30 K=1
C 16 DO 31 I=1,6
  H(I)=H(I+1)
  PR(I)=PR(I+1)
  HD(I)=HD(I+1)
  PRD(I)=PRD(I+1)
  PPR(I)=PPR(I+1)
  PPRD(I)=PPRD(I+1)
  HDD(I)=HDD(I+1)
C 31 HDDD(I)=HDDD(I+1)

```

```
      GOTO 1
7     GOTO(11,12,13,14,15),K
11    W1=H(1)
      P1=PR(1)
      WD1=HD(1)
      PD1=PRD(1)
      PP1=PPR(1)
      PPD1=PPRD(1)
      WDD1=HDD(1)
      WDDD1=HDDD(1)
      K=2
      GOTO 16
12    K=3
      GOTO 16
13    W2=H(1)
      P2=PR(1)
      WD2=HD(1)
      PD2=PRD(1)
      PP2=PPR(1)
      PPD2=PPRD(1)
      WDD2=HDD(1)
      WDDD2=HDDD(1)
      K=4
      GOTO 16
14    K=5
      GOTO 16
15    H(6)=H(7)
      H(4)=H(3)
      H(3)=H(1)
      H(2)=W2
      H(1)=W1
      PR(6)=PR(7)
      PR(4)=PR(3)
      PR(3)=PR(1)
      PR(2)=P2
      PR(1)=P1
      PPR(6)=PPR(7)
      PPR(4)=PPR(3)
      PPR(3)=PPR(1)
      PPR(2)=PP2
      PPR(1)=PP1
      HD(6)=HD(7)
      HD(4)=HD(3)
      HD(3)=HD(1)
      HD(2)=WD2
      HD(1)=WD1
      PRD(6)=PRD(7)
      PRD(4)=PRD(3)
      PRD(3)=PRD(1)
      PRD(2)=PD2
      PRD(1)=PD1
      PPRD(6)=PPRD(7)
      PPRD(4)=PPRD(3)
      PPRD(3)=PPRD(1)
      PPRD(2)=PPD2
```

```

PPRD(1)=PPD1
HDD(6)=HDD(7)
HDD(4)=HDD(3)
HDD(3)=HDD(1)
HDD(2)=WDD2
HDD(1)=WDD1
HDDD(6)=HDDD(7)
HDDD(4)=HDDD(3)
HDDD(3)=HDDD(1)
HDDD(2)=WDDD2
HDDD(1)=WDDD1
DETA=DETA+DETA
GOTO 10
21 IF(DETA-0.00000001)40,40,41
41 DO 42 I=1,3
Q(I)=.5*(H(5-I)+H(6-I))-.0625*(H(7-I)-H(6-I)-H(5-I)+H(4-I))
R(I)=.5*(PR(5-I)+PR(6-I))-.0625*(PR(7-I)-PR(6-I)-PR(5-I)
1 +PR(4-I))
S(I)=.5*(PPR(5-I)+PPR(6-I))-.0625*(PPR(7-I)-PPR(6-I)-PPR(5-I)
1 +PPR(4-I))
QD(I)=.5*(HD(5-I)+HD(6-I))-.0625*(HD(7-I)-HD(6-I)-HD(5-I)
1 +HD(4-I))
RD(I)=.5*(PRD(5-I)+PRD(6-I))-.0625*(PRD(7-I)-PRD(6-I)-
1 PRD(5-I))
SD(I)=.5*(PPRD(5-I)+PPRD(6-I))-.0625*(PPRD(7-I)-PPRD(6-I)
1 -PPRD(5-I)+PPRD(4-I))
QDD(I)=.5*(HDD(5-I)+HDD(6-I))-.0625*(HDD(7-I)-HDD(6-I)-
1 HDD(5-I)+HDD(4-I))
42 QDDD(I)=.5*(HDDD(5-I)+HDDD(6-I))-.0625*(HDDD(7-I)-HDDD(6-I)
1 -HDDD(5-I)+HDDD(4-I))
H(6)=H(5)
H(2)=H(3)
H(5)=Q(1)
H(3)=Q(2)
H(1)=Q(3)
PR(6)=PR(5)
PR(2)=PR(3)
PR(5)=R(1)
PR(3)=R(2)
PR(1)=R(3)
PPR(6)=PPR(5)
PPR(2)=PPR(3)
PPR(5)=S(1)
PPR(3)=S(2)
PPR(1)=S(3)
HD(6)=HD(5)
HD(2)=HD(3)
HD(5)=QD(1)
HD(3)=QD(2)
HD(1)=QD(3)
PRD(6)=PRD(5)
PRD(2)=PRD(3)
PRD(5)=RD(1)
PRD(3)=RD(2)
PRD(1)=RD(3)

```



```

PPRD(6)=PPRD(5)
PPRD(2)=PPRD(3)
PPRD(5)=SD(1)
PPRD(3)=SD(2)
PPRD(1)=SD(3)
HDD(6)=HDD(5)
HDD(2)=HDD(3)
HDD(5)=QDD(1)
HDD(3)=QDD(2)
HDD(1)=QDD(3)
HDDD(6)=HDDD(5)
HDDD(2)=HDDD(3)
HDDD(5)=QDDD(1)
HDDD(3)=QDDD(2)
HDDD(1)=QDDD(3)
ETA=ETA-2.*DETA
DETA=0.5*DETA
GOTO 10

```

C

C

CONSTANT GAP FILM THICKNESS WITH RIDER ROLLER

C

```

92  HON=HDDC*RS*((6.*VIS*U/T)**0.66667)*1.0E+06
    WRITE(3,*)RR,HON
    WRITE(122,191)RR,HON
191  FORMAT(1H ,F12.6,F12.0)
    RR=RR+1.0
    C1=CO*SQRT(1/RR)
    IF(RR .GT. 15.0) GOTO 40
    GOTO 91
40  STOP
    END

```

C

C

C

C

C

C

C

C

C

C

C

C

C

C

C

C

C

C

C

C

C

C

C

C

C

C

C

C

C

C

C

C

SUBROUTINE SEARCH(C1,C2,FLAG,SIO,SI)

```

REAL C1,C2,SIO,SI
LOGICAL FLAG

```

PARAMETER (PI=3.141593)

EPSI=1.0E-6

IF(FLAG) THEN

SI=-0.1

DSI=-0.05

ITER=0

21 ITER=ITER+1

IF(ITER .GT. 100) GOTO 22

DHS=(C2/C1)*((1./(COS(SI)**2))*(SIN(4*SIO)/32.+

1 SIN(2*SIO)/4.+3.*SIO/8.-3.*PI/16.)-SIN(2*SIO)/4.-

2 SIO/2.+PI/4.)

RHS=SIN(2*SI)/4.+SI/2.-((1/COS(SI))**2)*(SIN(4*SI)/32.+

1 SIN(2*SI)/4.+3.*SI/8.)

ERROR=RHS-DHS

```

        IF(ERROR .GT. 0. .AND. ERROR .LE. EPSI) GOTO 22
        IF((DHS .GT. RHS .AND. DSI .GT. 0.) .OR. (DHS .LT. RHS
1      .AND. DSI .LT. 0.)) DSI=-DSI/2.
        SI=SI+DSI
        GOTO 21
22     CONTINUE
      END IF
      IF(.NOT. FLAG) SI=-0.44355
      RETURN
      END

C
C
C
      REAL FUNCTION EQN1(C1,C2,BN,XP,C,CS,PSIS)
C
      REAL C1,C2,BN,XP,C,CS,PSIS
      PARAMETER (PI=3.141593)
C
      EQN1=(BN/C1)*((CS*XP/(8*C))*(2./C-1.)
1          +(XP*(CS-1.))/(2.*C)
2          +ATAN(XP)*(3.*CS/4.-1.)/2.-(PI/4.)*(3.*CS/4.-1.))
      RETURN
      END

C
C
C
      REAL FUNCTION EQN2(C1,C2,BN,XP,C,CS,PSIS)
C
      REAL C1,C2,BN,XP,C,CS,PSIS
      PARAMETER (PI=3.141593)
C
      EQN2=(BN/C2)*((CS*XP/(8*C))*(2./C-1.)
1          +(XP*(CS-1.))/(2.*C)
2          +ATAN(XP)*(3.*CS/4.-1.)/2.-TAN(PSIS)*(2./CS-1.)/8.
3          -TAN(PSIS)*(CS-1.)/(2.*CS)-(PSIS/2.)*(3.*CS/4.-1.))
      RETURN
      END

```

VITAⁱ

TAJUDDIN

Candidate for the Degree of
Master of Science

Thesis: MATHEMATICAL MODELLING OF AIR ENTRAINMENT IN WEB
HANDLING APPLICATIONS

Major Field: Mechanical Engineering

Biographical:

Personal Data: Born in Hyderabad, Pakistan, February
26, 1961, the son of Mr. and Mrs. Nazar Ali.

Education: Graduated from Government Dehli College,
Karachi, Pakistan, in July 1978; recieved Bach-
elor of Engineering Degree from N.E.D. Univer-
sity of Engineering & Technology in March 1985;
completed requirements for the Master of Science
Degree at Oklahoma State University in December,
1987.

Professional Experience: Installation and Mainte-
nance Engineer, Ameerjee Valijee & Sons, Karachi,
May, 1985; Research Assistant at Oklahoma State
University, School of Mechanical Engineering,
June, 1986 - present.